

INSTITUTO TECNOLÓGICO Y DE ESTUDIOS SUPERIORES DE OCCIDENTE

Maestría en Diseño Electrónico

Reconocimiento de Validez Oficial de Estudios de nivel superior según Acuerdo Secretarial 15018,
publicado en el *Diario Oficial de la Federación* el 29 de noviembre de 1976

DEPARTAMENTO DE ELECTRÓNICA, SISTEMAS E INFORMÁTICA



**PARAMETER EXTRACTION METHODOLOGY FOR
COMPOSITE RIGHT/LEFT-HANDED TRANSMISSION LINES
USING QUASI-STATIC MODELS**

Tesis para obtener el grado de

Maestro en Diseño Electrónico

Presenta:

Enrique Raúl Villa Loustaunau

Director de Tesis:

Dr. José Ernesto Rayas Sánchez

Tlaquepaque, Jalisco, Septiembre de 2014

MAESTRO EN INGENIERIA (2014)
Maestría en Diseño Electrónico

ITESO
Tlaquepaque, Jal., México

TÍTULO: **Parameter Extraction Methodology for Composite
Right/Left-Handed Transmission Lines using Quasi-static
Models**

AUTOR: Enrique Raúl Villa Loustaunau
Ingeniero en Electrónica y Sistemas Digitales (Instituto
Tecnológico de Hermosillo, México)

DIRECTOR DE TESIS: José Ernesto Rayas Sanchez
Departamento de Electrónica, Sistemas e Informática, ITESO
Ingeniero en Electrónica (ITESO, México)
Maestro en Sistemas Electrónicos (ITESM Campus Monterrey,
México)
Doctor en Ingeniería Eléctrica (Universidad McMaster, Canadá)
Senior, IEEE

NÚMERO DE PÁGINAS: ix, 142

Dedication

I dedicate this thesis to my wife Carolina, for being patient and supporting me through the Master Degree program.

To my parents for sharing their interest in science: my mother Elda Irene, for showing me unconditional love; and to my father Enrique Villa, for teaching me discipline and perseverance.

Summary

In this thesis, the parameter extraction process of equivalent circuit models of a composite right/left-handed (CRLH) transmission line (TL) is studied. First, an introduction to metamaterial (MTM) structures, and a brief description of the two main approaches of modeling a CRLH TL, are described. Next, it is reviewed the basic theory of modeling a purely right-handed (PRH) transmission lines by means of using ABCD-parameters. After obtaining a conventional TL model, we analyze our circuital responses and compare them with the expected behavior published in the literature. Next, it is reviewed the basic theory of modeling a purely left-handed (PLH) TL by means of using ABCD-parameters. After obtaining a model of PLH TL, we analyze our circuital responses and compare them with exact theoretical results published in MTM literature. Next, it is also reviewed the basic theory of modeling a CRLH TL, comparing our responses again with exact theoretical results. Next, based on previous learning of PRH TL, a parameter extraction (PE) strategy is employed on an actual microstrip structure simulated in Sonnet. Applying a minimax formulation using the Nelder-Mead method, the equivalent RGLC average values are extracted using Matlab. Later, a compilation of several CRLH TL structures are described, including its S-parameter responses. Two main groups of them are described: those using microstrip technology only, and those using surface mount technology (SMT) devices soldered over microstrip technology. Next, one of the structures is selected to finally implement a PE strategy, extracting its equivalent RGLC average values of the CRLH TL structure. It was found that the equivalent circuital model (implemented in Matlab), with parameter extracted by optimization, yields an acceptable approximation of the CRLH TL responses obtained by full-wave electromagnetic simulation (implemented in Sonnet) on a wide bandwidth.

Contents

Summary	v
Contents	vii
Introduction	1
1. A General Introduction to Metamaterials	5
1.1. INTRODUCTION	5
1.2. METAMATERIALS	6
1.3. BRIEF DESCRIPTION OF ELECTROMAGNETIC BEHAVIOR.....	9
1.4. MICROSTRUCTURE DEFINITION	10
1.5. RESONANT APPROACH TO IMPLEMENT METAMATERIALS	11
1.5.1 Importance of Broad Bandwith on Interconnections	15
1.6. TRANSMISSION LINE (TL) APPROACH TO IMPLEMENT METAMATERIALS.....	16
1.7. CONCLUSIONS	20
2. Modeling a Right-Handed Transmission Line in Matlab	21
2.1. INTRODUCTION	21
2.2. BASIC THEORY OF RIGHT-HANDED TRANSMISSION LINE MODEL.....	21
2.3. CALCULATING THE INPUT IMPEDANCE OF A RIGHT-HANDED TL WITH N SEGMENTS....	24
2.3.1 Theoretical Approach.....	24
2.3.2 Implementation in Matlab.....	26
2.4. CALCULATING THE GAIN AND INPUT IMPEDANCE OF A TRANSMISSION LINE WITH N SEGMENTS USING ABCD PARAMETERS	27
2.4.1 Theoretical Approach to Compute the Gain	27
2.4.2 Theoretical Approach to Compute the Input Impedance	31
2.4.3 Matlab Implementation.....	32
2.5. CONCLUSIONS	34
3. Modeling a Purely Left-Handed TL in Matlab with Equivalent Circuits ..	35
3.1. INTRODUCTION	35
3.2. BASIC THEORY OF THE LEFT-HANDED TRANSMISSION LINE MODEL	35
3.3. LOSSLESS MODEL OF A PURELY LEFT-HANDED TRANSMISSION LINE.....	38
3.3.1 Theoretical Approach to Compute the Gain	38
3.3.2 Theoretical Approach to Compute the Input Impedance	39
3.3.3 Theoretical Approach to Compute the S-parameters	40
3.3.4 Matlab Implementation	41
3.4. LOSSY MODEL OF THE PURELY LEFT-HANDED TRANSMISSION LINE.....	43
3.4.1 Characteristic Impedance for a Lossy PLH TL.....	44
3.4.2 Matlab Implementation.....	44
3.5. CONCLUSIONS	48

4. Modeling a Composite Right/Left-Handed TL in Matlab with Equivalent Circuits	51
4.1. INTRODUCTION	51
4.2. BASIC THEORY OF THE COMPOSITE RIGHT/LEFT-HANDED TRANSMISSION LINE MODEL 51	
4.2.1 Basic Concepts on Lossless CRLH Transmission Lines	52
4.2.2 Basic Concepts on Lossy CRLH Transmission Lines	56
4.3. LOSSLESS MODEL OF A COMPOSITE RIGHT/LEFT-HANDED TL	57
4.3.1 Theoretical Approach to Compute the S-parameters	57
4.3.2 Matlab Implementation	58
4.4. LOSSY MODEL OF A COMPOSITE RIGHT/LEFT-HANDED TL	63
4.4.1 Theoretical Approach to Compute the S-parameters	63
4.4.2 Matlab Implementation	64
4.5. CONCLUSIONS	70
5. A Parameter Extraction Process for Equivalent Circuit Models of a PRH TL in Matlab.....	71
5.1. INTRODUCTION	71
5.2. FORMULATION OF PARAMETER EXTRACTION (PE).....	71
5.3. THE STARTING POINT FOR PARAMETER EXTRACTION	73
5.4. PARAMETER EXTRACTION FOR THE LOSSLESS CASE	73
5.4.1 The Fine Model Using Sonnet	73
5.4.2 The Coarse Model Using Matlab	74
5.4.3 Responses before Parameter Extraction	74
5.4.4 The LC Extracted Parameters	75
5.4.5 Responses after Parameter Extraction.....	78
5.5. PARAMETER EXTRACTION FOR THE LOSSY CASE	79
5.5.1 The Fine Model Using Sonnet	79
5.5.2 The Coarse Model Using Matlab	79
5.5.3 Responses before Parameter Extraction	80
5.5.4 Initial RGLC Extracted Parameters	81
5.5.5 Responses after Initial parameter Extraction	82
5.5.6 An Enhanced PE for the Lossy Case.....	84
5.6. CONCLUSIONS	87
6. Physical Implementation of Composite Right/Left-Handed Transmission Lines	89
6.1. INTRODUCTION	89
6.2. COMPOSITE RIGHT/LEFT-HANDED TL WITH DISTRIBUTED IMPLEMENTATION.....	89
6.2.1 Conventional CRLH TL with Interdigital Capacitors.....	90
6.2.2 Simplified Extended CRLH TL with Interdigital Capacitors	91
6.2.3 Composite Right/Left-Handed TL with Wire Bonded Interdigital Capacitors	93
6.2.4 Another Composite Right/Left-Handed TL with Interdigital Capacitors	95
6.2.5 Composite Right/Left-Handed TL with Loading Series Capacitors	96
6.3. COMPOSITE RIGHT/LEFT-HANDED TRANSMISSION LINES WITH LUMPED COMPONENTS. 97	
6.3.1 Composite Right/Left-Handed TL with Discrete Series Capacitors	98

6.3.2	Coplanar Composite Right/Left-Handed TL with Discrete Series Capacitors	99
6.3.3	Composite Right/Left-Handed TL with discrete Series SMT Capacitors.....	101
6.4.	CONCLUSIONS	102
7.	A Parameter Extraction Process for Equivalent Circuit Models of a CRLH TL	103
7.1.	INTRODUCTION	103
7.2.	COMPOSITE RIGHT/LEFT-HANDED TRANSMISSION LINE.....	103
7.3.	DECOMPOSING THE CRLH STRUCTURE	104
7.3.1	Microstrip Line Segments	105
7.3.2	Microstrip Grounded Stub.....	105
7.3.3	Two Microstrip Lines Separated by a Capacitor over a Gap	105
7.3.4	Microstrip Line Connected to a Grounded stub by a Right-Angle Bend.....	106
7.3.5	Complete Unit-Cell of the CRLH Structure.....	107
7.4.	PROPOSED METHODOLOGY FOR PARAMETER EXTRACTION OF THE EQUIVALENT CIRCUITS	109
7.4.1	PE of the Conventional Microstrip Line 6.5 mm Long.....	109
7.4.2	PE of the Conventional Microstrip Line 5 mm Long.....	111
7.4.3	PE of the Conventional Microstrip Grounded Stub	112
7.4.4	PE of the Two Microstrip Lines Separated by a Capacitor over a Gap	113
7.4.5	PE of the Microstrip Line Connected to a Grounded Stub by a Right-Angle Bend ..	114
7.4.6	PE of the Complete Unit-Cell of the CRLH Structure.....	116
7.4.7	PE of the Complete CRLH TL Structure	118
7.5.	PARAMETER EXTRACTION CONSIDERING LOSSES	121
7.5.1	PE of the Lossy Microstrip Line 6.5 mm Long.....	121
7.5.2	PE of the Lossy Microstrip Line 5 mm Long.....	123
7.5.3	PE of the Lossy Microstrip Grounded Stub	124
7.5.4	PE of the Two Lossy Microstrip Lines Separated by a Capacitor over a Gap.....	125
7.5.5	PE of the Complete Lossy Unit-Cell of the CRLH Structure	126
7.5.6	PE of the Complete Lossy CRLH TL Structure.....	127
7.6.	CONCLUSIONS	129
	General Conclusions	131
	Appendix	135
A.	LIST OF INTERNAL RESEARCH REPORTS.....	137
	Bibliography	139
	Index	141

Introduction

In electronics design, there are potential applications of metamaterial (MTM) structures to high-speed interconnections. One of the objectives of high-speed analysis is to characterize the channel behavior, which can be done by obtaining the frequency responses of a particular high-speed interconnect in a specific bandwidth. There are several parameters that can influence its frequency response, including: the dielectric material and its thickness, the metal shape and its thickness, the structure's length, among others. It is also important to consider whether the high-speed interconnect is using discrete components, such as surface mount technology (SMT) devices, or it is using only distributed components, such as microstrip technology.

In this thesis, it is initially described the basic theory of left-handed, right-handed, and composite right/left-handed TL structures. Then, it is developed a parameter extraction strategy of the *RGLC* equivalent values of quasi-static TL circuit models, based on an actual 3D structure electromagnetically simulated.

An introduction to metamaterials, explaining the importance of these structures, is presented in the Chapter 1. The basic differences between a left-handed media (LHM) and a right-handed media (RHM) are described. The microstructure concept is briefly described to understand the unit-cell's equivalent circuit model of a high-speed interconnect structure. The two main strategies to create LH structures are explained: the resonant and non-resonant approaches. The importance of having a broad bandwidth on high-speed interconnections is briefly explained.

To initially understand the LH structure, first, a simple modeling of a conventional or RH transmission line (TL) is presented in Chapter 2. Basic concepts of the TL model approximation are described based on its equivalent lumped circuits. The input impedance and voltage gain approximations are developed using the ABCD-parameters in Matlab, and compared with results published in common literature. The results of Matlab implementations are presented, looking forward to develop a similar basic model for a left-handed TL.

In Chapter 3 it is presented a simple modeling process of a purely left-handed (PLH) TL. Basic concepts of a PLH TL model approximation are described based on its equivalent lumped

circuits for the lossless and lossy cases. The input impedance, voltage gain, and the S-parameter responses are computed using the ABCD-parameters in Matlab, and compared with exact theoretical results. The Matlab results are presented, looking forward to develop a similar basic model for a composite right/left-handed TL.

In Chapter 4 it is presented a simple modeling process of a composite right/left-handed CRLH TL. Basic concepts of a CRLH TL model approximation are described based on its equivalent lumped circuits for the lossless and lossy cases. The S-parameter responses are computed using the ABCD-parameters in Matlab, and compared with exact theoretical results.

Once the basic theory of a MTM TL as been previously described, a parameter extraction (PE) process for equivalent circuital models of a PRH TL is presented in Chapter 5. A minimax formulation using the Nelder-Mead method is used to extract the equivalent *RGLC* parameters. First, the S-parameter responses of a lossless 50- Ω microstrip line in Sonnet, and a lossless PRH TL circuital model, are obtained and compared. Then, its equivalent *LC* values are extracted by minimizing the Sonnet and Matlab response differences. Similarly, the equivalent *RGLC* values are extracted based the S-parameter response of a lossy 50- Ω microstrip line. The extracted *RGLC* values of the PRH TL are presented as a suitable strategy to develop a similar PE process for a CRLH TL.

A compilation of several physical implementations of CRLH transmission lines are presented in Chapter 6. This compilation is restricted to one dimension physical implementations, such as planar transmission lines and discrete component structures. The unit-cell's equivalent circuital model and the S-parameter responses of each implementation are presented and commented.

One of the CRLH TL physical implementations illustrated in Section 6.2 is selected, and decomposed into simpler conventional microstrip sub-structures. Then, a PE strategy similar to that one in Section 5.2 is applied to each sub-structure, as illustrated in Chapter 7. The S-parameter responses of a CRLH microstrip structure in Sonnet (fine model) and its equivalent CRLH circuital model in Matlab (coarse model) are obtained and compared. The equivalent circuital parameters in Matlab are extracted using the ABCD-parameter approximation of a TL. The results obtained in Sections 7.4 and 7.5 indicate that the equivalent circuital model, with parameter values extracted by optimization, yields a quite acceptable approximation of the CRLH TL responses obtained by full-wave electromagnetic.

The author wishes to express his sincere appreciation to Dr. José Ernesto Rayas Sánchez, full Professor and director of research in the Computer-Aided Engineering of Circuits and Systems (CAECAS) group at ITESO, for his expert guidance, continuous support and keen supervision throughout the development of this thesis. I would also like to thank Dr. Luis Rizo Domínguez and Dr. Jorge Pardiñas Mir, professors and researchers at ITESO, for their valuable reviews. The author also wants to express special thanks to the *Instituto Tecnológico de Estudios Superiores de Occidente* (ITESO), for its financial support through a Research Assistant Scholarship and all the resources facilitated. Finally, I wish to thank the Intel Guadalajara Board Development group for providing financial support through a scholarship, as well as Maria Isela Borroel Mora and Pedro Hermosillo Villalobos, for their support through the development of this thesis.

1. A General Introduction to Metamaterials

1.1. Introduction

In this chapter, a brief introduction to metamaterials is made, describing the basic concepts related to these structures, as well as some potential applications to high-speed interconnections. In general terms, the possible set of applications that could be achieved with metamaterial theory, from the frequency point of view, exists from near DC (better electromagnets) to visible light (invisibility cloaking and error free optics) [Breed-07]. The objective of this chapter is to show the metamaterial basic concepts that may allow, in the following chapters, the implementation of high speed interconnections exploiting metamaterials properties.

It is also explained in this chapter the two main methodologies to model structures with LH properties, which are the resonant and non-resonant approaches. In Section 1.2 it is explained the meaning of metamaterials, and what are the properties that mainly define the particular behavior of such structures. This section also gives a quick historic overview of the main researches on the field until the first metamaterial was created. In Section 1.3, a high level explanation of the electromagnetic behavior is shown, and it is also described how the electromagnetic fields are affected by the particular properties of metamaterials. In Section 1.4 it is explained the microstructure concept, which relates the working wavelength with the physical dimension of the so called unit cell, that integrates any structure. In Section 1.5 it is explained how a metamaterial structure can be implemented following a resonant approach, which was the method used by John Pendry et al. a few years ago, based on a periodic structural arrangement. Also the narrow bandwidth effect of such structures is highlighted. An explanation of the transmission line approach to implement metamaterials by the non-resonant approach, and its advantages over resonant models in broad bandwidth applications, are described in Section 1.6. And finally the conclusions of this chapter are presented in Section 1.7.

1. A General Introduction to Metamaterials

1.2. Metamaterials

Metamaterials can be defined as “artificially created structures that exhibit electromagnetic properties not observed on the normal elements that are found in nature”. Meta means “beyond” in Greek. These structures exhibit opposite behaviors to what is found in natural materials. For example, natural materials such as glass, diamond, etc., have positive values of electrical permittivity (response to an electric field), magnetic permeability (response to a magnetic field), and index of refraction. But metamaterials have negative values for index of refraction and negative values for permittivity (ϵ) and/or permeability (μ). In general ϵ and μ are the main determinants of a material’s response to electromagnetic (EM) waves [Kshetrimayum-04].

The four possible combinations for permittivity and permeability properties and also an illustration of the examples of the materials in such combinations are shown in the Fig. 1-1. Only two of those combinations allow the signal propagation effect [Rincón-07], which are the quadrants I and III. On the first quadrant there are positive values of ϵ and μ ; this media corresponds to the common dielectric materials.

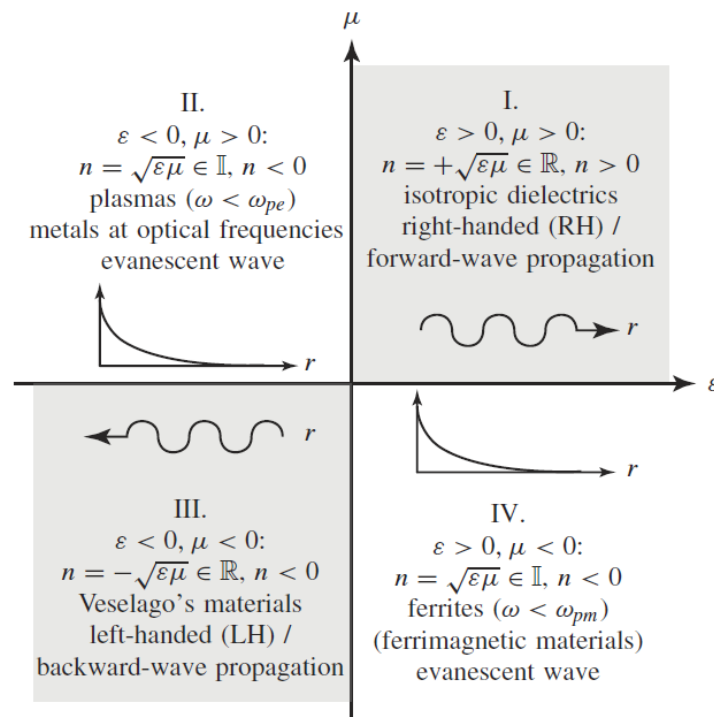


Fig. 1-1 The four possible combinations of ϵ and ν . Figure taken from [Caloz-06].

1. A General Introduction to Metamaterials

On the second quadrant we have negative permittivity and positive permeability ($\varepsilon < 0$, $\mu > 0$). In this case the propagation constant is complex and hence there will be only evanescent modes, making the propagation effect impossible. In this quadrant, we have in nature plasmas as well as metals at optic frequencies [Madrid-05], [Holden-96].

In the third quadrant both ε and μ have negative values, and the transmission effect or wave propagation is possible. It is only possible in artificial materials.

In the fourth quadrant we have permittivity (ε) with positive values and permeability (μ) with negative values, and there is a similar situation to the second quadrant, with evanescent effects where there is no wave propagation; this is the case of resonant ferromagnetic or anti-ferromagnetic systems [Pendry-04].

However this thesis will focus on the third quadrant only, which are structures with negative values of electrical permittivity (ε) and magnetic permeability (μ) simultaneously, and correspondingly a real and negative refractive index, since the refractive index [Pendry-04] corresponds to

$$n = -\sqrt{\varepsilon\mu} \quad (1-1)$$

Originally the concept of negative permittivity/permeability was described by the Russian scientist, V. G. Veselago [Veselago-68] in 1968. Although he researched how the electromagnetic (EM) waves would propagate in such materials ($\varepsilon < 0$ and $\mu < 0$) and what would be their properties, the experimental verifications occurred 30 years later [Kshetrimayum-04].

The first concept that was experimentally verified was the negative permittivity ($\varepsilon < 0$). In 1996 John B. Pendry et al. proposed that a periodic array of copper wires with a specific radius and spacing produces an electromagnetic response that corresponds to materials with negative permittivity [Holden-96] in a reduced frequency band. Then in 1999, he proposed that a periodic array of structures formed as concentric split-rings, also called Split-Ring Resonators (SRRs), would have a frequency band where μ is negative [Kshetrimayum-04], [Robbins-99].

At that time the behavior of those structures provided only negative permittivity effect (periodic array of copper wires [Holden-96]) and negative permeability effect (periodic array of SRRs [Robbins-99]) independently. The easiest way to build a structure that contains both properties simultaneously ($\varepsilon < 0$ and $\mu < 0$), was to create a periodic structure composed of pairs

1. A General Introduction to Metamaterials

of such elements. This was achieved by combining one element array that produces the effect of negative ϵ , with the other element array that produces the effect of negative μ . That would be a metamaterial with both negative ϵ and μ , just as Veselago pointed out in his work [Veselago-68].

“The first metamaterial was fabricated by interleaving split ring resonators (SSRs) and copper wires. The experiment used a 2-D array of repeated unit cells of copper strips and split ring resonators (SRR) on interlocking strips of standard circuit board materials. The scattering angle measured from the transmitted beam through a prism fabricated from these metamaterial structures showed a frequency band with the index of refraction negative. In such metamaterials, an array of SRRs contributes to the negative μ , the copper wire array contributes to the negative ϵ and the combined array results in a negative permeability and permittivity material. David Smith and his colleges at UCSD reported the outcome in 2001 April issue of Science” [Kshetrimayum-04]. Fig. 1-2 shows an example of the first metamaterial created.

In Fig. 1-3 there is a similar example of metamaterials, in which each cell has a dimension of $50 \mu\text{m} \times 50 \mu\text{m}$ for response at terahertz frequencies, which falls in the little-used spectrum between millimeter waves and long infrared light waves [Averitt-06].

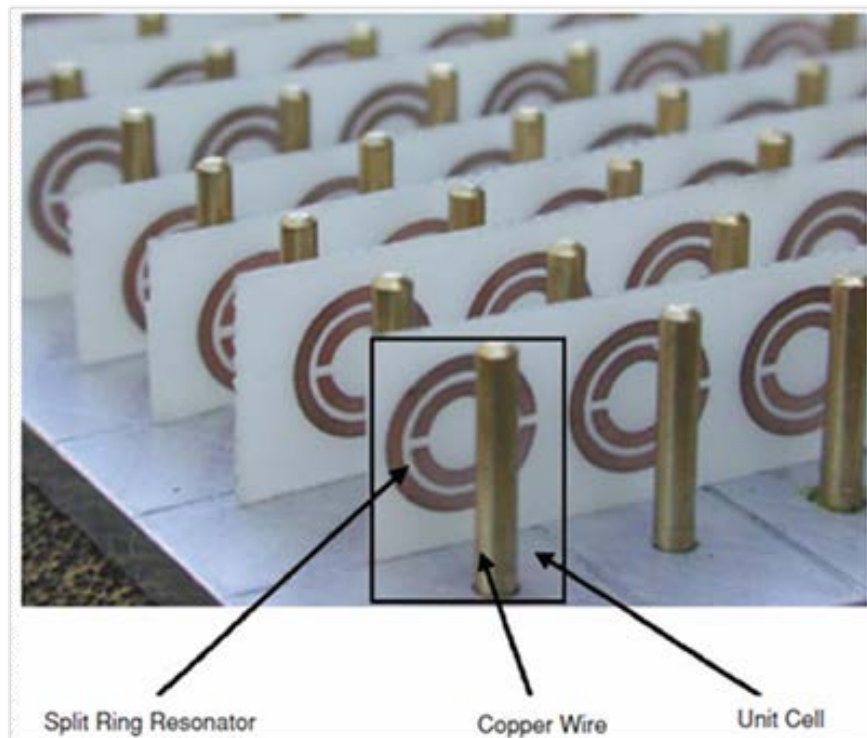


Fig. 1-2 Photograph of the first metamaterial. Figure taken from [Kshetrimayum-04].

1. A General Introduction to Metamaterials

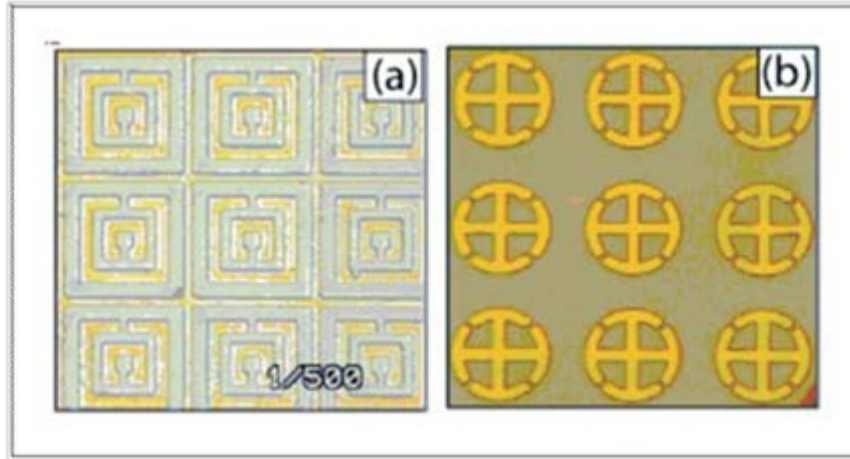


Fig. 1-3 Magnetic and electric metamaterial structures: a) Nested resonant loops of different sizes, and b) purely electric resonators (i.e., no loop to reinforce the magnetic lines of force). Figure taken from [Kshetrimayum-04].

1.3. Brief Description of Electromagnetic Behavior

The normal Transverse Electro-Magnetic (TEM) behavior of the electromagnetic waves traveling on “natural” media (positive ϵ and μ) follows a right-handed triplet as it is shown in Fig. 1-4. This means that the group velocity S and phase vector k are going parallel and in the same direction, while the electric (E) and magnetic (H) fields are traveling orthogonally to each other and orthogonally to the energy propagation direction. The phase vector k represents the direction of the traveling waves; whereas the energy propagation direction or group velocity is indicated by the Poynting vector S .

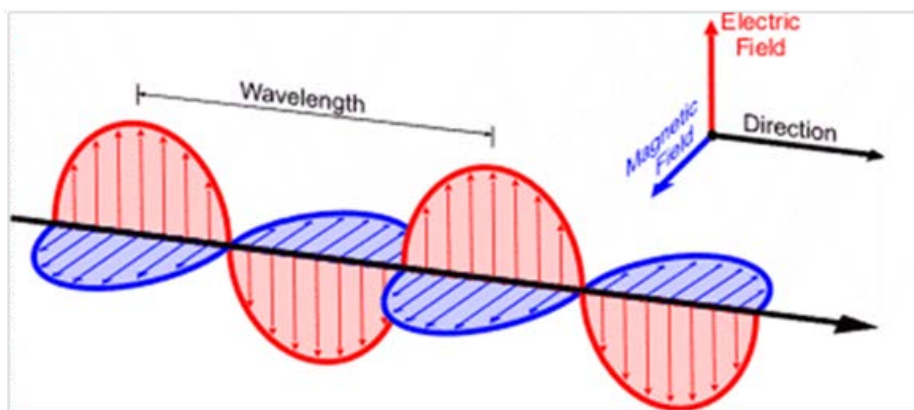


Fig. 1-4 Transverse electro-magnetic (TEM) propagation using positive ϵ and μ ¹.

¹ http://www.srh.noaa.gov/jetstream//remote/remote_intro.htm

1. A General Introduction to Metamaterials



Fig. 1-5 Poynting vector S and phase vector k : a) going in the same direction, and b) going on opposite directions².

A consequence of having negative ϵ and μ is that when changing their sign in two of the four Maxwell's equations, there is a left-handed triplet of electric field E , magnetic field H and phase vector k . This implies that the phase vector k and the group velocity vector S are in opposite directions as indicated in Fig. 1-5. Thereby, the waves flow in a backwards fashion (i.e. the wave phase appears to undulate backwards while the energy propagates along the incident energy in a forward direction). In other words, while the energy is propagated moving away from the source, the wave front is traveling in opposite direction, toward the source. That is the reason why these structures are also known as Left-Handed Media (LHM), or Backward Wave Media (BWM) [4], [Kshetrimayum-04]. In summary,

- a) If $\epsilon > 0$ and $\mu > 0$, then E , H , and k form a right triplet.
- b) If $\epsilon < 0$ and $\mu < 0$, then E , H , and k form a left triplet.

On the other hand, the energy propagation direction given by S always forms a right triplet regarding the E and H vectors.

1.4. Microstructure Definition

Every material is a composite of atoms, molecules, or bigger elements that could be simply called, unit cells. The response of any material to the electromagnetic radiation of frequency ω depends on the condition.

$$a \ll \lambda \quad (1-2)$$

where a represents the characteristic dimension of the unit cell, and λ represents the working wavelength. An effectively homogenous structure is a structure whose structural average cell

² http://www.srh.noaa.gov/jetstream//remote/remote_intro.htm

1. A General Introduction to Metamaterials

size a is much smaller than the working wavelength. In [Caloz-06] it is used the condition $a = \lambda/4$, as the effective homogeneity limit or effective-homogeneity condition, to distinguish lumped components ($a < \lambda/4$) from quasi-lumped components ($\lambda/4 < a < \lambda/2$), and distributed components $a > \lambda/2$.

If this effective-homogeneity condition is satisfied, the structure behave as a real homogeneous material in the sense that electromagnetic waves are essentially myopic to the internal structure of the material and only probe the average, or effective, macroscopic and well-defined constitutive parameters, which depend on the nature of the unit cell. Otherwise there would be the possibility that the internal unit cells of the structure could diffract as well as refract the radiation, in such way that all developed metamaterial theory so far would be invalid.

1.5. Resonant Approach to Implement Metamaterials

Metamaterial theory was confirmed by using microstructures that behaves as resonant elements, which helped to provide the negative values for both permittivity and permeability. The electromagnetic response of metals in the visible region and near ultraviolet is dominated by the negative epsilon concept [Pendry-99], or negative permittivity effect. Since normally the negative epsilon concept is presented on the spectral range between visible and near ultraviolet frequencies, John Pendry et al. wanted to displace the negative permittivity effect to lower frequencies (microwave). According to [Pendry-96], by confining electrons to thin wires it is possible displace the negative permittivity effect at lower frequencies. So the final microstructure

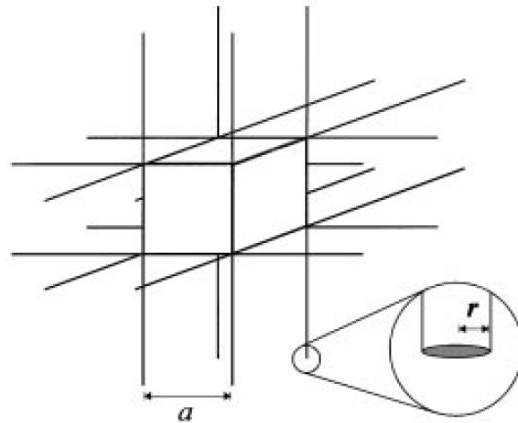


Fig. 1-6 Thin wire lattice developed by John Pendry et al. Figure taken from [Pendry-96].

1. A General Introduction to Metamaterials

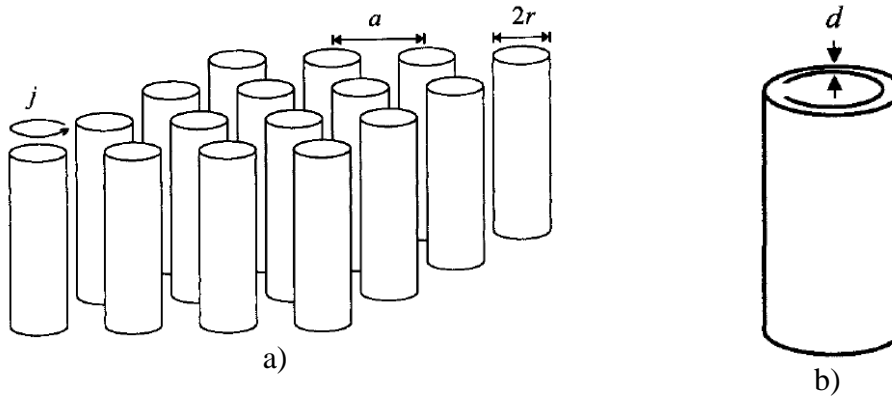


Fig. 1-7 Structure created by John Pendry et al.: a) square structure of metallic cylinders designed to present magnetic properties in parallel direction of cylinders axis, b) cylinder details. Figure taken from [Pendry-99].

was created as a periodic lattice of very thin metal wires of the order of $1\mu\text{m}$ in radius [Pendry-96], and a defined spacing among wires (i.e., Fig. 1-6). According to the analysis in [Pendry-96] and [Madrid-05], if this structure is feed by an electric field in the same direction than the thin wires orientation, negative values of ϵ will be provided in a reduced frequency range. Modifying the very thin metal wires radius and the periodicity of the lattice it is possible to modify the frequency range in which this structure presents negative permittivity values. According to [Madrid-05], these calculations are already corroborated with real measurements.

John Pendry et al. analyzed some structures [Pendry-99] to achieve negative permeability, one of those was a capacitive array of sheets wound on cylinders that he called split ring as shown in Fig. 1-7b, whose top view is shown in Fig. 1-8. The split ring structure consist of two metallic sheets separated by a distance d , were a cut on each sheet avoids the current to flow in any of the two rings as shown in Fig. 1-8. Applying a variable magnetic field parallel to the cylinder axis, currents are induced on each split ring and according to [Madrid-05]

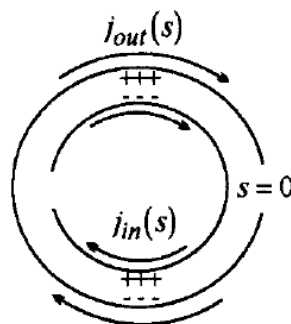


Fig. 1-8 Induced currents due to the applied magnetic field on a split ring. Figure taken from [Pendry-99].

1. A General Introduction to Metamaterials

and [Pendry-99], and the negative permeability effect may be achieved on a reduced frequency range. There is a problem with the structures based on cylinders, they have magnetic properties whether the field is aligned with the cylinder axis, but they also have a totally non-magnetic response if the field is in other directions. To avoid this limitation, a slice of the cylinders was cut as is shown in Fig. 1-8, and the sheet was thickened to recover the lost section of metal. In this manner, a compact structure whose magnetic effect is not lost when the field arrives in other directions was created. This structure is also known as Edge-Coupled Split Ring Resonator (EC-SRR) as indicated in Fig. 1-9a, and Fig. 1-9b shows its equivalent circuit model. The EC-SRR acts as a resonator, so it can be modeled by a tank circuit as indicated in Fig. 1-9b, where L_s represents the inductive behavior introduced by the conductors that creates the split-rings, and C_s models the capacitive effect created by the separation d among the rings and the splits of each ring. The EC-SRR is the first non-magnetic structure that provides negative values of magnetic permeability when it is implemented on arrays of periodic elements [Ballesta-07] (see Fig. 1-7a). According to [Caloz-06] the EC-SRR can be excited by an axial variable magnetic field parallel to the Z axis or by a variable electric field polarized in the Y axis. The magnetic field could be external to the media, or can also be propagated by a coplanar line. These fields will induce a current in each ring, that current will not be able to complete the circuit of each ring due to the apertures at the left and right side of each ring as indicated in Fig. 1-9a. So those currents are going from one ring to the other by the displacement current of the distributed capacitance between them. This means that the larger the capacitance between the rings, the larger the

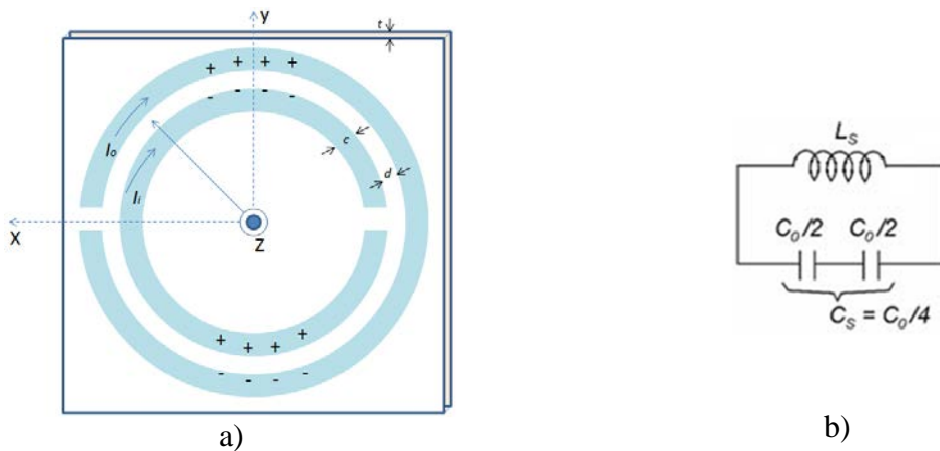


Fig. 1-9 Edge-coupled split ring resonator: a) scheme of an edge coupled split-ring resonator, b) electric model as a tank circuit. Figure taken from [Ballesta-09].

1. A General Introduction to Metamaterials

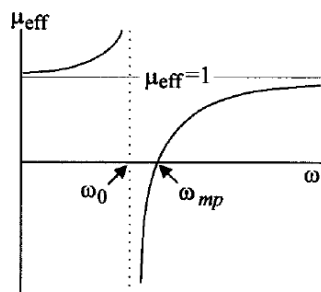


Fig. 1-10 The effective magnetic permeability of the model of the structure created by John Pendry, showing resonant values dictated by the capacitance between the sheets and the magnetic inductance of the cylinder. Below the resonant frequency μ_{eff} is enhanced, but above the resonance, μ_{eff} is less than unity and may be negative close to the resonance value. Figure taken from [Pendry-99].

current flux among them. According to the analysis in [Madrid-05] and [Pendry-99], the circulating current induces on its part a magnetic field which can lead to an effective negative permeability [Rincón-07] ($\mu < 0$) in a small frequency range, just above the resonance frequency (but close to it), and below the magnetic plasma frequency [Pendry-99] as is shown in Fig. 1-10.

An example of the metamaterial unit-cell with both permittivity and permeability negative values in a reduced bandwidth, is shown in the Fig. 1-11a. Similarly to the first metamaterial structure in Fig. 1-2, we can use a periodic structure as indicated in Fig. 1-11b. According to the simulations in [Lippens-04], it is possible to have an electric field along the wire, and provide a similar effect in one direction, which can work as a common interconnection case (see Fig. 1-12b). As indicated in Fig. 1-12a, the unit-cell needs to obey the microstructure principle. The EC-SRR and wire dimensions must be properly designed to ensure $\mu < 0$ and $\varepsilon < 0$ simultaneously in a reduced bandwidth of interest.

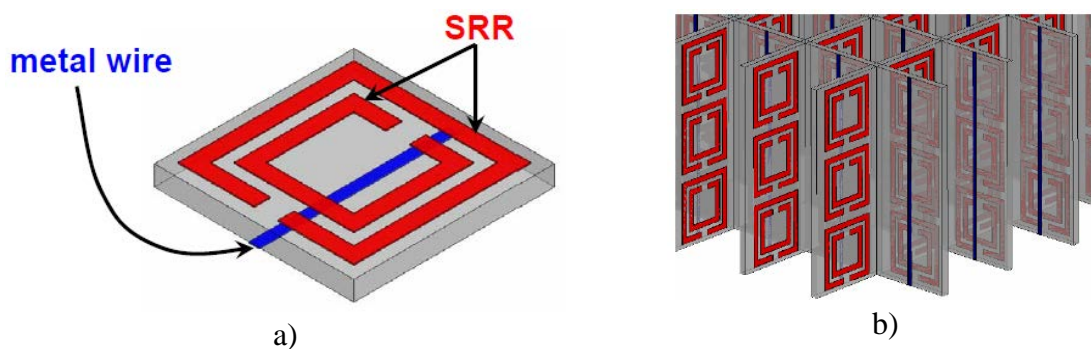


Fig. 1-11 SRR implementation example: a) SRR based LHM unit cell, the metal wire provides $\varepsilon < 0$, and the SRR at resonance frequency provides $\mu < 0$; b) periodic structure with both negative properties ($\varepsilon < 0$ and $\mu < 0$) simultaneously. Figure taken from [Lai-04].

1. A General Introduction to Metamaterials

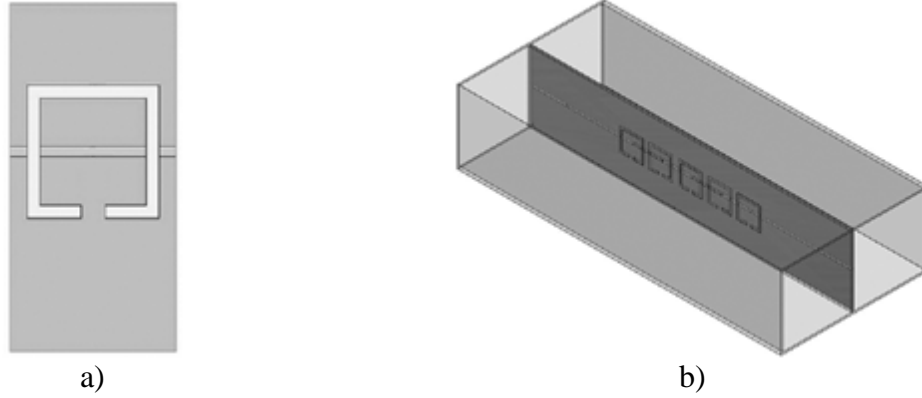


Fig. 1-12 SRR implementation example: a) SRR based LHM unit cell, with both the metal wire and the SRR in the same substrate, b) periodic structure with five unit cells. Figure taken from [Decoopman-04].

1.5.1 Importance of Broad Bandwidth on Interconnections

Metamaterials based on EC-SRR and its variations seem of little practical interest for engineering applications with broad bandwidth because these structures are resonant, and consequently exhibit high loss and narrow bandwidth [Caloz-06]. In a resonator, the loaded quality factor (Q_l) is related with the unloaded quality factor (Q_u) and external quality factor (Q_e). In terms of losses, the total transmission loss (proportional to $1/Q_l$) through a resonator is equal to the sum of the dielectric/ohmic losses (proportional to $1/Q_u$) in the resonator, and the coupling losses (proportional to $1/Q_e$) in the transitions with the external circuits. This can be represented as following

$$\frac{1}{Q_l} = \frac{1}{Q_u} + \frac{1}{Q_e} \quad (1-3)$$

The loaded quality factor is a quantity that can be obtained directly from the measurement equipment from the magnitude of the transmission parameter (S_{21}) as

$$Q_l = \frac{f_r}{B} \quad (1-4)$$

where f_r is the resonance frequency for $|S_{21}|$ response and B is the corresponding -3dB bandwidth (in Hz). On the other hand, the unloaded quality factor can be defined as following

$$Q_u = \omega \frac{\text{average_energy_stored_in_resonator}}{\text{power_dissipated_in_resonator}} \quad (1-5)$$

where ω is the angular frequency (rad/s). As can be seen from (1-3) and (1-4), there is trade-off

1. A General Introduction to Metamaterials

between bandwidth and the transmission level. Minimum transmission loss, or equivalently maximum Q_l , is achieved at the resonant frequency f_r , by minimizing the bandwidth B . Assuming that Q_u is maximized, good transmission characteristics can be obtained, but bandwidth is so restricted that a modulated signal, even with the modest bandwidth, cannot be transmitted without distortion through the resonant structure. Bandwidth can naturally be increased, but this immediately results in a decrease of Q_l according to (1-4). Due to this weakness of the resonant-type metamaterial, an alternative architecture is needed for metamaterial structures with broad bandwidth.

1.6. Transmission Line (TL) Approach to Implement Metamaterials

Propagation of waves with antiparallel phase and group velocity is not a new phenomenon. Originally the backward wave concept was introduced by Brillouin and Pierce in the late 1940s. For Brillouin, the backward waves referred to the negative space harmonics contributing in the Fourier series expansion of fields in periodic structures [Caloz-06]. Meanwhile, for Pierce et al. backward waves were related to the phenomenon of backward amplification in traveling wave tubes [Caloz-06]. They used the circuit shown in Fig. 1-13, as the equivalent circuit for a line supporting a backward wave [Caloz-06], [Cripps-06]. As we can see, it is the dual of the conventional right-handed TL model shown in Fig. 1-14.

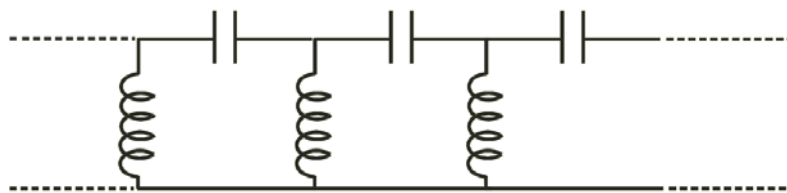


Fig. 1-13 Equivalent circuit model for a transmission line supporting a backward wave. Figure taken from [Cripps-06].

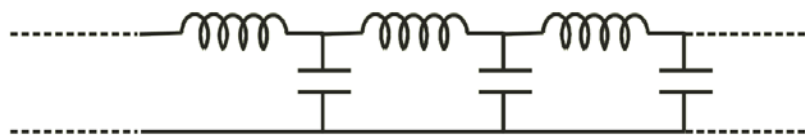


Fig. 1-14 Equivalent circuit model for a right-handed transmission line. Figure taken from [Cripps-06].

1. A General Introduction to Metamaterials

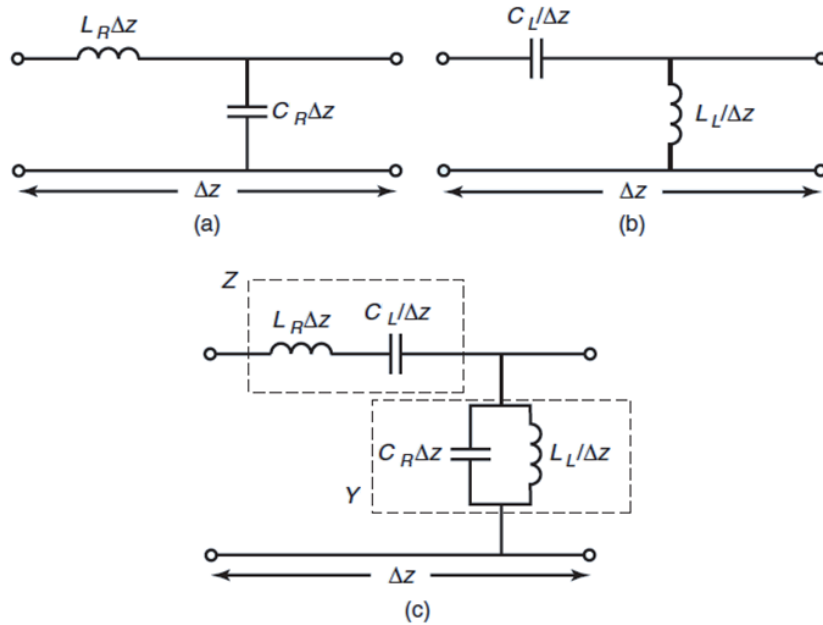


Fig. 1-15 Equivalent circuit models for: a) purely right-handed TL (PRH TL), b) purely left-handed TL (PLH), c) composite right/left handed TL (CRLH TL). Figure taken from [Lai-04].

The conventional or purely right-handed (PRH) transmission line model [Caloz-06] shown in Fig. 1-15a, can be represented as a combination of a per-unit length series inductance L_R (H/m) and a per-unit length shunt capacitance C_R (F/m). On the other hand, a purely left-handed (PLH) model [Caloz-06] shown in Fig. 1-15b, is the combination of a times-unit length series capacitance C_L (F×m), and a times-unit length shunt inductance L_L (H×m). As can be observed one model is the dual of the other one.

In reality, a PLH structure is not physically possible because RH parasitic series inductance (L) and shunt capacitance (C) effects cannot be avoided. The parasitic shunt capacitance is due to development of voltage gradients in the real dielectric structure, and the parasitic series inductance is due the current flow along the metallization [Lai-04]. For these reasons, a composite right/left-handed (CRLH) model, shown in Fig. 1-15c, represents the most general and realistic equivalent circuit model of a structure with LH attributes (neglecting losses).

At low frequencies, L_R and C_R tend to behave as short and open circuits, respectively, so that the equivalent circuit is essentially reduced to the series- C_L /shunt- L_L circuit, which has LH attributes [Caloz-06]. This LH circuit is of high-pass nature, therefore below a certain cutoff, a

1. A General Introduction to Metamaterials

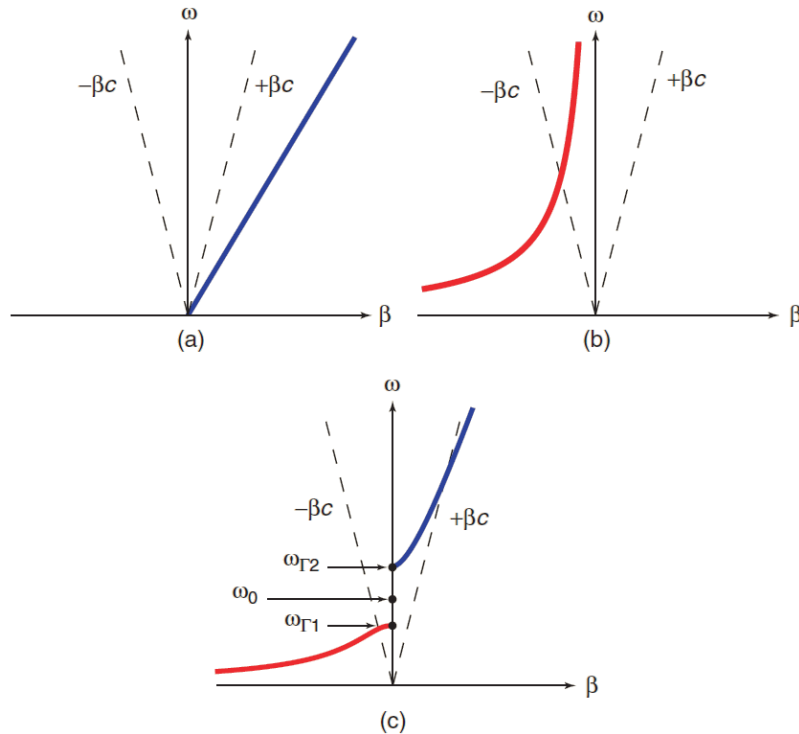


Fig. 1-16 Dispersion diagrams for the TLs in free space (c is the speed of light): a) homogeneous RH TL, b) homogeneous LH TL, c) homogeneous CRLH TL (unbalanced). Figure taken from [Lai-04].

LH stop-band is present. At high frequencies, C_L and L_L tend to be short and open, respectively, so that the equivalent circuit is essentially reduced to the series- L_R /shunt- C_R circuit, which corresponds to a conventional lossless transmission line [Caloz-06]. This RH circuit is of low-pass nature, therefore above a certain cutoff, a RH stop-band is present.

The dispersion diagram of the PRH and PLH circuits are shown in Fig. 1-16a and Fig. 1-16b respectively. The series resonance $\omega_{\Gamma 1}$ and shunt resonance $\omega_{\Gamma 2}$ are different, so that a gap exists between the LH and the RH ranges, as shown in Fig. 1-16c. However, if these resonances are made equal, or are balanced, this gap disappears and an infinite-wavelength propagation [Caloz-06] is achieved at the transition frequency ω_0 , as shown in Fig. 1-17b. Although a CRLH structure has both a LH range and a RH range, the dispersion curve in each of these ranges significantly differs from that of the PLH and PRH structures, respectively, because of the combined effects of LH and RH contributions at all frequencies (see Fig. 1-16 and Fig. 1-17b).

There are two possible implementations for approximating the CRLH model [Lai-07]: one with discrete components as indicated in Fig. 1-18b, and the other one with distributed components as indicated in Fig. 1-18c.

1. A General Introduction to Metamaterials

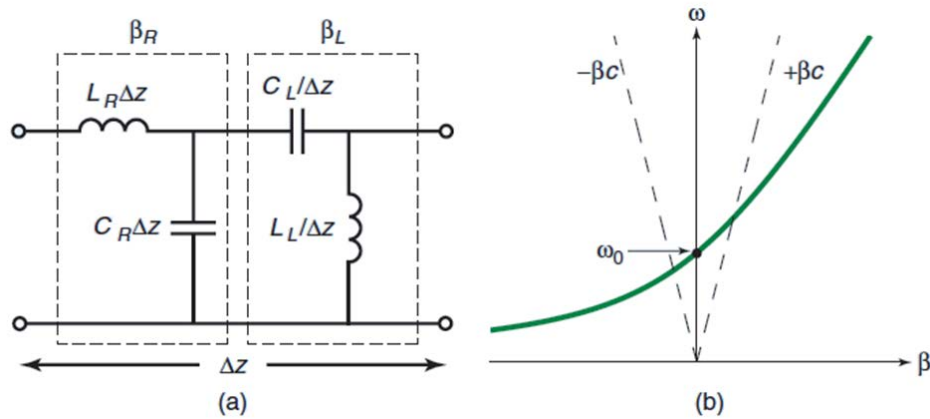


Fig. 1-17 Balanced form of CRLH TL: a) Simplified equivalent circuit model, b) Dispersion diagram showing seamless LH to RH transition. Figure taken from [Lai-04].

When the CRLH model is physically implemented using lumped elements, it has the working frequency limited by each lumped component's equivalent circuit, both the capacitance and the inductance. In other words, at relatively high frequencies the parasitic values of each lumped element can reassert and modify the resultant capacitive and inductive equivalent values. The main advantage of the lumped implementation is that, whether a capacitance and inductance value needs to be slightly different than current implementation, it does not require a major

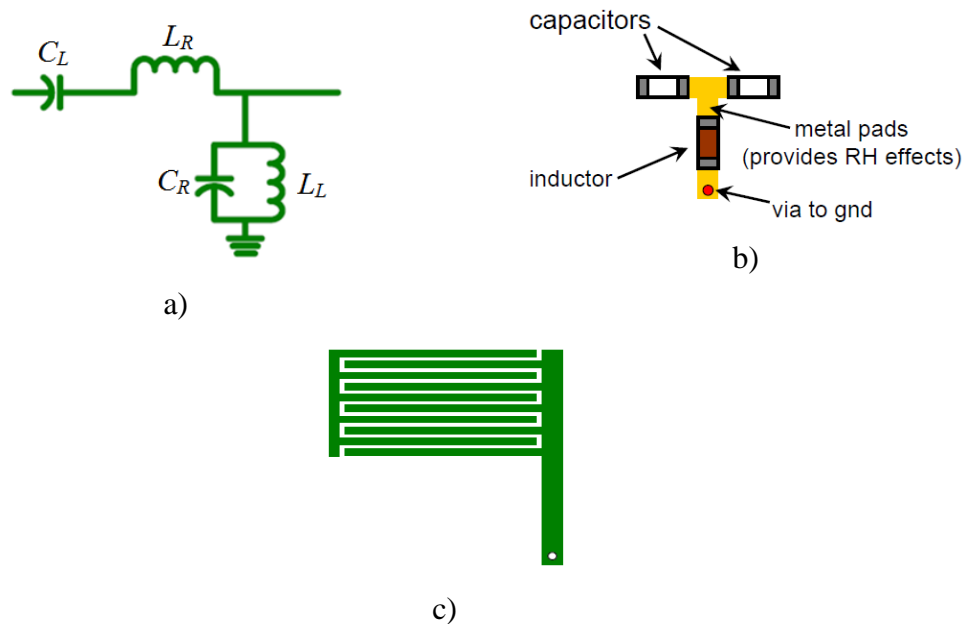


Fig. 1-18 Composite right/left-handed TL model implementation: a) CRLH TL circuit model, b) lumped element implementation, c) distributed microstrip implementation based on interdigital capacitor. Figure taken from [Lai-04].

1. A General Introduction to Metamaterials

design change. In some cases is just a matter of changing the discrete elements. On the other hand, if the CRLH model is physically implemented in distributed manner, as shown in Fig. 1-18c, it has a much higher frequency limit. The inductive and capacitive values are obtained from the geometrical shape and material properties. A consequence of these implementations is that, if the capacitance or inductance per-unit length values require a slight change, a major change on the physical implementation must be done. Although the lumped component solution may be apparently easier to implement physically, the lumped solution is valid only on relatively mid-low-frequencies. Most of the interconnection cases require broad bandwidth, which in general are in the high-frequency range.

1.7. Conclusions

The basic concepts of metamaterials, and also the effects of the main properties that produce the left-handed behavior were explained in this chapter. The microstructure concept and its importance for artificial structures to create left-handed media, were explained. Two methodologies to create LH materials, as resonant and non-resonant structures, were introduced, including an example of each of these structures. The importance of having broad bandwidth in high-speed interconnections was briefly explained. The transmission line approach to LHM modeling as a non-resonant approach was explained, and also its advantages over the resonant approaches were highlighted.

2. Modeling a Right-Handed Transmission Line in Matlab

2.1. Introduction

A simple modeling procedure of a conventional (right-handed) transmission line (TL) using lumped element approximations is made in this chapter. The objective of this work is to develop a basic method for modeling transmission lines in Matlab, to be later applicable for left-handed transmission lines based on lumped element approximations.

It is explained in this chapter the methodology used to approximate the input impedance and voltage gain of a right-handed (RH) transmission line model. The corresponding *Matlab* implementations, and its results, are also described.

In Section 2.2 it is briefly reviewed the basic theory of conventional RH transmission line models. A number of exact theoretical results are used to validate the Matlab implementations. In Section 2.3 it is described the theoretical approach to obtain an iterative equation that approximates the input impedance response of a RH transmission line with N segments, as well as the Matlab implementation and corresponding numerical results. In Section 2.4 it is explained the theoretical approach to compute the voltage gain of the equivalent RH transmission line of N segments, and also its input impedance at the TL, by using the ABCD parameters of each lumped element. Finally, the conclusions and future work description are presented in Section 2.5.

2.2. Basic Theory of Right-Handed Transmission Line Model

A common transmission line can be implemented by a conductor-pair, as shown in Fig. 2-1 [Ludwig-00]. Many other physical types of transmission lines can be implemented, such as microstrip lines, coaxial cables, etc. In any case, the circuitual model of a transmission line can be represented as shown in the lower part of Fig. 2-1. The actual interconnect is modeled using an infinite number of R , L , C , and G sections, whose length tend to zero ($\Delta z \rightarrow 0$). In this case the energy propagation path from the source to the load is achieved through one conductor, and the

2. Modeling a Right-Handed Transmission Line in Matlab

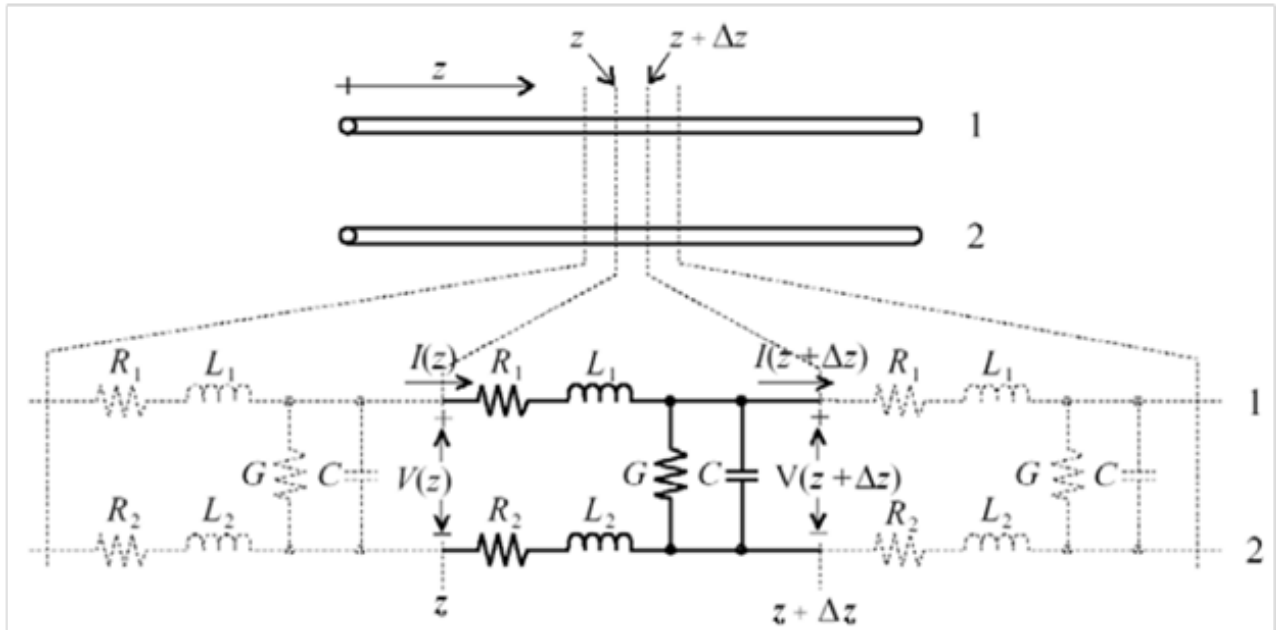


Fig. 2-1 Equivalent circuit for a transmission line indicating voltage and current definitions. Above are two conductors that represent a transmission line, as conductor 1 and 2; below is the equivalent circuit with lumped elements. Figure taken from [Pozar-05].

other conductor provides the return path for the energy. To simplify the analysis [Thierauf-04], it is possible to represent both inductances and resistances in a single component, respectively, as indicated in Fig. 2-2. In this case, all lumped elements are represented in per-unit-length values. The series inductance L represents the total self-inductance of the two conductors, including the return path, the shunt capacitance C is due to the close proximity of the two conductors. The series resistance R represents the resistance due to the finite conductivity of the conductor including its return path, and the shunt conductance G is due to the dielectric loss in the material between the conductors. A segment of a transmission line can be represented as a cascade of sections as that one shown in Fig. 2-2.

The way signals are propagated on a transmission line depends on the conductor's physical shape, the material properties, and the signal characteristics. For the conventional or right-handed transmission line, some of these properties can be explained by the complex propagation constant (γ) [Pozar-05], defined as

$$\gamma = \alpha + j\beta = \sqrt{(R + j\omega L)(G + j\omega C)} \quad (2-1)$$

where α represents the attenuation constant (losses), and β indicates the phase constant or propagation constant.

2. Modeling a Right-Handed Transmission Line in Matlab

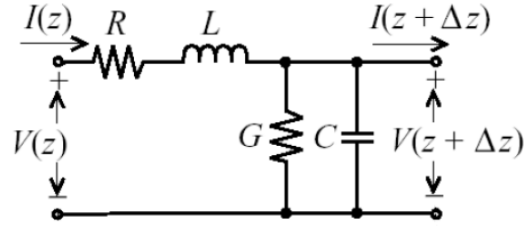


Fig. 2-2 Single TL segment with only one R and L to simplify calculations (as opposed to that one in Fig. 1). Figure taken from [Poazar-05].

The transmission line characteristic impedance can be defined as [Poazar-05],

$$Z_0 = \sqrt{\frac{R + j\omega L}{G + j\omega C}} \quad (2-2)$$

while the input impedance along a lossless transmission line [Poazar-05] is given by

$$Z_{in} = Z_0 \frac{Z_L + jZ_0 \tan \beta l}{Z_0 + jZ_L \tan \beta l} \quad (2-3)$$

where Z_L represents the load impedance, and l is the transmission line physical length.

Essentially, the quality of any signal being transmitted over a TL depends, among other factors, on the impedance mismatch. This mismatch can occur at the interconnection between the transmission line and the source, or between the transmission line and the load circuitry. These impedance differences produce signal reflections exactly where the impedance difference exists, and naturally, these reflections can be decreased by reducing the impedance mismatches.

The wavelength on the transmission line, λ , can be obtained as

$$\lambda = \frac{2\pi}{\beta} \quad (2-4)$$

The phase velocity v_p is related to the wavelength as follows

$$v_p = \lambda f = \frac{\omega}{\beta} \quad (2-5)$$

It is seen from (2-3) that $Z_{in} = Z_L$ when the transmission line length is a half wavelength ($l = \lambda/2$), regardless of the characteristic impedance used. Also, if the line is a quarter-wavelength long ($l = \lambda/4$), the transmission line's input impedance is related to the load impedance by

$$Z_{in} = \frac{Z_0^2}{Z_L} \quad (2-6)$$

The previous cases for the input impedance will be used for validating our results in the following section.

2. Modeling a Right-Handed Transmission Line in Matlab

2.3. Calculating the Input Impedance of a Right-Handed TL with N Segments

2.3.1 Theoretical Approach

The following approach to compute the input impedance from the transmission line's equivalent circuit is based on a recursive equation applied to a number of TL segments. The calculation considers a general lossy transmission line model. Fig. 2-3a shows the equivalent circuit of a TL considering only one segment, whose corresponding input impedance is given by

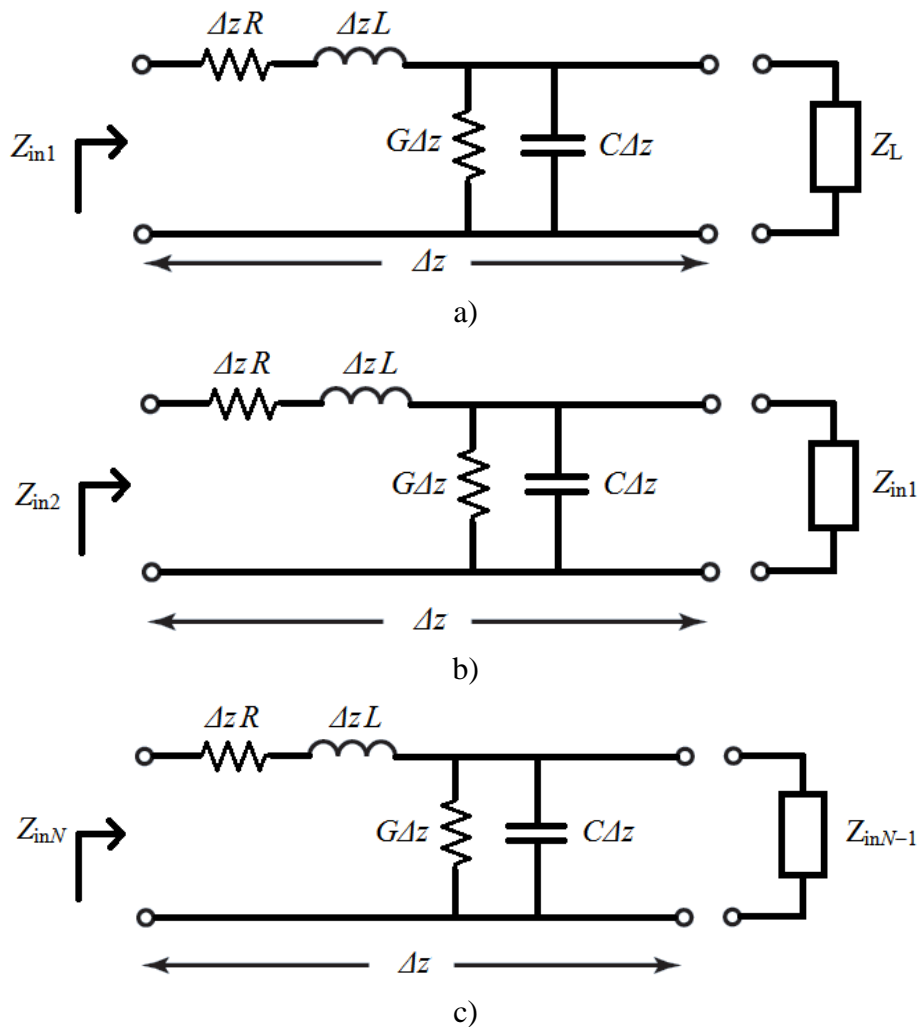


Fig. 2-3 Input impedance with N lossy TL segments: a) using only one lossy TL segment, b) using two lossy segments, and c) using N segments.

2. Modeling a Right-Handed Transmission Line in Matlab

$$Z_{in1} = R\Delta z + j\omega L\Delta z + \frac{1}{\Delta z G} \left\| \frac{1}{j\omega C\Delta z} \right\| Z_L \quad (2-7)$$

which can be reduced to

$$Z_{in1} = \Delta z(R + j\omega L) + \frac{Z_L}{Z_L j\omega C\Delta z + 1 + Z_L G\Delta z} \quad (2-8)$$

Fig. 2-3b shows the case of a TL with two cascaded segments. Its input impedance can be similarly calculated as

$$Z_{in2} = R\Delta z + j\omega L\Delta z + \frac{1}{\Delta z G} \left\| \frac{1}{j\omega C\Delta z} \right\| Z_{in1} \quad (2-9)$$

which can also be reduced to

$$Z_{in2} = \Delta z(R + j\omega L) + \frac{Z_{in1}}{Z_{in1} j\omega C\Delta z + 1 + Z_{in1} G\Delta z} \quad (2-10)$$

Generalizing the previous approach to N segments, a recursive equation can be written as follows

$$Z_{in(N)} = \Delta z(R + j\omega L) + \frac{Z_{in(N-1)}}{Z_{in(N-1)} j\omega C\Delta z + 1 + Z_{in(N-1)} G\Delta z} \quad (2-11)$$

```
function mZin = Zin(N,f,Tlength,R,G,L,C,ZL)
%Usage mZin = Zin(N,f,Tlength,R,G,L,C,ZL)
% N: number of transmission line segments.
% f: frequency of interest (in Hertz).
% Tlength: transmission line length (in meters).
% R: Resistance per-unit length in ohms/m.
% G: Conductance per-unit length in Seimens/m.
% L: Inductance per-unit length in Henrys/m.
% C: Capacitance per-unit length in Farads/m.
% ZL: Load impedance connected to the TL in Ohms.
% mZin: Magnitude of the input impedance for N segments (scalar).
%-----
j = sqrt(-1);
dz = Tlength/N;%Length of the Transmission line segments.
w = 2*pi*f;%Omega.
N = N+1;
Zin = ZL;
for k = 2:N
    Zin_old = Zin;
    Zin = dz*(R+j*w*L)+((Zin_old)/((j*w*C*dz*Zin_old)+1+Zin_old*G*dz));
end
mZin = abs(Zin);
```

Fig. 2-4 Matlab script used to compute the input impedance for N segments, using recursive as shown in (2-11).

2. Modeling a Right-Handed Transmission Line in Matlab

2.3.2 Implementation in Matlab

An example of a Matlab script for this computation is shown in Fig. 2-4. It is possible to use this code to compute the input impedance of a lossless TL by simply doing $R = G = 0$.

As a first example, consider a lossless case with $L = 0.3456 \mu\text{H/m}$, and $C = 0.1382 \text{ nF/m}$. This corresponds to $Z_0 = 50 \text{ ohms}$, and considering that $Z_L = 50 \text{ ohms}$, it is confirmed in Fig. 2-5a that as we increase N , the magnitude of the input impedance is closer to 50 ohms.

Fig. 2-5b shows a second example using a lossy case, where $R = 0.2 \Omega/\text{m}$, $G = 0.1 \text{ Siemens/m}$, $L = 0.3456 \mu\text{H/m}$, $C = 0.1382 \text{ nF/m}$, and $Z_L = 50 \text{ ohms}$. It is also confirmed that Z_{in} is closer to 50 ohms as we increase N .

The Z_{in} approximation for both lossless and lossy cases, in general also depends on the transmission line length [Pozar-05]. The third example shows a lossless case similar to the first one but considering only 96 segments, and $Z_L = 30 \text{ ohms}$. In this case the transmission line length is 0.1809 m long, which according to (2-1) and (2-4) corresponds to a quarter-wavelength line at $f = 200 \text{ MHz}$; and also corresponds to a half-wavelength line at 400 MHz, as confirmed in Fig. 2-6. The input impedance obeys (2-6) and (2-3), hence $Z_{\text{in}} = (50)2/30 = 83.33 \text{ ohms}$ at 200 MHz, and similarly $Z_{\text{in}} = Z_L = 30 \text{ ohms}$ at 400 MHz, as confirmed also in Fig. 2-6.

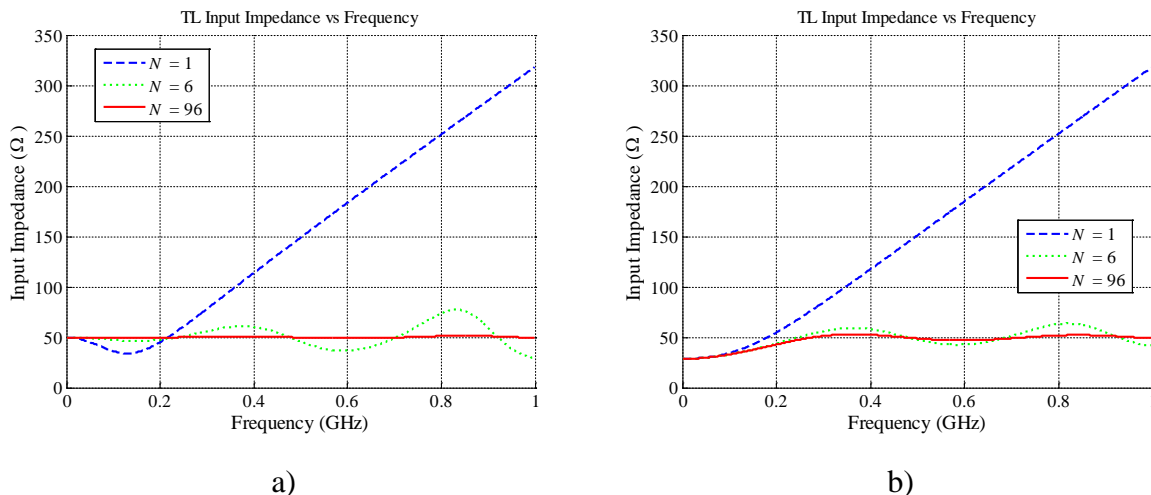


Fig. 2-5 Input impedance of a transmission line using 1, 6 and 96 segments, where $Z_0 = Z_L = 50 \Omega$ and 0.15 m long: a) for the lossless case where $L = 0.3456 \mu\text{H/m}$, $C = 0.1382 \text{ nF/m}$, b) for the lossy case where $R = 0.2 \Omega/\text{m}$, and $G = 0.1 \text{ Siemens/m}$, $L = 0.3456 \mu\text{H/m}$, and $C = 0.1382 \text{ nF/m}$.

2. Modeling a Right-Handed Transmission Line in Matlab

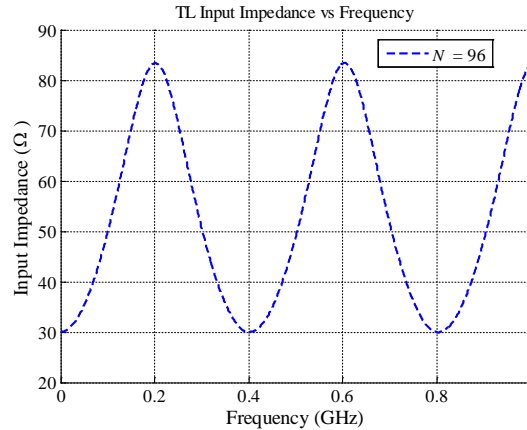


Fig. 2-6 Input impedance of a lossless transmission line 0.1809 m long, approximated by 96 segments, with $L = 0.3456 \mu\text{H/m}$, $C = 0.1382 \text{ nF/m}$, and $Z_L = 30 \text{ ohms}$.

The presented examples shows that the proposed Matlab script shown in Fig. 2-4 makes a good approximation of the basic transmission line theory as we increase the number of segments.

2.4. Calculating the Gain and Input Impedance of a Transmission Line with N Segments using ABCD Parameters

2.4.1 Theoretical Approach to Compute the Gain

An iterative procedure to obtain the voltage gain on a transmission line with N segments is developed. ABCD parameters are used to compute the voltage gain of the circuit shown in Fig. 2-7, since the output of one segment can feed the input of the next segment, to finally obtain the relation V_o/V_i . The three main elements are the load impedance, the transmission line itself, and the source impedance.

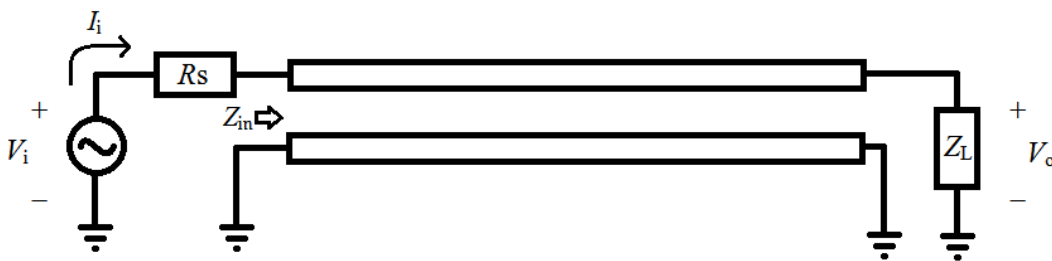


Fig. 2-7 Elements on the approximation of the voltage gain (V_o/V_i): source resistor (R_s), transmission line, and load impedance (Z_L).

2. Modeling a Right-Handed Transmission Line in Matlab

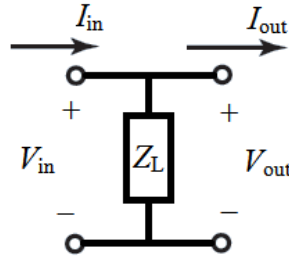


Fig. 2-8 Voltages and currents at the load segment required for the ABCD parameters.

The ABCD parameters of each element are obtained based on their electrical models shown in Fig. 2-8 to Fig. 2-10. By using ABCD parameters, it is possible to use the output voltages/currents from one segment, to feed the input voltages/currents of the next segment, and so on. Fig. 2-11 represents an example of this idea, the ABCD parameters of the load impedance (Z_L) represented as segment 0, the ABCD parameters of the transmission line represented with two segments (1 and 2 in this case), and the ABCD parameters of the source impedance (R_S) represented as the third segment.

The analysis starts from the load element towards the source's series impedance and through the transmission line model. In case of the transmission line segments, a cumulative

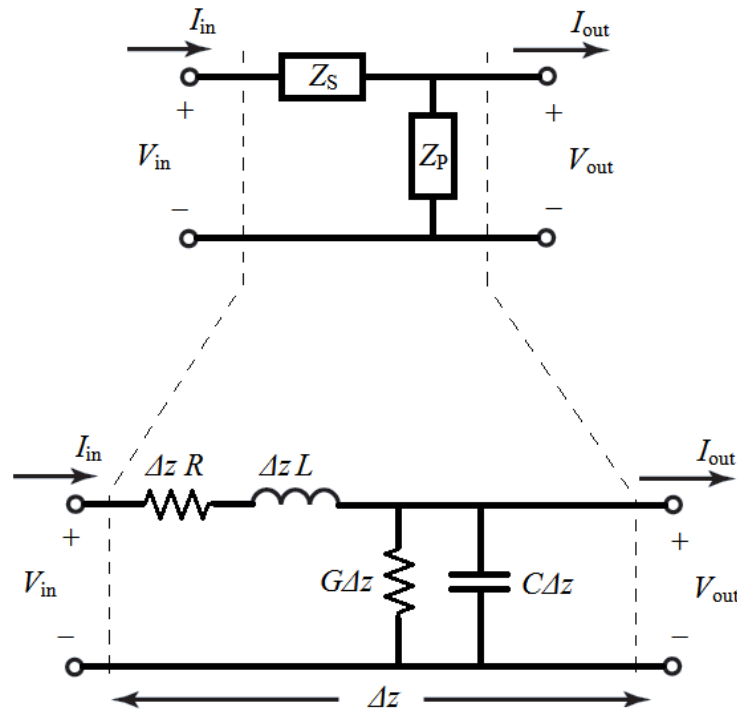


Fig. 2-9 Voltages and currents of each transmission line segment according to the ABCD parameters, and series and parallel impedances Z_S and Z_P representing the corresponding lumped elements of the TL segment.

2. Modeling a Right-Handed Transmission Line in Matlab

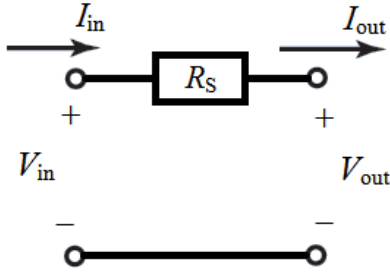


Fig. 2-10 Voltages and currents of the series resistor at the generator side according to the ABCD parameters.

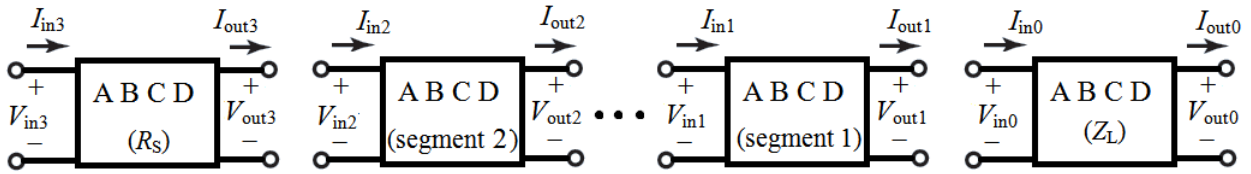


Fig. 2-11 Cascaded segments by using the transmission matrix (ABCD) for each of the elements, such as Z_L , the transmission line with 2 segments, and the generator's series resistor (R_S).

computation is achieved considering N transmission line segments (in case of Fig. 2-11, $N = 2$).

As an example to obtain ABCD parameters, consider the case of the load impedance Z_L . This element can be modeled as an isolated passive impedance in shunt connection. Its input/output voltages and currents in the ABCD parameters scheme are shown in Fig. 2-8. The equivalent equations of such element are

$$\begin{aligned} V_{in} &= AV_{out} + BI_{out} \\ I_{in} &= CV_{out} + DI_{out} \end{aligned} \quad (2-12)$$

To find the A and C parameters it is important to remember that no current is flowing in the output direction, since $I_{out} = 0$. The relation between the input and output voltages in (2-12) are re-written as

$$V_{in} = AV_{out} \quad (2-13)$$

From Fig. 2-8 it is seen that $V_{in} = V_{out}$. Hence, $A = 1$. Similarly, the relationship between the input current and output voltage is

$$I_{in} = CV_{out} \quad (2-14)$$

According to (2-14), and Ohm's law in Fig. 2-8, the C parameter value corresponds to the inverse of Z_L , $C = 1/Z_L$.

2. Modeling a Right-Handed Transmission Line in Matlab

The B and D parameters can be obtained by doing $V_{\text{out}} = 0$, imposing a short circuit on port 2. Hence the B parameter is written as

$$V_{\text{in}} = BI_{\text{out}} \quad (2-15)$$

Under this condition (see Fig. 2-8), the input and output currents are the same, $I_{\text{out}} = I_{\text{in}}$. The current goes through the least resistance path (short circuit) and $B = V_{\text{in}}/I_{\text{in}}$. Since $V_{\text{out}} = 0 = V_{\text{in}}$, we find by solving (2-15) that $B = 0$.

The relationship between the input and output currents is represented by the D parameter as

$$I_{\text{in}} = DI_{\text{out}} \quad (2-16)$$

Since the input and output currents are the same, we find that $D = 1$.

In summary, the ABCD parameters for the load segment (see Fig. 2-8) are

$$\begin{bmatrix} V_{\text{in}} \\ I_{\text{in}} \end{bmatrix} = \begin{bmatrix} A & B \\ C & D \end{bmatrix} \begin{bmatrix} V_{\text{out}} \\ I_{\text{out}} \end{bmatrix} = \begin{bmatrix} 1 & 0 \\ 1/Z_L & 1 \end{bmatrix} \quad (2-17)$$

A similar procedure [Pojar-05] can be followed to obtain the ABCD parameters of the rest of the components represented in Fig. 2-11. The ABCD parameter for a transmission line segment (see Fig. 2-9) is computed as follows

$$\begin{bmatrix} A & B \\ C & D \end{bmatrix} = \begin{bmatrix} 1 & Z_S \\ 0 & 1 \end{bmatrix} \begin{bmatrix} 1 & 0 \\ 1/Z_P & 1 \end{bmatrix} = \begin{bmatrix} 1 + \frac{Z_S}{Z_P} & Z_S \\ \frac{1}{Z_P} & 1 \end{bmatrix} \quad (2-18)$$

where Z_S and Z_P are

$$Z_S = \Delta z R + \Delta z j \omega L \quad (2-19)$$

$$Z_P = \frac{1}{\Delta z G + \Delta z j \omega C} \quad (2-20)$$

The ABCD parameter of the generator's series segment (R_S), according to Fig. 2-10, is

$$\begin{bmatrix} A & B \\ C & D \end{bmatrix} = \begin{bmatrix} 1 & R_S \\ 0 & 1 \end{bmatrix} \quad (2-21)$$

Once we have the ABCD parameter matrix for each element (see Fig. 2-11), we multiply the ABCD matrices for all segments. The resulting matrix of the transmission line in case of Fig. 2-11, for two transmission line segments, is computed as

2. Modeling a Right-Handed Transmission Line in Matlab

$$T_{NS} = \begin{bmatrix} 1 & R_S \\ 0 & 1 \end{bmatrix} \begin{bmatrix} 1 + \frac{Z_{S1}}{Z_{P1}} & Z_{S1} \\ \frac{1}{Z_{P1}} & 1 \end{bmatrix} \cdots \begin{bmatrix} 1 + \frac{Z_{SN}}{Z_{PN}} & Z_{SN} \\ \frac{1}{Z_{PN}} & 1 \end{bmatrix} \begin{bmatrix} 1 & 0 \\ 1/Z_L & 1 \end{bmatrix} \quad (2-22)$$

The general case for the transmission line's resulting matrix (T_{NS}) for N transmission line segments can be calculated as

$$T_{2S} = \begin{bmatrix} 1 & R_S \\ 0 & 1 \end{bmatrix} \begin{bmatrix} 1 + \frac{Z_S}{Z_P} & Z_S \\ \frac{1}{Z_P} & 1 \end{bmatrix} \begin{bmatrix} 1 + \frac{Z_S}{Z_P} & Z_S \\ \frac{1}{Z_P} & 1 \end{bmatrix} \begin{bmatrix} 1 & 0 \\ 1/Z_L & 1 \end{bmatrix} \quad (2-23)$$

Finally the resulting equation is

$$\begin{bmatrix} V_i \\ I_i \end{bmatrix} = T_{NS} \begin{bmatrix} V_o \\ 0 \end{bmatrix} = \begin{bmatrix} A_T & B_T \\ C_T & D_T \end{bmatrix} \begin{bmatrix} V_o \\ 0 \end{bmatrix} \quad (2-24)$$

It is seen from (2-24) that the total A parameter, A_T contains the relationship V_i/V_o , and its inverse contains the required voltage gain value,

$$A_v = \frac{1}{A_T} \quad (2-25)$$

2.4.2 Theoretical Approach to Compute the Input Impedance

Similarly to the voltage gain computation, the input impedance at the transmission line can also be approximated by using ABCD parameters. Based on (2-24), it is possible to know the total input impedance, including the source resistance, by knowing the interconnect input voltage and current, as follows

$$V_i = A_T V_o \quad (2-26)$$

$$I_i = C_T V_o \quad (2-27)$$

The input impedance indicated in Fig. 2-7 can be calculated from (2-26) and (2-27) as follows

$$Z_{in} = \frac{V_i}{I_i} - R_S = \frac{A_T}{C_T} - R_S \quad (2-28)$$

2. Modeling a Right-Handed Transmission Line in Matlab

2.4.3 Matlab Implementation

Fig. 2-12 shows an example of the Matlab script used to compute the voltage gain and input impedance. It contains an iterative process to compute the cumulative ABCD-parameter matrix for N transmission line segments.

Fig. 2-13a shows the magnitude of the input impedance of a lossless TL approximation, whose response is the same as the one shown in Fig. 2-5. This response confirms that the ABCD parameters approximation leads to the same response, as those obtained by the cumulative

```
function [mZin,mAv] = Av(N,f,Tlength,Rs,R,G,L,C,ZLoad)
%Usage [mZin,mAv] = Av(N,f,Tlength,Rs,R,G,L,C,ZLoad)
%   N:      Number of transmission line segments.
%   f:      Frequency of interest in Hertz.
%   Tlength: Transmission line length in meters.
%   Rs:     Source Impedance (ohms).
%   R:     Resistance per-unit length in ohms/m.
%   G:     Conductance per-unit length in Seimens/m.
%   L:     Inductance per-unit length in Henrys/m.
%   C:     Capacitance per-unit length in Farads/m.
%   ZLoad:  Load Impedance (in ohms).
%   mAv:   Magnitude of the Voltage Gain for N segments (scalar).
%   mZin:  Magintude of the Input Impedance at the TL input (scalar).
%-----
j = sqrt(-1);
%---ABCD-parameter matrix of the load resistor segment.
ABCD_ZLoad=[1 0;1/ZLoad 1];
dz = Tlength/N;% Length of the Transmission line segments.
w = 2*pi*f;
%---ABCD-parameters for each TL segment
A = 1+(dz*R+dz*j*w*L)*(G*dz+j*w*C*dz);
B = (dz*R+dz*j*w*L);
C = G*dz+j*w*C*dz;
D = 1;
ABCD_TL=[A B;C D];
%---Iterative procedure to compute the ABCD matrix for N
%---transmission line segments.
if N>=2
    ABCD_TL_old=ABCD_TL;
    for i=2:N
        ABCD_TL_new=ABCD_TL*ABCD_TL_old;
        ABCD_TL_old=ABCD_TL_new;
    end
    ABCD_TL=ABCD_TL_new;
end
%---ABCD-parameters matrix of the Rs element.
ABCD_RS=[1 Rs;0 1];
%---Computing the Transmission Line Resultant Matrix for all segments,
%---considering also a transmission line with N segments.
TLRM=ABCD_RS*ABCD_TL*ABCD_ZLoad;
Av_inv=TLRM(1,1);
%---Obtaining the magnitude of the voltage gain.
mAv = 1/abs(Av_inv);
%---Obtaining the magnitude of the input impedance at the TL input.
mZin= abs((TN(1,1)/TN(2,1))-Rs);
```

Fig. 2-12 Matlab script used to compute the magnitude of the voltage gain of a simple transmission line circuit with load and source resistors.

2. Modeling a Right-Handed Transmission Line in Matlab

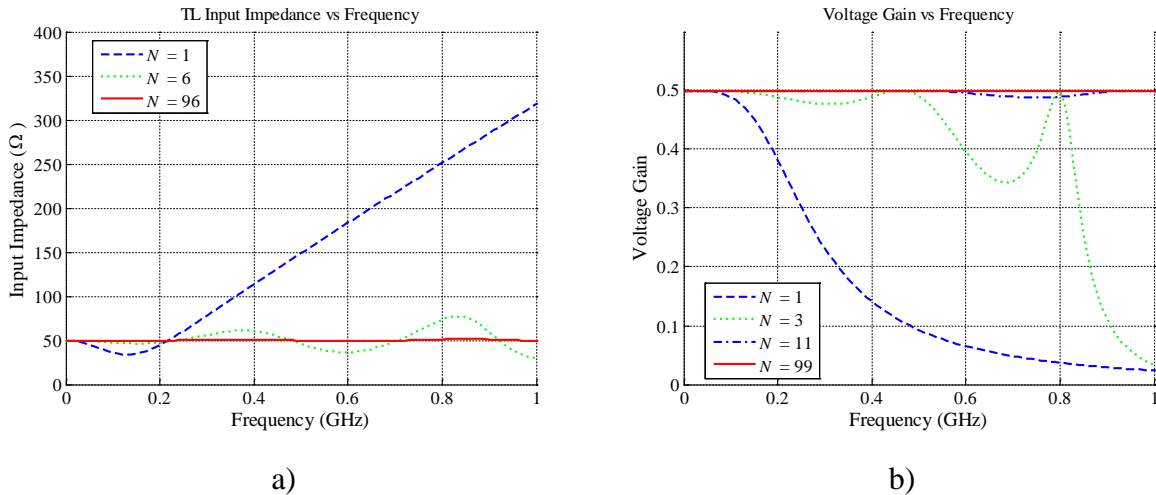


Fig. 2-13 Matlab approximation of a lossless TL up to 1 GHz, for 1, 6 and 96 segments, when $Z_0 = Z_L = R_S = 50 \Omega$, and the TL length is 0.15 m: a) the magnitude of the input impedance at the transmission line, b) the voltage gain magnitude.

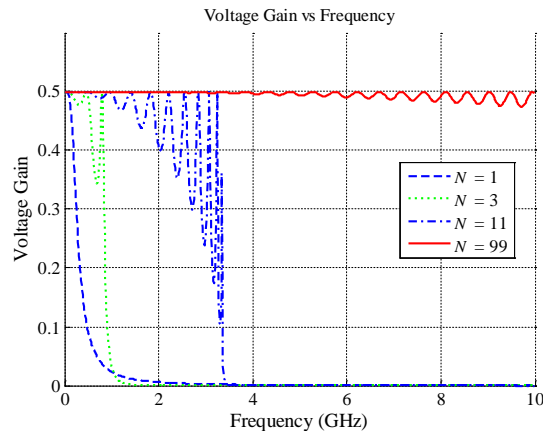


Fig. 2-14 Voltage gain magnitude approximation up to 10 GHz using 1, 3, 11, and 99 transmission line segments, when $R_S = 50$ ohms, $R = G = 0$, $Z_0 = Z_L = 50$ ohms.

analysis using the generalized input impedance equation described in Section 2.3.1.

Fig. 2-13b shows the magnitude of the voltage gain of a lossless TL approximation up to 1 GHz, when $R_S = Z_L = 50 \Omega$ for N TL segments. As can be observed in Fig. 2-7, since there is impedance matching on every circuit segment (generator's series resistor, load impedance, and the transmission line's characteristic impedance), the expected voltage gain magnitude is 0.5. It is shown in Fig. 2-13b this is true as we increase the number of segments.

The number of segments used to describe the response of any TL it is very important. For three TL segments, according to Fig. 2-13b, the voltage gain response differs from the expected

2. Modeling a Right-Handed Transmission Line in Matlab

value above 200 MHz. Similarly, for one TL segment, the response is only valid for less than 1 MHz. As observed in Fig. 2-13b, the best approximation between the four cases is given for 99 TL segments.

Fig. 2-14 shows the voltage gain magnitude of a lossless TL approximation up to 10 GHz for N segments, where $R_S = Z_L = 50$ ohms. Using 99 TL segments, the circuit response is relatively good up to 4GHz. But the response starts differing from the expected value ($A_v = 0.5$) at frequencies above 4GHz. In this case the logic should say that the improvement of the response can be also achieved by increasing the number of TL segments. But it is important to remember that modeling a transmission line based only on *RLGC* elements has some inherent limits due to the nature of the model itself. There are effects at very high frequencies that cannot be modeled by simple cascaded *RLGC* elements. Those can only be seen by doing electromagnetic simulations of the physical geometries in the transmission line itself, at the physical level.

2.5. Conclusions

Basic concepts of a conventional transmission line were presented to develop a simple model of the input impedance, and the voltage gain, using Matlab. The first input impedance approximation was computed considering the transmission line's lumped element model for N segments and load impedance. The second input impedance and the voltage gain approximations were computed by using the ABCD parameters of basic circuit elements, such as generator series resistor, the N TL segments considering its lumped element model, and the load impedance. These scripts can be used for lossless, low-loss and lossy cases. It was demonstrated that simple right-handed transmission line approximations can be achieved by using lumped element models in the low frequency range, where the RGLC transmission line model response is still valid.

Both approximations are presented looking forward to develop in the next chapter a similar basic model for the left-handed TL.

3. Modeling a Purely Left-Handed TL in Matlab with Equivalent Circuits

3.1. Introduction

As explained in Chapter 1, a metamaterial high-speed interconnect can also be modeled using an equivalent transmission line approach. The objective of this work is to develop a basic procedure to model purely left-handed transmission lines (TL) in Matlab, by using the lossless and lossy lumped element approximations. It is explained in this chapter a methodology used to approximate the input impedance, voltage gain, and the S-parameter magnitudes of a purely left-handed (PLH) transmission line. The corresponding Matlab implementations, and its results, are also described.

In Section 3.2, it is briefly reviewed the basic theory of purely left-handed transmission line models. A number of exact theoretical results from [Caloz-06] and [Caloz-02] are used to validate the Matlab implementations. In Section 3.3, it is described the theoretical approach to compute the input impedance, the voltage gain, and the S-parameters of a lossless PLH TL with N segments. Similarly, the same approximations using a lossy model of a purely left-handed TL with N segments are described in Section 3.4. The Matlab implementation and corresponding numerical results are also presented in Section 3.3 and Section 3.4. Finally, the conclusions and future work description are presented in Section 3.5.

3.2. Basic Theory of the Left-Handed Transmission Line Model

Transmission line theory is a powerful analysis and design tool for conventional materials. Fig. 3-1 shows an example of an ideal and homogeneous TL that is perfectly uniform. It is called ideal because it can transmit signals at all frequencies, from zero to infinity. It is uniform because it has invariant cross section along the direction of propagation. Although homogeneous TL are commonly used in RH transmission lines, such as coaxial or microstrip lines, for left-handed materials this is not possible because there are no available real

3. Modeling a Purely Left-Handed TL in Matlab with Equivalent Circuits

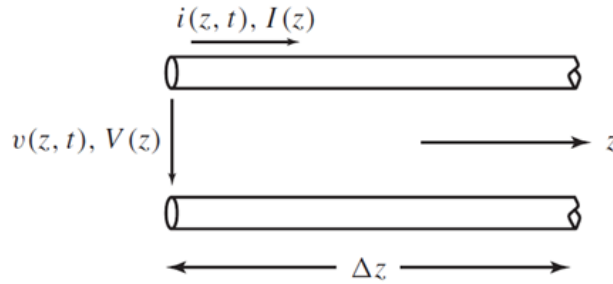


Fig. 3-1 Representation of an ideal (transmitting from $\omega = 0$ to $\omega = \infty$) homogeneous (perfectly uniform) TL in the form of its incremental model (length $\Delta z \rightarrow 0$) with time-domain or steady-state voltage/currents, $v(z,t) / i(z,t)$ or $V(z) / I(z)$, respectively. Figure taken from [Caloz-06].

homogeneous LH materials in nature [Caloz-06]. However, it is possible to construct effectively homogeneous artificial LH TL structures that mimic ideal TL in a restrictive range of frequencies. A difference between a perfectly homogeneous TL and an effective homogeneous TL is that in the former case we have an incremental length $\Delta z \rightarrow 0$, whereas in the latter case we have a finite Δz that satisfies [Caloz-06]

$$\Delta z \ll \lambda_g, \text{ (at least } \Delta z < \frac{\lambda_g}{4} \text{)} \quad (3-1)$$

where λ_g represents the guided wavelength and Δz is typically equal to the average unit cell size.

A purely left-handed TL can be modeled using an equivalent TL model [Caloz-02] as shown in Fig. 3-2, which is useful for the lossy and lossless cases. The series impedance (Z) and shunt admittance (Y) are represented as per-unit-length immittances. The per-unit length impedance Z (Ω/m) is constituted by a LH times-unit-length capacitance, C_L ($F \times m$), in parallel with its LH times-unit-length conductance, G_L ($S \times m$). Similarly, the per-unit-length admittance

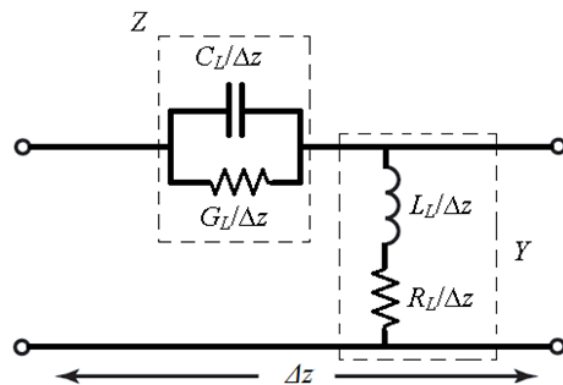


Fig. 3-2 Equivalent circuit model for a purely left-handed (PLH) transmission line, for both, lossy and lossless cases. Figure taken from [Caloz-02].

3. Modeling a Purely Left-Handed TL in Matlab with Equivalent Circuits

Y (S/m) is constituted by a LH times-unit-length inductance L_L (H×m) in series with a LH times-unit-length resistance R_L (Ω ×m). The left-handed parameters are presented as times-unit-length elements, to mathematically maintain Z and Y as per-unit-length immittances.

Similarly to the right-handed TL case, in the LH case the way the signals are propagated on a transmission line depends on the conductor's physical shape, the material properties of the artificial LH structure, and also depends on the signal characteristics. Some of these characteristics can be explained by the propagation constant (γ) [Caloz-06], defined as

$$\gamma = \alpha + j\beta = \sqrt{ZY} \quad (3-2)$$

where α represents the attenuation constant (losses), and β indicates the phase constant.

The characteristic impedance of a lossless PLH TL can be defined as [Caloz-06],

$$Z_0 = \sqrt{\frac{Z}{Y}} = +\sqrt{\frac{L_L}{C_L}} \quad (3-3)$$

where Z_0 is positive and depends on the LH parameters (L_L and C_L).

The phase constant of a lossless PLH TL can be defined as [Caloz-06],

$$\beta = -\frac{1}{\omega\sqrt{L_L C_L}} \quad (3-4)$$

where ω represents the angular frequency of the signal, and β is negative. This is different from the lossless right-handed (RH) case, which is positive [Pozar-05].

The phase velocity of a lossless PLH TL is defined as [Caloz-06],

$$v_p = \frac{\omega}{\beta} = -\omega^2\sqrt{L_L C_L} \quad (3-5)$$

where v_p is frequency-dependent, and is negative. This is different from the lossless RH case, which is constant and positive [Pozar-05].

The group velocity of a lossless PLH TL is defined as [Caloz-06],

$$v_g = \left(\frac{\partial\beta}{\partial\omega}\right)^{-1} = +\omega^2\sqrt{L_L C_L} \quad (3-6)$$

where v_g is associated with the direction of power flow, is always positive, and is frequency dependent.

As observed in (3-5) and (3-6), the group/phase velocities have the same magnitude, and they are anti-parallel as consequence of the LH properties. In the lossless left-handed case, the

3. Modeling a Purely Left-Handed TL in Matlab with Equivalent Circuits

group/phase velocities are frequency dependent. In the lossless right-handed case, the group/phase velocities are constant [Pozar-05].

The resulting PLH structure is a high-pass filter mimicking the LH transmission line in its band-pass. The cutoff frequency of this high-pass filter can be approximated as follows. In [Caloz-02] it is imposed that the transmission line segment is smaller than $\lambda_g/5$, although any other restriction could be selected to ensure (3-1). Hence, the validity range of the approximation can be estimated as [Caloz-02]

$$f > \frac{5}{(2\pi)^2 \sqrt{L_u C_u}} \quad (3-7)$$

where L_u and C_u are computed [Caloz-02] as follows

$$L_u = \frac{L_L}{l/N} \quad (3-8)$$

$$C_u = \frac{C_L}{l/N} \quad (3-9)$$

where l is the TL length, and N is the number of transmission line segments.

The approximation in (3-7) is valid for a small number of transmission line segments, although its generalization for $N \rightarrow \infty$ [Caloz-02] can be used to find the cutoff frequency, as follows

$$f_c \approx \frac{1}{4\pi \sqrt{L_u C_u}} \quad (3-10)$$

These approximations will be used later to validate the Matlab scripts developed in this chapter.

3.3. Lossless Model of a Purely Left-Handed Transmission Line

3.3.1 Theoretical Approach to Compute the Gain

Following a similar process to that one in Section 2.4.1, the voltage gain of a TL with N segments can be computed using its equivalent ABCD parameters (see Fig. 2-7 and Fig. 2-11). As explained in previous chapter, the main elements are the load impedance, the transmission line, and the source impedance. The circuitual model of a PLH TL is illustrated in Fig. 3-3.

3. Modeling a Purely Left-Handed TL in Matlab with Equivalent Circuits

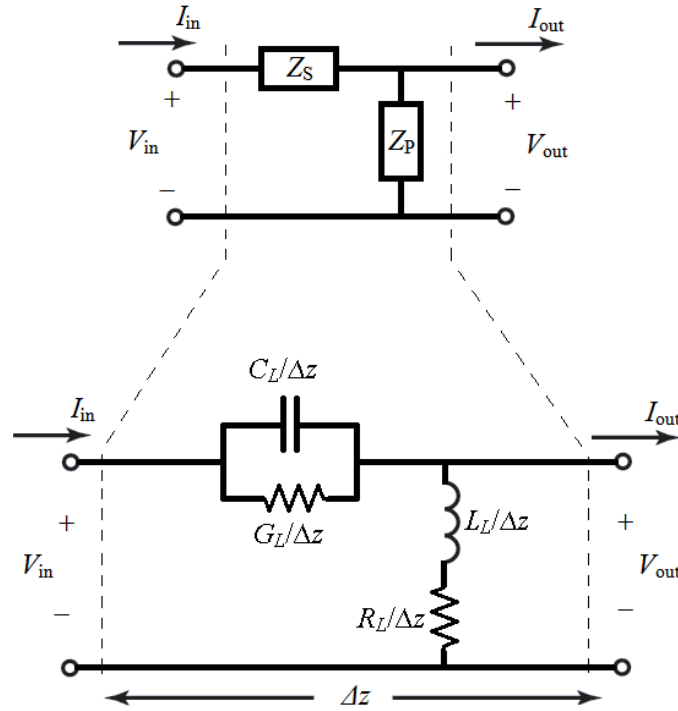


Fig. 3-3 Voltages and currents of each transmission line segment according to the ABCD parameters, and series and parallel impedances Z_S and Z_P representing the corresponding lumped elements of a PLH TL segment.

where Z_S and Z_P , for lossless PLH transmission lines, are

$$Z_S = \frac{\Delta z}{j\omega C_L} \quad (3-11)$$

$$Z_P = \frac{j\omega L_L}{\Delta z} \quad (3-12)$$

The ABCD parameter matrices for the load and the series impedances are the same as the ones used in Section 2.4.1. Once the equivalent Z_S and Z_P parameters for the PLH transmission line are properly defined in (2-22), the voltage gain response can also be obtained from (2-25).

3.3.2 Theoretical Approach to Compute the Input Impedance

Following a similar process to that one in Section 2.4.2, once the equivalent Z_S and Z_P parameters for the PLH transmission line are properly defined in (2-22), the input impedance can also be obtained from (2-28).

3. Modeling a Purely Left-Handed TL in Matlab with Equivalent Circuits

3.3.3 Theoretical Approach to Compute the S-parameters

According to [Pozar-05], once the transmission line's resulting ABCD matrix (T_{NS}) has been calculated, it is possible to compute the corresponding S-parameters as,

$$S_{11} = \frac{A + B/Z_{REF} - CZ_{REF} - D}{A + B/Z_{REF} + CZ_{REF} + D} \quad (3-13)$$

$$S_{12} = \frac{2(AD - BC)}{A + B/Z_{REF} + CZ_{REF} + D} \quad (3-14)$$

$$S_{21} = \frac{2}{A + B/Z_{REF} + CZ_{REF} + D} \quad (3-15)$$

$$S_{22} = \frac{-A + B/Z_{REF} - CZ_{REF} + D}{A + B/Z_{REF} + CZ_{REF} + D} \quad (3-16)$$

where the parameters A, B, C, D corresponds to A_T, B_T, C_T, D_T in (2-24), and Z_{REF} corresponds to the termination impedance at the ports, which usually is 50Ω .

```
function [Z0,SN11,SN12,SN21,SN22,mZin,mAv] = PLH_TL(N,f,Tlength,Rs,RL,GL,LL,CL,ZLoad)
%Usage [Z0,SN11,SN12,SN21,SN22,mZin,mAv] = PLH_TL(N,f,Tlength,Rs,RL,GL,LL,CL,ZLoad)
j = sqrt(-1);
ABCD_ZLoad=[1 0;1/ZLoad 1];%<-ABCD-Parameter of ZL.
dz = Tlength/N;%<-Length of each TL segments.
w = 2*pi*f;
%----ABCD-parameters for each PLH TL segment
ZS = dz/(j*w*CL+GL);
ZP = (j*w*LL+RL)/dz;
A = 1+ZS/ZP;
B = ZS;
C = 1/ZP;
D = 1;
ABCD_TL=[A B;C D];
%----Iterative procedure, the ABCD matrix for N transmission line segments.
if N>=2
    ABCD_TL_old=ABCD_TL;
    for i=2:N
        ABCD_TL_new=ABCD_TL*ABCD_TL_old;
        ABCD_TL_old=ABCD_TL_new;
    end
    ABCD_TL=ABCD_TL_new;
end
ABCD_RS=[1 Rs;0 1];%<-ABCD-Parameter matrix of Rs.
TN=ABCD_RS*ABCD_TL*ABCD_ZLoad;%<-Computing the Resultant Matrix for all segments.
Av_inv=TN(1,1);
mAv = 1/abs(Av_inv);%<-Obtaining the magnitude of the voltage gain.
mZin= abs((TN(1,1)/TN(2,1))-Rs);%<-Obtaining the magnitude of the Zin at the TL.
Z0=abs(sqrt(ZS*ZP));%<-Obtaining the magnitude of the TL's characteristic impedance
Z_Ref=50;%<-Reference impedance to compute S-parameters
[SN11,SN12,SN21,SN22] = ABCD2SPARAM(TN,Z_Ref);%<-Computing S-parameters from TN
```

Fig. 3-4 Cascaded segments by using the transmission matrix (ABCD) for each of the elements illustrated in Fig. 2-11.

3. Modeling a Purely Left-Handed TL in Matlab with Equivalent Circuits

3.3.4 Matlab Implementation

Fig. 3-4 shows the Matlab code used to compute A_v , Z_0 , and the S-parameters of the diagram illustrated in Fig. 2-7. As observed, a cumulative analysis across the TL elements in Fig. 2-11 is performed using the ABCD parameters. The LH parameters considered in the lossless case ($R_L = G_L = 0$) are: $L_L = 64 \text{ nH}\times\text{m}$, $C_L = 25.6 \text{ pF}\times\text{m}$, and the TL length is 10 m. The values are selected from [Caloz-02] to compare results with our Matlab implementation.

Fig. 3-5 shows the input impedance magnitude, $|Z_{in}|$, and it is observed that the response seems to be of high pass nature. At low frequencies the input impedance is above 400Ω , and as the frequency increases, the input impedance reaches the expected value, 50Ω . This is also valid as N increases, for 100 TL segments ($N = 100$) the input impedance response reaches 50Ω above 100 MHz.

Fig. 3-6a shows the voltage gain magnitude, and it is also observed the high pass nature. At very low frequencies the voltage gain magnitude is zero, after the cutoff the voltage gain magnitude starts to rise.

Fig. 3-6b shows the voltage gain within the 100 MHz range, according to (3-10) and having the LH parameters as indicated in [Caloz-02], for $N = 20$ ($L_{u20} = 128 \text{ nH}$, $C_{u20} = 51.2 \text{ pF}$), the expected cutoff frequency is $f_c = 31.08 \text{ MHz}$. Around this frequency the TL starts transmitting, and the voltage gain starts to rise towards the expected magnitude value, 0.5.

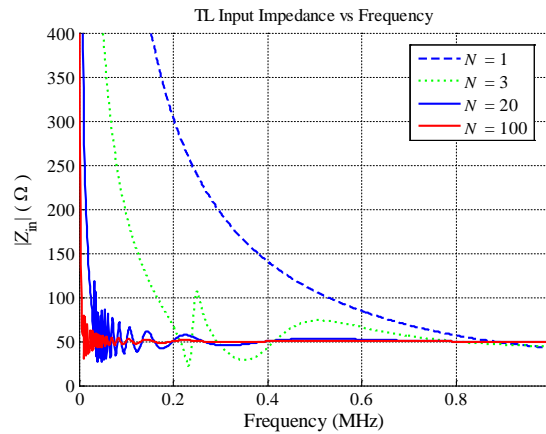


Fig. 3-5 Magnitude of the input impedance (Z_{in}) of a lossless transmission line using 1, 3, 20 and 100 segments. The TL parameters are $L_L = 64 \text{ nH}\times\text{m}$, $C_L = 25.6 \text{ pF}\times\text{m}$, $Z_0 = Z_L = 50 \text{ ohms}$ and 10 m long.

3. Modeling a Purely Left-Handed TL in Matlab with Equivalent Circuits

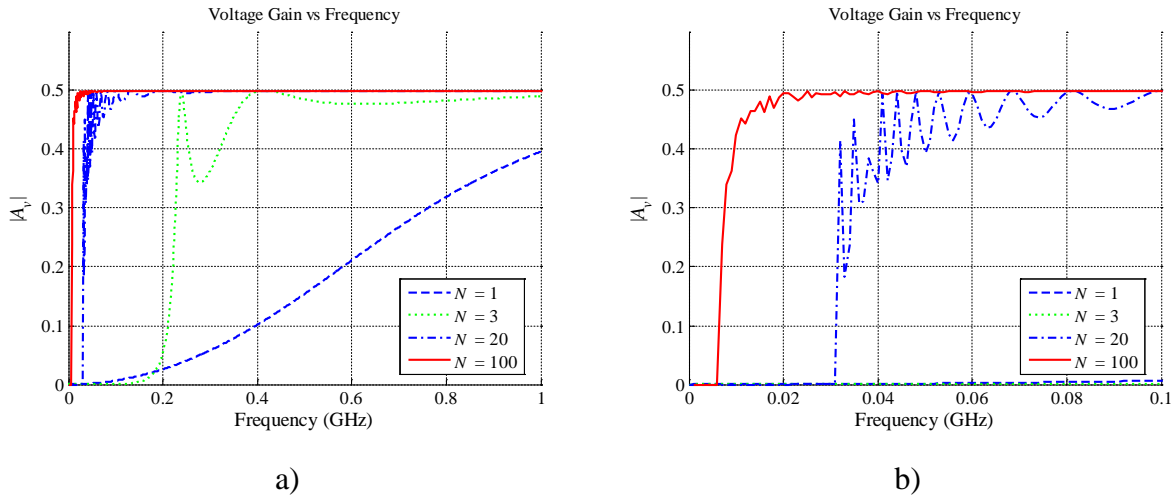


Fig. 3-6 Voltage gain magnitude, $|A_v|$, approximation up to 1 GHz using 1, 3, 20, and 100 transmission line segments, when $R_S = 50 \Omega$, $Z_0 = Z_L = 50 \Omega$: a) frequency up to 1 GHz, b) frequency up to 100 MHz.

In order to compare the Matlab approximation with the response in [Caloz-02], no series impedance exist at the source, and the TL termination is open circuit ($R_S = 0 \Omega$ and $Z_L = \infty \Omega$). Fig. 3-7a and Fig. 3-7b shows the Matlab approximation responses of $|S_{11}|$ and $|S_{21}|$, respectively, for N TL segments. It is seen that our responses are practically identical to the theoretically obtained responses in [Caloz-02] (see Fig. 3-8), for $N = 20$. Also it is observed, in Fig. 3-9, that the cutoff frequencies also coincides with [Caloz-02] for $N = 20$ and $N = 100$, where $f_c = 31.08$ MHz and $f_c = 6.21$ MHz, respectively.

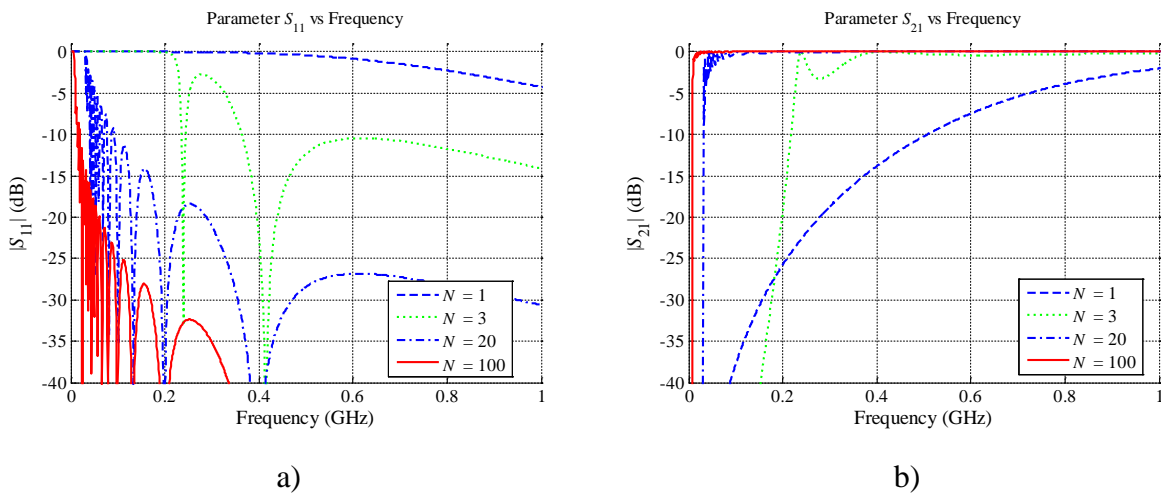


Fig. 3-7 The S-parameter response for a lossless transmission line using 1, 3, 20 and 100 segments, up to 1 GHz. $R_S = 0 \Omega$, and $Z_L = \infty \Omega$. The LH parameters are $L_L = 64$ nH \times m, $C_L = 25.6$ pF \times m, and 10 m long: a) the magnitude of S_{11} , b) the Magnitude of S_{21} .

3. Modeling a Purely Left-Handed TL in Matlab with Equivalent Circuits

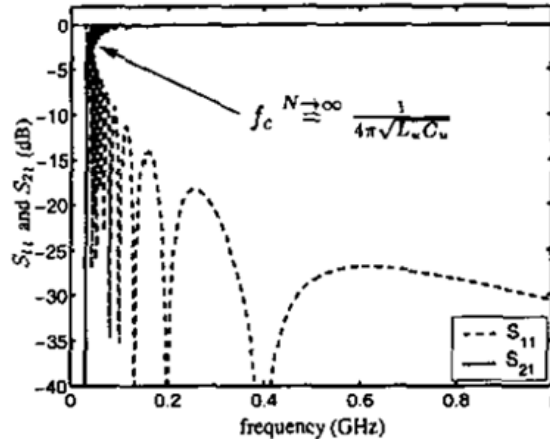


Fig. 3-8 Result for a lossless LH-TL with ideal lumped-elements in [Caloz-02]. Parameters: TL length = 10 m, $C_L = 25.6$ pF×m, and $L_L = 64$ nH×m. Figure extracted from [Caloz-02].

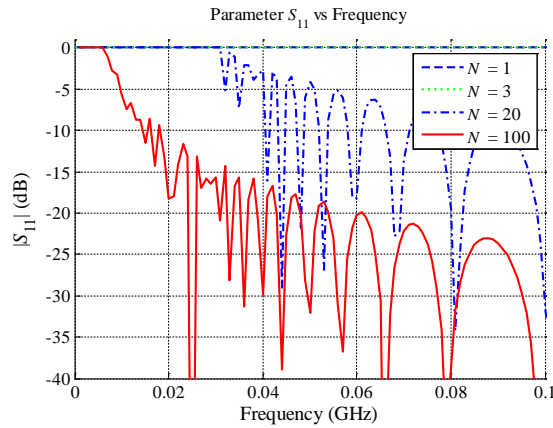


Fig. 3-9 Magnitude of S_{11} for a lossless PLH transmission line using 1, 3, 20 and 100 segments, up to 100 MHz. $R_S = 0$, and $Z_L = \infty$. The LH parameters are $L_L = 64$ nH×m, $C_L = 25.6$ pF×m, and 10 m long.

As observed in previous results, the proposed Matlab model provides excellent approximations for lossless purely left-handed transmission lines.

3.4. Lossy Model of the Purely Left-Handed Transmission Line

The voltage gain, input impedance, and S-parameter values for the lossy case are computed similarly to the procedure explained in Section 3.3. Now we take into account all the left-handed parameters: R_L , G_L , C_L , and L_L . Although the same script is used (see Fig. 3-4), now the transmission line model uses the lossy PLH parameters, hence, Z_S and Z_P are now

3. Modeling a Purely Left-Handed TL in Matlab with Equivalent Circuits

$$Z_s = \frac{\Delta z}{j\omega C_L + G_L} \quad (3-17)$$

$$Z_p = \frac{j\omega L_L + R_L}{\Delta z} \quad (3-18)$$

Hence, $|A_v|$ can also be obtained from (2-25), and the input impedance at the transmission line, Z_{in} , can be approximated from (2-28). Similarly, the S-parameters can also be computed using (3-13)-(3-16). Notice that, in order to compute the S-parameters, it is necessary the proper termination impedance at the input/output ports [Pozar-05], which are usually 50 Ω .

3.4.1 Characteristic Impedance for a Lossy PLH TL

The characteristic impedance of a LH transmission line is [Caloz-06],

$$Z_0 = \sqrt{\frac{Z}{Y}} \quad (3-19)$$

According to (3-17)-(3-18) and Fig. 3-2, the characteristic impedance would be,

$$Z_{0Lossy} = \sqrt{\frac{Z}{Y}} = \sqrt{\frac{\frac{1}{j\omega C_L + G_L}}{\frac{1}{j\omega L_L + R_L}}} = \sqrt{\frac{j\omega L_L + R_L}{j\omega C_L + G_L}} \quad (3-20)$$

were the lossy parameters in Fig. 3-2, (R_L , G_L), are considered. If those parameters are overridden, the lossy TL characteristic impedance (3-20) becomes the lossless TL characteristic impedance (3-3).

3.4.2 Matlab Implementation

Fig. 3-10 and Fig. 3-11 show the magnitudes of the input impedance, $|Z_{in}|$, and voltage gain, $|A_v|$, respectively. Current approximation was computed with the values: $L_L = 64 \text{ nH}\times\text{m}$, $C_L = 25.6 \text{ pF}\times\text{m}$, $R_L = 0.1 \text{ }\Omega\times\text{m}$, $G_L = 0$, and the TL length is 10 m. As can be observed, it seems that given the low resistive loss in the inductive element in shunt connection, there is a relatively low impact on the input impedance response. By comparing Fig. 3-11b and Fig. 3-6b, for $N = 100$, it is seen that low resistive loss, displaces the voltage gain's BW response a few Hertz to

3. Modeling a Purely Left-Handed TL in Matlab with Equivalent Circuits

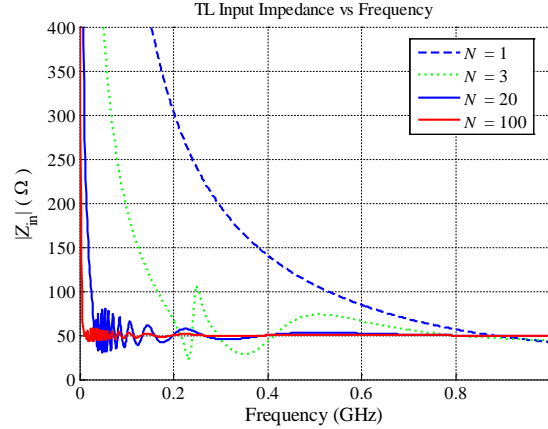


Fig. 3-10 Magnitude of the input impedance for a lossy TL for 1, 3, 20 and 100 segments, up to 1 GHz. $R_S = 50 \Omega$, $Z_L = 50 \Omega$. The LH parameters are $L_L = 64 \text{ nH} \times \text{m}$, $C_L = 25.6 \text{ pF} \times \text{m}$, $R_L = 0.1 \Omega \times \text{m}$, $G_L = 0$, and 10 m long.

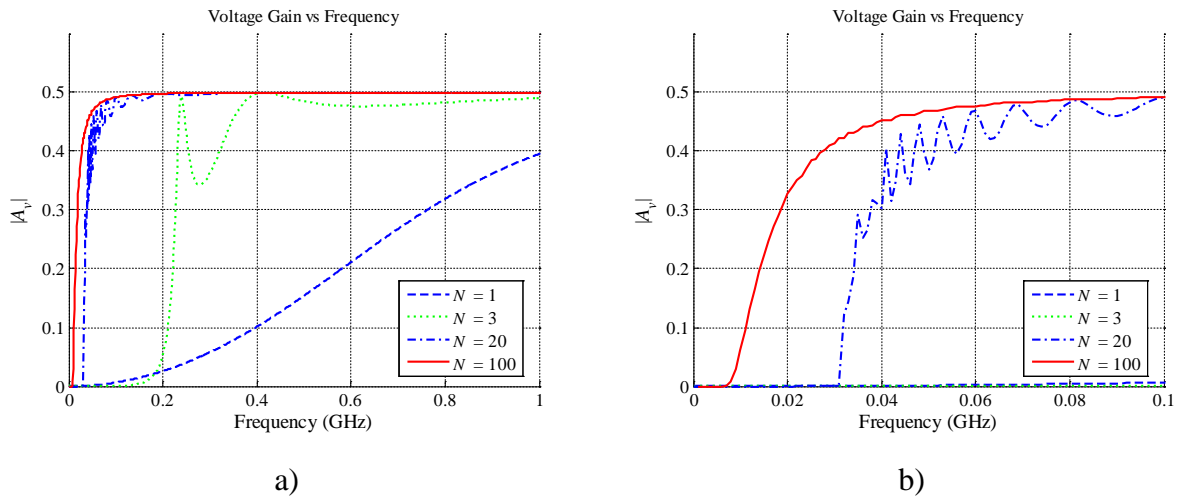


Fig. 3-11 Magnitude of the voltage gain for a lossy TL for 1, 3, 20 and 100 segments, up to 1 GHz. $R_S = 50 \Omega$, $Z_L = 50 \Omega$. The LH parameters are $L_L = 64 \text{ nH} \times \text{m}$, $C_L = 25.6 \text{ pF} \times \text{m}$, $R_L = 0.1 \Omega \times \text{m}$, $G_L = 0$, and 10 m long: a) frequency up to 1 GHz, b) frequency up to 100 MHz.

higher frequencies. Here, the voltage gain response reaches the expected value, 0.5, above 100 MHz (see Fig. 3-11b); while in the lossless case (see Fig. 3-6b), the voltage magnitude reaches the expected value, approximately at 40 MHz.

Fig. 3-12 and Fig. 3-13 show the magnitudes of the input impedance, $|Z_{in}|$, and voltage gain $|A_v|$, respectively. The Matlab approximation was computed with the following values: $L_L = 64 \text{ nH} \times \text{m}$, $C_L = 25.6 \text{ pF} \times \text{m}$, $R_L = 0$, $G_L = 0.01 \text{ S} \times \text{m}$, and the TL length is 10 m. At low frequencies, the Z_{in} response is smaller than that one for the lossless case (see Fig. 3-5).

3. Modeling a Purely Left-Handed TL in Matlab with Equivalent Circuits

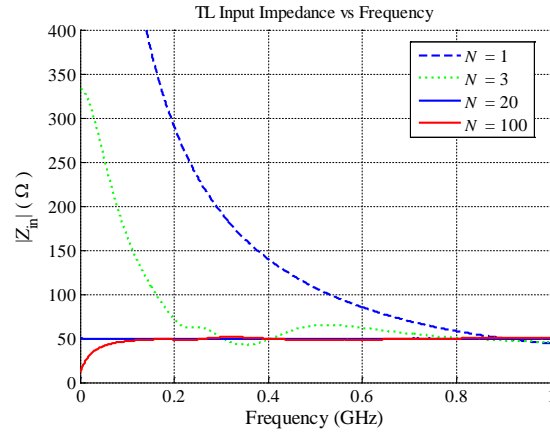


Fig. 3-12 Magnitude of the input impedance for a lossy TL for 1, 3, 20 and 100 segments, up to 1 GHz. $R_S = 50 \Omega$, $Z_L = 50 \Omega$. The LH parameters are $L_L = 64 \text{ nH}\times\text{m}$, $C_L = 25.6 \text{ pF}\times\text{m}$, $R_L = 0$, $G_L = 0.01 \text{ S}\times\text{m}$, and 10 m long.

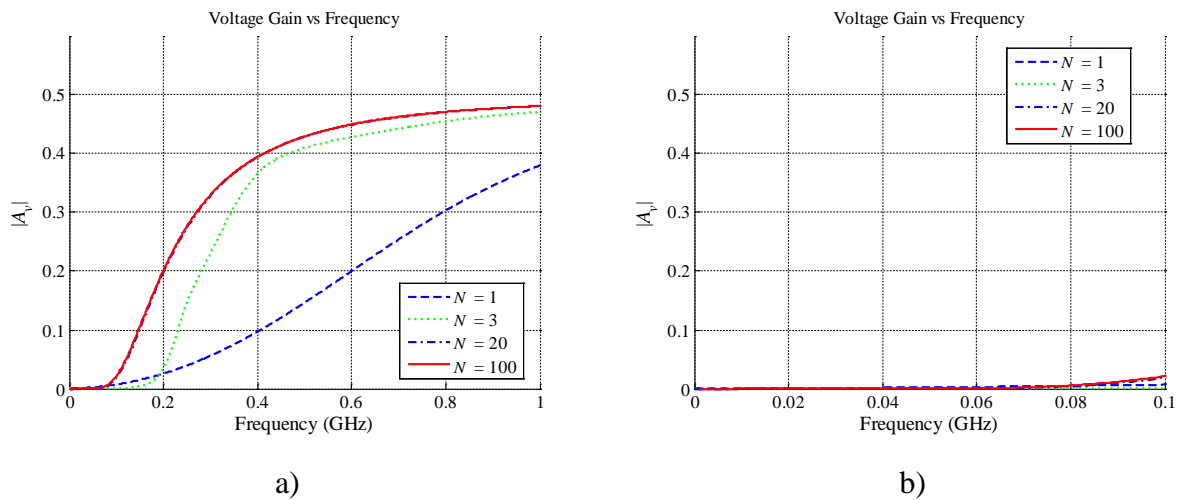


Fig. 3-13 Magnitude of the voltage gain for a lossy TL for 1, 3, 20 and 100 segments, up to 1 GHz. $R_S = 50 \Omega$, $Z_L = 50 \Omega$. The LH parameters are $L_L = 64 \text{ nH}\times\text{m}$, $C_L = 25.6 \text{ pF}\times\text{m}$, $R_L = 0$, $G_L = 0.01 \text{ S}\times\text{m}$, and 10 m long: a) frequency up to 1 GHz, b) frequency up to 100 MHz.

Although the expected input impedance value (50Ω) is the same after 2 MHz in both cases, in the very low frequency range the input impedance tends to 10Ω . On the other hand, as N increases, it seems that the voltage gain bandwidth is displaced more than 80 MHz to higher frequencies (see Fig. 3-13b). Apparently, the Matlab approximation using the lossy model (see Fig. 3-3) and a small conductance loss (G_L) at the proposed TL length (10 m), has a larger impact on the transmission line model, than the resistive losses (R_L) using the same TL length.

3. Modeling a Purely Left-Handed TL in Matlab with Equivalent Circuits

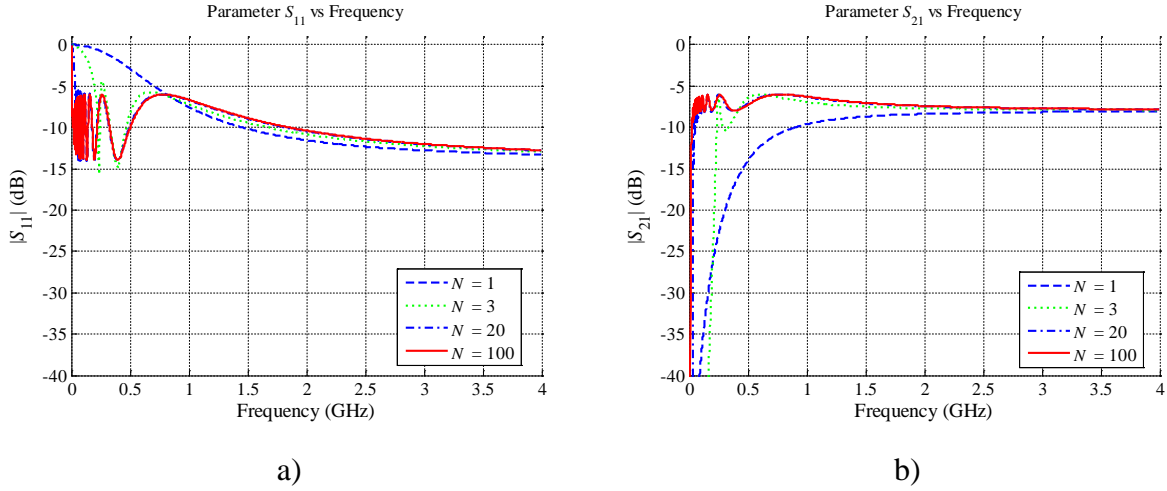


Fig. 3-14 The Matlab S-parameter responses, in decibels, for a lossy TL using 1, 3, 20 and 100 segments, up to 4 GHz. $R_S = 50 \Omega$, $Z_L = 50 \Omega$. The LH parameters are $L_L = 64 \text{ nH}\times\text{m}$, $C_L = 25.6 \text{ pF}\times\text{m}$, $R_L = 0.1 \Omega\times\text{m}$, $G_L = 0$, and $l = 10 \text{ m}$: a) magnitude of S_{11} , b) magnitude of S_{21} .

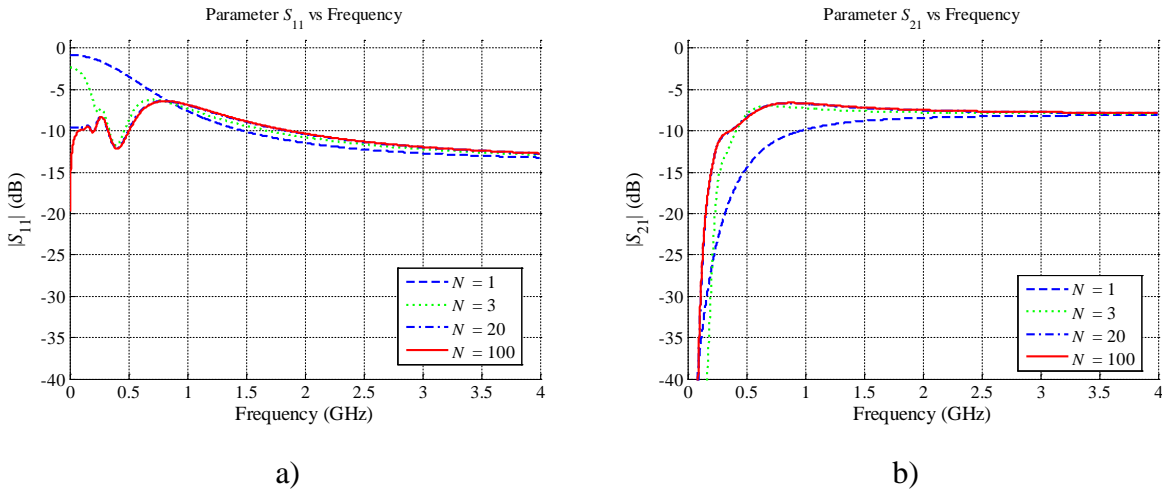


Fig. 3-15 The Matlab S-parameter responses, in decibels, for a lossy TL using 1, 3, 20 and 100 segments, up to 4 GHz. $R_S = 50 \Omega$, $Z_L = 50 \Omega$. The LH parameters are $L_L = 64 \text{ nH}\times\text{m}$, $C_L = 25.6 \text{ pF}\times\text{m}$, $R_L = 0$, $G_L = 0.01 \text{ S}\times\text{m}$, and $l = 10 \text{ m}$: a) magnitude of S_{11} , b) magnitude of S_{21} .

Fig. 3-14a and Fig. 3-14b show the $|S_{11}|$ and $|S_{21}|$ responses, respectively, using the following transmission line parameters: $L_L = 64 \text{ nH}\times\text{m}$, $C_L = 25.6 \text{ pF}\times\text{m}$, $R_L = 0.1 \Omega\times\text{m}$, $G_L = 0$.

Fig. 3-15a and Fig. 3-15b show the $|S_{11}|$ and $|S_{21}|$ responses, respectively, using the following transmission line parameters: $L_L = 64 \text{ nH}\times\text{m}$, $C_L = 25.6 \text{ pF}\times\text{m}$, $R_L = 0$, $G_L = 0.01 \text{ S}\times\text{m}$. In both cases $l = 10 \text{ m}$.

3. Modeling a Purely Left-Handed TL in Matlab with Equivalent Circuits

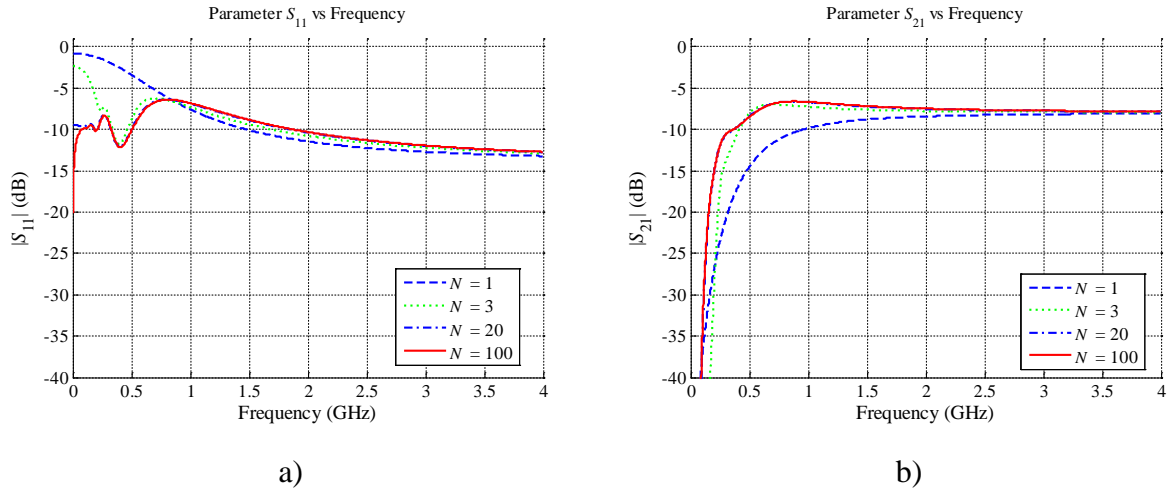


Fig. 3-16 The Matlab S-parameter responses in decibels for a lossy TL for 1, 3, 20 and 100 segments, up to 4 GHz. $R_S = 50 \Omega$, $Z_L = 50 \Omega$. The LH parameters are $L_L = 64 \text{ nH} \times \text{m}$, $C_L = 25.6 \text{ pF} \times \text{m}$, $R_L = 0.1$, $G_L = 0.01 \text{ S} \times \text{m}$, and 10 m long: a) magnitude of S_{11} , b) magnitude of S_{21} .

By comparing Fig. 3-14b and Fig. 3-15b, it seems that the cutoff frequency is moved to higher frequencies. The transmission response, when only conductance loss is present (see Fig. 3-15b), seems to reach to a stable response in a smooth manner. On the other hand, when only resistive loss is present (see Fig. 3-14b), the response reaches the expected value in an abrupt manner and the cutoff frequency is less affected. This is the expected behavior when cascading a large number of high-pass LC sections (or TL segments).

The combined effects of the lossy parameters R_L and G_L (see Fig. 3-16) compared with the individually obtained R_L and G_L effects, confirms that the conductance loss (at $l = 10 \text{ m}$) in the series capacitor produces dominant effects on the interconnects' response than the resistive loss in the shunt inductor (see Fig. 3-3). Also, the bandwidth response is moved a few thousands of Hertz to higher frequencies.

3.5. Conclusions

Basic concepts of a LH transmission line were presented to develop a simple model of this component. The input impedance, the voltage gain, and S-parameter calculations were achieved using the ABCD parameters of each interconnect element, for N transmission line segments. Although these scripts were used for the lossless purely left-handed case, it was

3. Modeling a Purely Left-Handed TL in Matlab with Equivalent Circuits

possible to achieve acceptable results by using lossy left-handed TL models. The individual impact of the lossy parameters were observed, and also analyzed. The left-handed conductance loss has larger effect than the left-handed resistive loss in PLH transmission lines.

It was demonstrated that simple left-handed transmission line approximations can be achieved by using the lumped element models in the low frequency range, where the *RGLC* transmission line model response is still valid.

Both approximations were presented looking forward to develop a similar basic model for the composite right/left-handed TL in the next chapter.

4. Modeling a Composite Right/Left-Handed TL in Matlab with Equivalent Circuits

4.1. Introduction

The objective of this work is to develop a basic procedure to model composite right/left-handed (CRLH) transmission lines (TLs) in Matlab using the lossless and lossy lumped element approximations. It is explained in this chapter a methodology used to approximate the S-parameter magnitudes of a composite right/left-handed transmission line interconnect. The corresponding Matlab implementations, and its results, are also described.

In Section 4.2, it is briefly reviewed the basic theory of CRLH TL models. A number of exact theoretical results from [Caloz-06] are used to validate the Matlab implementations. In Section 4.3, it is described the theoretical approach to compute the S-parameters of a lossless CRLH TL with N segments. Similarly, the same approximations using a lossy model of a composite right/left-handed TL with N segments are described in Section 4.4. The Matlab implementation and corresponding numerical results are also presented in Section 4.3 and Section 4.4. Finally, the conclusions and future work description are presented in Section 4.5.

4.2. Basic Theory of the Composite Right/Left-Handed Transmission Line Model

A purely left-handed (PLH) transmission line (TL) model is studied in Chapter 3, but as commented in Chapter 1, a PLH TL cannot exist physically. Even if we provide only series capacitance and shunt inductance effects, parasitic series inductance and shunt capacitances effects, increasing as frequency increases, will unavoidably occur due the currents flowing in the metallization and voltage gradients developing between the metal patterns of the trace and the ground plane. Thus, the CRLH model represents the most general metamaterial structure possible.

Composite right/left-handed TL structures also share the unit-cell size constraint required

4. Modeling a Composite Right/Left-Handed TL in Matlab with Equivalent Circuits

in the purely left-handed structures, $\Delta z < \lambda_g/4$, explained in Chapter 3. A composite right/left-handed TL can be modeled using an equivalent TL lossless model [Caloz-06], as shown in Fig. 1-15, where some circuits can be used as transmission line models; either for right-handed (conventional) TL (see Fig. 1-15a), the left-handed TL (see Fig. 1-15b), or the composite left/right-handed TL (see Fig. 1-15c) [Caloz-06]. In any case, the series impedance (Z) and shunt admittance (Y) are represented as per-unit-length immittances. The per-unit length impedance Z (Ω/m) is constituted by a RH per-unit-length inductance, L_R (H/m), in series with a LH times-unit-length capacitance, C_L (F \times m). Similarly, the per-unit-length admittance Y (S/m) is constituted by a RH per-unit-length capacitance C_R (F/m) in parallel with a LH times-unit-length inductance L_L (H \times m). The left-handed parameters are presented as times-unit-length elements, to mathematically maintain Z and Y as per-unit-length immittances.

If the LH immittances are zero, $Z_L = -j/(\omega C_L) = 0$ (or $C_L = \infty$) and $Y_L = -j/(\omega L_L) = 0$ (or $L_L = \infty$), only the RH immittances $Z_R = j\omega L_R$ and $Y_R = j\omega C_R$ remain, and the model in Fig. 1-15c reduces to the conventional RH TL lossless model shown in Fig. 1-15a. Similarly, if the RH immittances are zero, $Z_R = j\omega L_R = 0$ and $Y_R = j\omega C_R = 0$, the model in Fig. 1-15c reduces to the LH TL lossless model shown in Fig. 1-15b.

Similarly to the right-handed TL case, in the CRLH TL case the way the signals are propagated on a transmission line depends on the conductor's physical shape, the material properties of the structure, and the signal characteristics. Some of these signal propagation characteristics can be explained by the propagation constant (γ) [Caloz-06],

$$\gamma = \alpha + j\beta = \sqrt{ZY} \quad (4-1)$$

where α represents the attenuation constant (losses), and β indicates the phase constant.

Further CRLH characteristics will be explained for the lossless and lossy cases individually, to be later confirmed with exact theoretical results [Caloz-06].

4.2.1 Basic Concepts on Lossless CRLH Transmission Lines

In the particular case of the CRLH TL lossless model, the per-unit length impedance and per-unit length admittance can be defined as [Caloz-06],

4. Modeling a Composite Right/Left-Handed TL in Matlab with Equivalent Circuits

$$Z = j \left(\omega L_R - \frac{1}{\omega C_L} \right) \quad (4-2)$$

$$Y = j \left(\omega C_R - \frac{1}{\omega L_L} \right) \quad (4-3)$$

The complex propagation constant can be explicitly defined as [Lai-04],

$$\gamma = \alpha + j\beta = js(\omega) \sqrt{\omega^2 L_R C_R + \frac{1}{\omega^2 L_L C_L} - \left(\frac{L_R}{L_L} + \frac{C_R}{C_L} \right)} \quad (4-4)$$

where $s(\omega)$ is the following sign function [Lai-04],

$$s(\omega) = \begin{cases} -1 & \text{if } \omega < \min\left(\frac{1}{\sqrt{L_R C_L}}, \frac{1}{\sqrt{L_L C_R}}\right) \text{ LH range,} \\ +1 & \text{if } \omega > \max\left(\frac{1}{\sqrt{L_R C_L}}, \frac{1}{\sqrt{L_L C_R}}\right) \text{ RH range,} \end{cases} \quad (4-5)$$

due to the presence of the negative sign in (4-4), the propagation constant γ is not necessarily purely imaginary $\gamma = j\beta$ (band pass); it can be purely real $\gamma = \alpha$ (stop band) in some frequency ranges despite of the fact that the line is lossless. This stop band is a unique characteristic of the CRLH TL, which is not present in the purely right-handed (PRH) or in the PLH cases.

The CRLH dispersion/attenuation relation (4-4) is plotted in Fig. 4-1. Fig. 4-1a shows the CRLH dispersion and attenuation curves for energy propagation along both the positive and

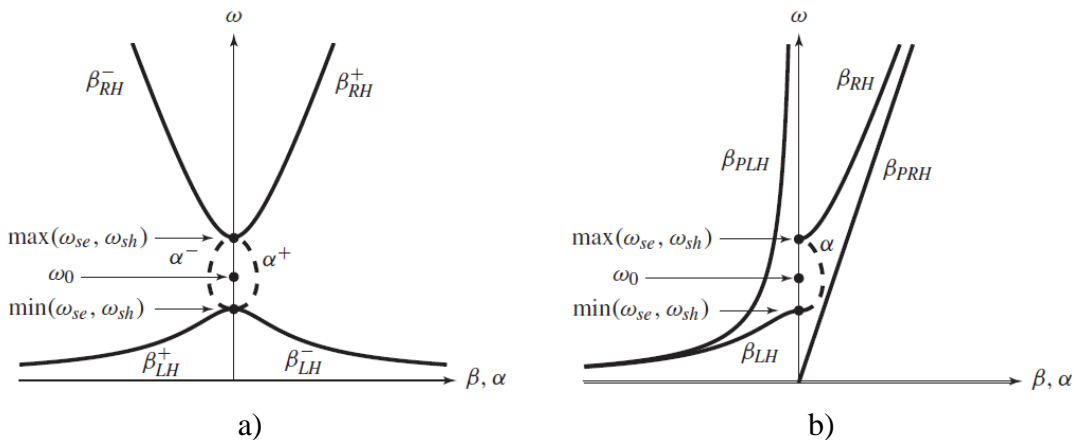


Fig. 4-1 Dispersion/attenuation diagrams for a CRLH TL. The labels “RH” and “LH” indicate the RH and LH frequency branches, respectively; a) energy propagation along $+z$ and $-z$ directions, b) comparison of the CRLH, PLH (β_{PLH}) and PRH (β_{PRH}) TLs for energy propagation long the $+z$ direction ($v_g > 0$). Figure taken from [Caloz-06].

4. Modeling a Composite Right/Left-Handed TL in Matlab with Equivalent Circuits

negative z directions. Super index + or – denote the positive or negative z direction of propagation. Fig. 4-1b shows these curves in the positive z -direction of propagation as compared with the dispersion curves of the corresponding PRH and PLH TLs. This second graph shows how the CRLH dispersion curves tends to the PLH and PRH dispersion curves at lower and higher frequencies, respectively. The previously mentioned stop band, shown by α in Fig. 4-1b, is caused by the different series and shunt resonances [Caloz-06],

$$\omega_{se} = \frac{1}{\sqrt{L_R C_L}} \quad (4-6)$$

$$\omega_{sh} = \frac{1}{\sqrt{L_L C_R}} \quad (4-7)$$

where ω_{se} and ω_{sh} (in rad/s) represent the resonance frequencies of the CRLH TL lossless model. When the series and shunt resonances are different, the CRLH TL is said to be unbalanced. On the other hand, when the series and shunt resonances are equal, $L_R C_R = L_L C_L$, in which case the line will be called balanced, the CRLH gap closes up with nonzero group velocity.

The sign function (4-5) is understood by considering Fig. 4-1a. If $\omega < \min(\omega_{se}, \omega_{sh})$, the phase velocity, given by (4-10), and group velocity, given by (4-11), have opposite signs (i.e., they are antiparallel), meaning that the TL is LH and that β is therefore negative. In contrast, in the RH range $\omega > \max(\omega_{se}, \omega_{sh})$, the phase and group velocities have the same sign, meaning that the TL is RH and that β is therefore positive. Thus, the real dispersion diagram for propagation of energy (v_g) in the $+z$ direction is the one shown in Fig. 4-1b, which is flipped around the ω axis if propagation of energy occurs in the $-z$ direction.

The Z_0 of the CRLH TL lossless model [Caloz-06] can be defined as

$$Z_0 = \sqrt{\frac{Z}{Y}} = Z_L \sqrt{\frac{L_R C_L \omega^2 - 1}{L_L C_R \omega^2 - 1}} \quad (4-8)$$

where Z_0 is positive and depends on the CRLH lossless parameters (L_R , C_R , L_L , C_L), and Z_L is the PLH characteristic impedance defined as

$$Z_L = \sqrt{\frac{L_L}{C_L}} \quad (4-9)$$

Notice that the characteristic impedance of a CRLH is frequency-dependent even if the TL is considered lossless.

4. Modeling a Composite Right/Left-Handed TL in Matlab with Equivalent Circuits

The phase velocity of a lossless CRLH TL is defined as [Caloz-06],

$$v_p = \frac{\omega}{\beta} = s(\omega) \frac{\omega}{\sqrt{\omega^2 L_R C_R + \frac{1}{\omega^2 L_L C_L} - \left(\frac{L_R}{L_L} + \frac{C_R}{C_L} \right)}} \quad (4-10)$$

where v_p may be frequency-dependent and negative or positive, depending on the RH and LH parameters and the frequency range.

The group velocity of CRLH lossless model [Caloz-06] is defined as

$$v_g = \left(\frac{\partial \beta}{\partial \omega} \right)^{-1} = \frac{\sqrt{\omega^2 L_R C_R + \frac{1}{\omega^2 L_L C_L} - \left(\frac{L_R}{L_L} + \frac{C_R}{C_L} \right)}}{\left| \omega L_R C_R - \frac{1}{\omega^3 L_L C_L} \right|} \quad (4-11)$$

where v_g is associated with the direction of power flow and is always positive.

By doing $L_R = C_R = 0$, the RH effects are eliminated from (4-10)-(4-11) and only the LH effects remain. The phase velocity is negative and the group velocity is positive, they are antiparallel as expected. On the other hand, if $L_L = C_L = \infty$ the LH effects are vanished; only the RH effects are present, and v_p and v_g are both positive. It is seen that the CRLH model has both LH properties and RH properties; the combined response is different from the ones individually obtained, due to the combined effects of LH and RH contributions to all frequencies.

The cutoff frequency of the PRH case can be computed [Caloz-06] as

$$f_c^{PRH} = \frac{1}{\pi \sqrt{L_R C_R}} \quad (4-12)$$

The cutoff frequency of the PLH case can be computed [Caloz-06] as

$$f_c^{PLH} = \frac{1}{4\pi \sqrt{L_L C_L}} \quad (4-13)$$

The cutoff frequencies for the CRLH balanced case can be computed [Caloz-06] as

$$f_{cL}^{bal} = f_R \left| 1 - \sqrt{1 + \frac{f_L}{f_R}} \right| \quad (4-14)$$

$$f_{cR}^{bal} = f_R \left(1 + \sqrt{1 + \frac{f_L}{f_R}} \right) \quad (4-15)$$

where $f_R = 1/(2\pi\sqrt{L_R C_R})$, and $f_L = 1/(2\pi\sqrt{L_L C_L})$.

4. Modeling a Composite Right/Left-Handed TL in Matlab with Equivalent Circuits

The transition frequency for the CRLH case, where the LH response (present at lower frequencies) goes to the RH response (at higher frequencies), can be computed [Caloz-06] as

$$\omega_0 = \frac{1}{\sqrt[4]{L_R C_R L_L C_L}} \quad (4-16)$$

The transition frequency, ω_0 , can also be understood as the maximum attenuation frequency, in the unbalanced case; or the minimum attenuation frequency, in the balanced case.

The cutoff frequencies for the CRLH unbalanced case can be computed [Caloz-06] as

$$f_{cL} = \frac{\omega_0}{2\pi} \sqrt{\frac{\left[k + \left(2\sqrt{L_L C_L} \right)^2 \right] \times \omega_0^2 - \sqrt{\left[k + \left(2\sqrt{L_L C_L} \right)^2 \right]^2 \times \omega_0^4 - 4}}{2}} \quad (4-17)$$

$$f_{cR} = \frac{\omega_0}{2\pi} \sqrt{\frac{\left[k + \left(2\sqrt{L_L C_L} \right)^2 \right] \times \omega_0^2 + \sqrt{\left[k + \left(2\sqrt{L_L C_L} \right)^2 \right]^2 \times \omega_0^4 - 4}}{2}} \quad (4-18)$$

where $k = L_R C_L + L_L C_R$.

The equations above will be used to confirm the correct behavior of the Matlab script developed in this Chapter.

4.2.2 Basic Concepts on Lossy CRLH Transmission Lines

In the particular case of the CRLH TL lossy model, the per-unit length impedance and per-unit length admittance are defined as

$$Z = j\omega \frac{L_R}{2} + \frac{R_R}{2} + \frac{1}{j\omega 2C_L + 2G_L} \quad (4-19)$$

$$Y = j\omega C_R + G_R + \frac{1}{j\omega L_L + R_L} \quad (4-20)$$

where R_R and G_R represent the RH losses, and similarly, R_L and G_L represent the LH losses.

The characteristic impedance of the CRLH TL lossy model can be defined as

$$Z_0 = \sqrt{\frac{Z}{Y}} = \sqrt{\frac{j\omega L_L + R_L}{j\omega C_L + G_L}} \times \sqrt{\frac{L_R C_L \omega^2 - j\omega L_R G_L - R_R(j\omega C_L + G_L) - 1}{L_L C_R \omega^2 - j\omega C_R R_L - G_R(j\omega L_L + R_L) - 1}} \quad (4-21)$$

As observed in (4-21), by removing the right/left-handed losses ($R_R = G_R = R_L = G_L = 0$), the lossy characteristic impedance becomes the lossless characteristic impedance (4-8), as expected.

4. Modeling a Composite Right/Left-Handed TL in Matlab with Equivalent Circuits

4.3. Lossless Model of a Composite Right/Left-Handed TL

4.3.1 Theoretical Approach to Compute the S-parameters

An iterative procedure, similar to that one in Chapter 3 to obtain the resulting S-parameters of an interconnection using a transmission line with N segments, is developed in this Chapter. The transmission line's unit-cell used as the CRLH TL model, is illustrated in Fig. 4-2. The symmetric unit-cell is used to allow us to compare our results with the ones provided by [Caloz-06], where a symmetric unit-cell is also used.

The ABCD parameter matrix for each CRLH transmission line lossless segment (see Fig. 4-2) is computed as follows

$$\begin{bmatrix} A & B \\ C & D \end{bmatrix} = \begin{bmatrix} 1 & Z_S \\ 0 & 1 \end{bmatrix} \begin{bmatrix} 1 & 0 \\ \frac{1}{Z_P} & 1 \end{bmatrix} \begin{bmatrix} 1 & Z_S \\ 0 & 1 \end{bmatrix} = \begin{bmatrix} 1 + \frac{Z_S}{Z_P} & Z_S \left(2 + \frac{Z_S}{Z_P} \right) \\ \frac{1}{Z_P} & 1 + \frac{Z_S}{Z_P} \end{bmatrix} \quad (4-22)$$

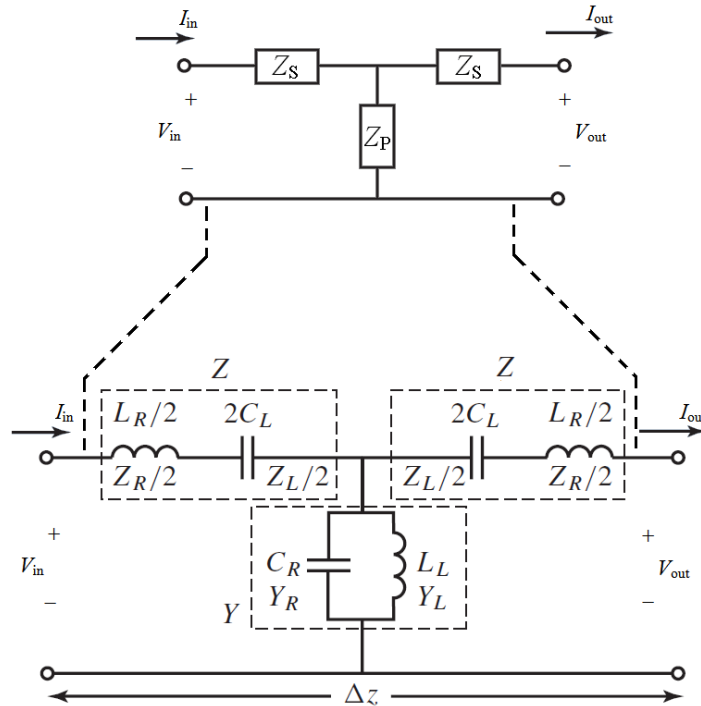


Fig. 4-2 Segment of a lossless CRLH TL. The series and parallel impedances, (Z_S and Z_P) representing the corresponding lumped elements of a CRLH TL symmetric model, with identical infinitesimal immittances as the asymmetric unit-cell in [Caloz-06].

4. Modeling a Composite Right/Left-Handed TL in Matlab with Equivalent Circuits

where Z_S and Z_P are

$$Z_S = j\omega \frac{L_R}{2} \Delta z + \frac{\Delta z}{j\omega 2C_L} \quad (4-23)$$

$$Z_P = \frac{1}{j\omega C_R \Delta z + \frac{\Delta z}{j\omega L_L}} \quad (4-24)$$

Now the ABCD parameter matrix is adjusted for the transmission line's unit-cell symmetric model as indicated in (4-22) and illustrated in Fig. 4-2. Then, Z_S and Z_P are also defined for the lossless case as indicated in (4-23) and (4-24). Finally, the S-parameter results can be computed as explained in Section 3.3.

4.3.2 Matlab Implementation

The Matlab code used to compute the CRLH lossless model is shown in Fig. 4-3, where Z_S and Z_P are defined as per-unit length values.

```
function [SN11,SN12,SN21,SN22] = CRLH_TL(N,f,Tlength,Rs,LL,CL,LR,CR,RR,GR,RL,GL,ZLoad)
%   SNxx:   Parameter Sxx at the basic TL interconnect for N segments.
%   ZLoad:  Represents the Load Impedance (in ohms).
%   N:      Transmission Line Segments.
%   f:      Frequency of interest in Hertz.
%   Tlength: The transmission line length in meters.
%   Rs:     Represents the source's voltage
j = sqrt(-1);
ABCD_ZLoad=[1 0;0 1/ZLoad];%<-ABCD-parameter matrix of ZL.
dz = Tlength/N;
w = 2*pi*f;
%----ABCD-parameters for each TL segment
ZS = j*w*(LR/2)*dz+(dz*(RR/2))+dz/((j*w*CL*2)+(GL*2));
ZP = 1/((j*w*CR*dz)+(dz*GR)+(dz/(j*w*LL+RL)));
A = 1+(ZS/ZP);
B = ZS*(1+(ZS/ZP+1));
C = 1/ZP;
D = 1+(ZS/ZP);
ABCD_TL=[A B;C D];
%----Iterative procedure to compute the ABCD matrix for N TL segments.
if N>=2
    ABCD_TL_old=ABCD_TL;
    for i=2:N
        ABCD_TL_new=ABCD_TL*ABCD_TL_old;
        ABCD_TL_old=ABCD_TL_new;
    end
    ABCD_TL=ABCD_TL_new;
end
ABCD_RS=[1 Rs;0 1];%<-ABCD-parameters matrix of Rs.
TN=ABCD_RS*ABCD_TL*ABCD_ZLoad;
%----Computing the S-parameters from the ABCD-parameters.
Z_Ref=50;
[SN11,SN12,SN21,SN22] = ABCD2SPARAM(TN,Z_Ref);
```

Fig. 4-3 Matlab script used to compute the S-parameters for a CRLH TL using N segments.

4. Modeling a Composite Right/Left-Handed TL in Matlab with Equivalent Circuits

In the CRLH lossless responses in [Caloz-06], the computed unit-cell is dimensionless, and most of their calculations are achieved in a dimensionless unit-cell. The provided capacitive or inductive values in [Caloz-06] are not defined as per-unit-length or times-unit-length values, since they represent only a single TL segment. On the other hand, the unit-cell in our Matlab script is associated with a physical length $\Delta z = 1/N$ (m). To properly match our responses with the ones in [Caloz-06], we need a TL length (l) such that given the N TL segments, our Matlab unit-cell values corresponds to the same values used in [Caloz-06]. In this case, $l = 10$ m, $N = 10$, $\Delta z = 1$ m.

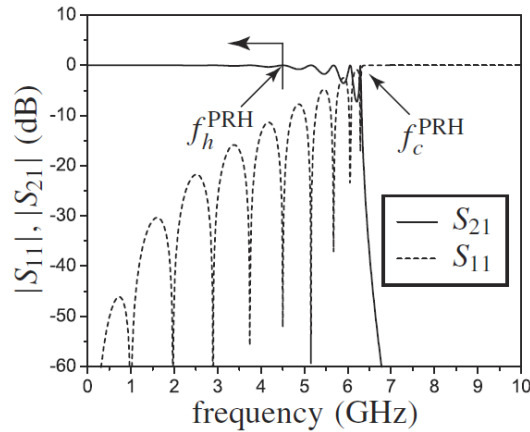


Fig. 4-4 PRH response in [Caloz-06] using a symmetric unit-cell, for the parameters $N = 10$, $L_L = C_L = 0$, $L_R = 2.5$ nH, $C_R = 1$ pF, $Z_0 = 50 \Omega$; magnitude of $S_{21,N}$ and $S_{11,N}$.

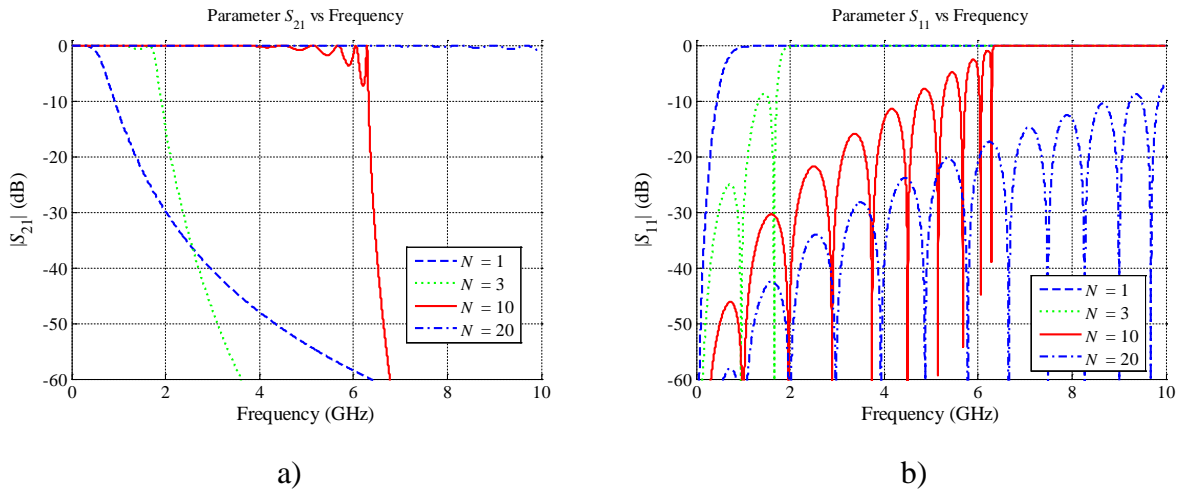


Fig. 4-5 Matlab response for the PRH case, up to 10 GHz using 1, 3, 10, and 20 transmission line segments, when $R_S = 0$, $Z_L = \infty$, $L_R = 2.5$ nH/m, $C_R = 1$ pF/m, $Z_0 = 50 \Omega$, and $L_L = C_L = \infty$: a) the magnitude of S_{21} , b) the magnitude of S_{11} .

4. Modeling a Composite Right/Left-Handed TL in Matlab with Equivalent Circuits

Fig. 4-4 show some of the responses obtained in [Caloz-06] for the PRH case. The Matlab computation was achieved with $R_S = 0$, $Z_L = \infty$, $L_L = C_L = \infty$, and $L_R = 2.5$ nH/m, $C_R = 1$ pF/m. This means that no left-handed parameters are present, no series impedance in the source, and the TL is terminated in open circuit.

Fig. 4-5a and Fig. 4-5b show the Matlab approximation response of $|S_{21}|$ and $|S_{11}|$, respectively, for N TL segments. It is seen that our responses (see Fig. 4-5) are practically identical to the responses in [Caloz-06] (see Fig. 4-4) for $N = 10$. The -10 dB cut-off frequency for $|S_{21}|$ response (see Fig. 4-5a), for $N = 10$, coincides with (4-12) at $f_c^{\text{PRH}} = 6.37$ GHz. As indicated in [Caloz-06] and illustrated in Fig. 4-4, our Matlab approximation $|S_{11}|$ also exhibits $N - 1$ reflection peaks (see Fig. 4-5b). At low frequencies, the peaks are equidistant as a consequence of the fact that the unit cell electrical length is proportional to the frequency [Caloz-06].

Fig. 4-6 show some of the responses obtained in [Caloz-06] for the PLH case. This computation was achieved with $R_S = 0$, $Z_L = \infty$, $L_L = 2.5$ nH×m, $C_L = 1$ pF×m, and $L_R = C_R = 0$.

Fig. 4-7a and Fig. 4-7b show our Matlab approximation response of $|S_{21}|$ and $|S_{11}|$, respectively, for N transmission line segments. It is seen that our responses (see Fig. 4-7) are practically identical to the responses in [Caloz-06] (see Fig. 4-6) for $N = 10$. The cut-off frequency for $|S_{21}|$ response (see Fig. 4-7a), for $N = 10$, coincides with (4-13) at $f_c^{\text{PLH}} = 1.59$ GHz. As indicated in [Caloz-06], our Matlab approximation $|S_{11}|$ exhibits $N - 1$ reflection peaks (see Fig. 4-7b).

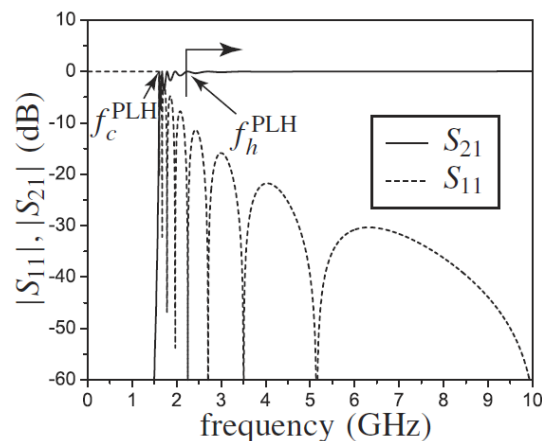


Fig. 4-6 PLH response in [Caloz-06] using a symmetric unit-cell, for the parameters $N = 10$, $L_L = 2.5$ nH, $C_L = 1$ pF, $L_R = C_R = 0$, and $Z_0 = 50 \Omega$; magnitude of $S_{21,N}$ and $S_{11,N}$.

4. Modeling a Composite Right/Left-Handed TL in Matlab with Equivalent Circuits

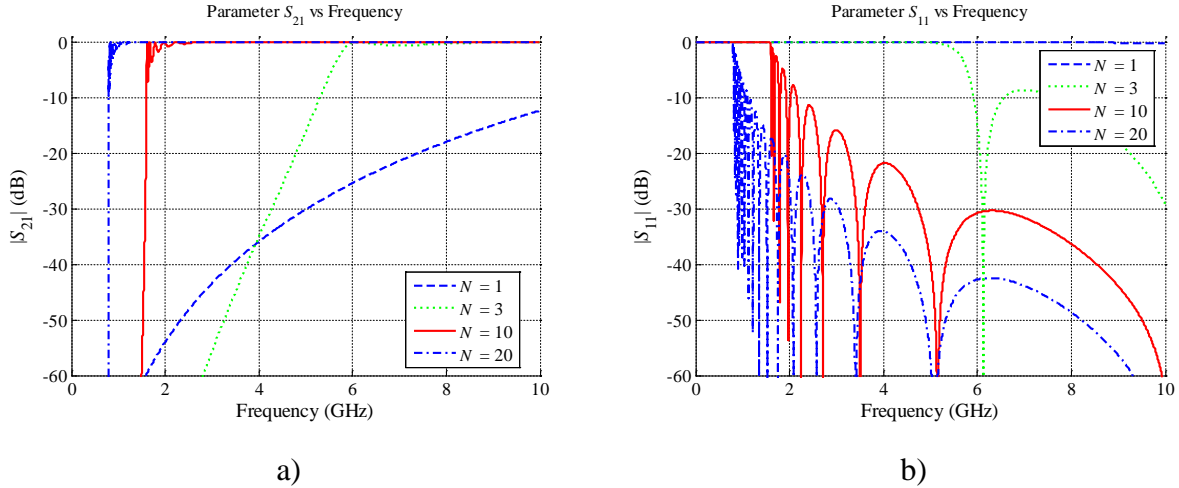


Fig. 4-7 Matlab response for the PLH case, up to 10GHz using 1, 3, 10, and 20 transmission line segments, when $R_S = 0$, $Z_L = \infty$, $L_R = C_R = 0$, $L_L = 2.5 \text{ nH}\times\text{m}$, $C_L = 1 \text{ pF}\times\text{m}$, and $Z_0 = 50 \Omega$: a) the magnitude of S_{21} , b) the magnitude of S_{11} .

Fig. 4-8 show some of the responses obtained in [Caloz-06] for the CRLH lossless balanced case, where $L_R C_L = L_L C_R$. The Matlab approximation is achieved with $R_S = 0$, $Z_L = \infty$, $L_L = 2.5 \text{ nH}\times\text{m}$, $C_L = 1 \text{ pF}\times\text{m}$, $L_R = 2.5 \text{ nH/m}$, and $C_R = 1 \text{ pF/m}$.

Fig. 4-9a and Fig. 4-9b show our Matlab approximation response of $|S_{21}|$ and $|S_{11}|$, respectively, for N TL segments. It is seen that our responses (see Fig. 4-9) are practically identical to the responses in [Caloz-06] (see Fig. 4-8) for $N = 10$. The cut-off frequencies for $|S_{21}|$ response (see Fig. 4-8), for $N = 10$, coincides with (4-14) at $f_{cL}^{\text{bal}} = 1.31 \text{ GHz}$, and also with (4-15) at $f_{cR}^{\text{bal}} = 7.68 \text{ GHz}$. The transition frequency from the LH region to the RH region,

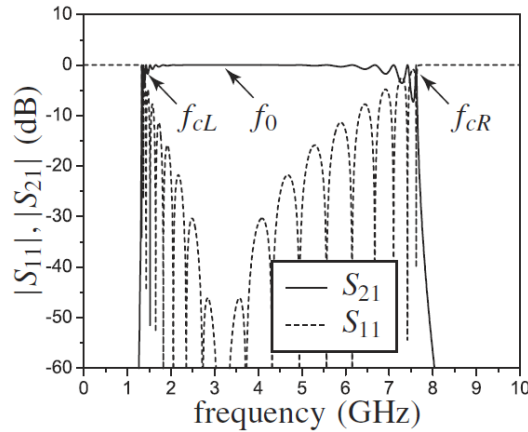


Fig. 4-8 CRLH response in [Caloz-06] (balanced case) using symmetric unit-cell, for the parameters $N = 10$, $L_L = 2.5 \text{ nH}$, $C_L = 1 \text{ pF}$, $L_R = 2.5 \text{ nH}$, $C_R = 1 \text{ pF}$, $Z_L = Z_R = 50 \Omega$; magnitude of $S_{21,N}$ and $S_{11,N}$.

4. Modeling a Composite Right/Left-Handed TL in Matlab with Equivalent Circuits

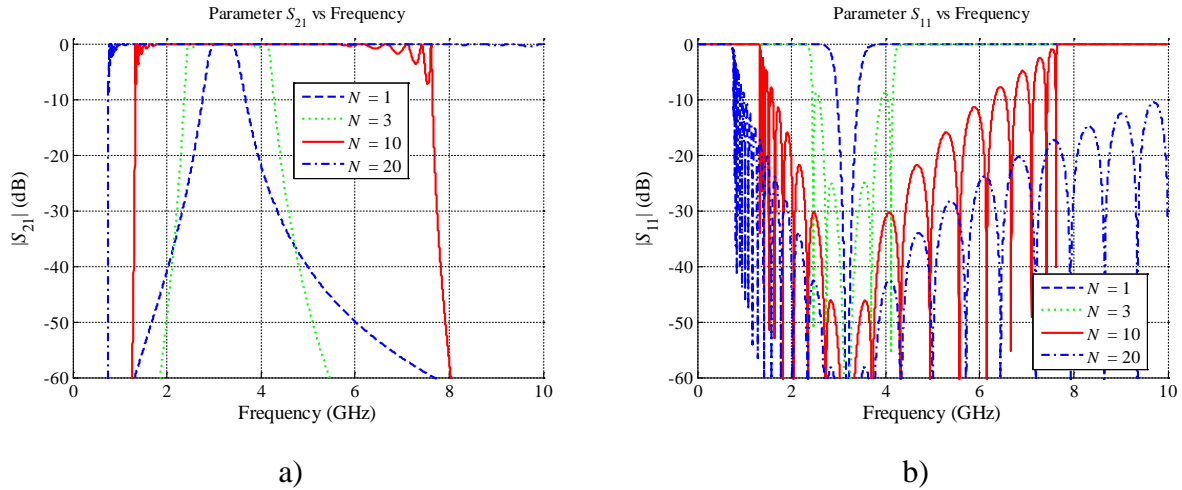


Fig. 4-9 Matlab response for the CRLH lossless balanced case, up to 10 GHz using 1, 3, 10, and 20 transmission line segments, when $R_S = 0$, $Z_L = \infty$, $L_R = 2.5$ nH/m, $C_R = 1$ pF/m, $L_L = 2.5$ nH×m, $C_L = 1$ pF×m, $Z_0 = 50 \Omega$: Ω : a) the magnitude of S_{21} , b) the magnitude of S_{11} .

according to (4-16), occurs at $f_0 = 3.18$ GHz. As observed in our responses (see Fig. 4-9b), the attenuation value at the transition frequency is really low, as expected for the balanced case.

Fig. 4-10 show some of the responses obtained in [Caloz-06] for the CRLH lossless unbalanced case, where $L_R C_L \neq L_L C_R$. This computation was achieved with $R_S = 0$, $Z_L = \infty$, $L_L = 2.5$ nH×m, $C_L = 0.75$ pF×m, and $L_R = 2$ nH/m, $C_R = 1$ pF/m. This means that all the composite right/left-handed effects are present simultaneously.

Fig. 4-11a and Fig. 4-11b show our Matlab approximation response of $|S_{21}|$ and $|S_{11}|$, respectively, for N TL segments. It is seen that our responses are practically identical to the

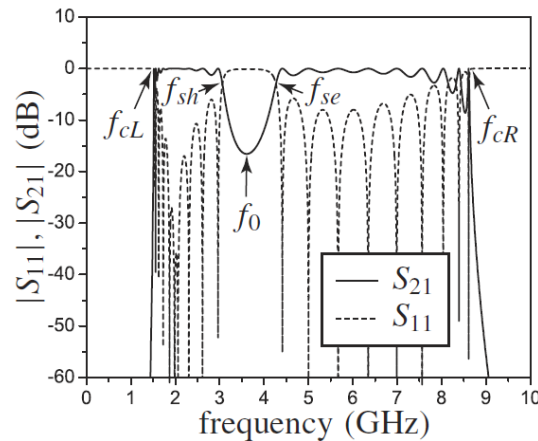


Fig. 4-10 CRLH response obtained in [Caloz-06] (unbalanced case) using symmetric unit-cell, for the parameters $N = 10$, $L_L = 2.5$ nH, $C_L = 0.75$ pF, $L_R = 2$ nH, $C_R = 1$ pF, $Z_L = 57.54 \Omega$, $Z_L = 44.72 \Omega$; magnitude of $S_{21,N}$ and $S_{11,N}$.

4. Modeling a Composite Right/Left-Handed TL in Matlab with Equivalent Circuits

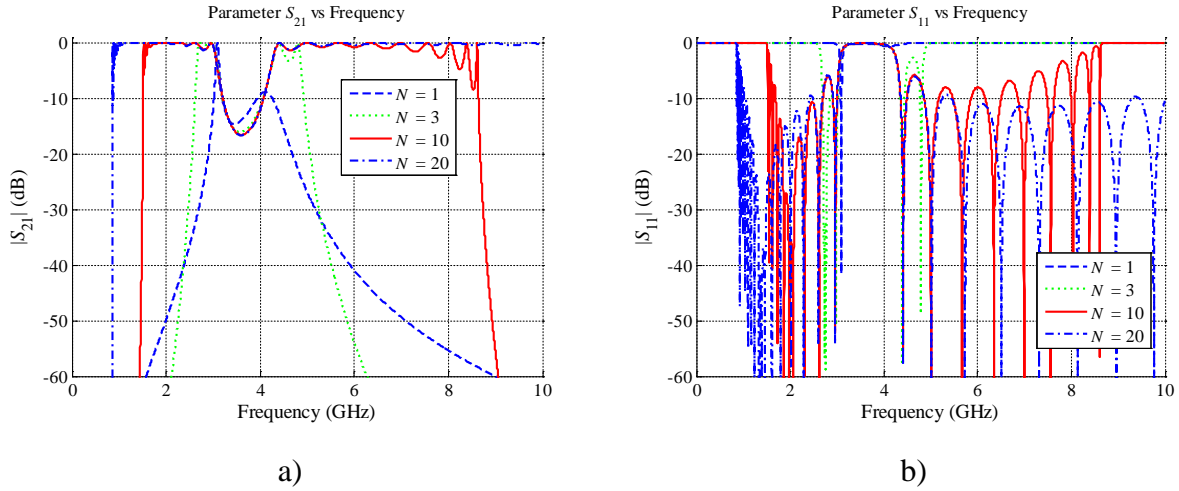


Fig. 4-11 Matlab response for the CRLH lossless unbalanced case, up to 10 GHz using 1, 3, 10, and 20 transmission line segments, when $R_S = 0$, $Z_L = \infty$, $L_R = 2$ nH/m, $C_R = 1$ pF/m, $L_L = 2.5$ nH×m, $C_L = 0.75$ pF×m, $Z_0 = 50 \Omega$: Ω : a) the magnitude of S_{21} , b) the magnitude of S_{11} .

responses in [Caloz-06] (see Fig. 4-10) for $N = 10$. The cut-off frequencies for $|S_{21}|$ response (see Fig. 4-11a) for $N = 10$, coincides with (4-17) at $f_{cL} = 1.51$ GHz, and also with (4-18) at $f_{cR} = 8.69$ GHz. The transition frequency from the LH region to the RH region, according to (4-16), occurs at $f_0 = 3.62$ GHz. As observed in our responses (see Fig. 4-11), there is a gap with the maximum attenuation value (stop band), as expected in the unbalanced case.

Notice that equations (4-4)-(4-24) represent the capacitance/inductance values of the unit-cell illustrated in Fig. 4-2.

4.4. Lossy Model of a Composite Right/Left-Handed TL

4.4.1 Theoretical Approach to Compute the S-parameters

Similarly to Section 4.3, the lossy model of the CRLH TL is illustrated in Fig. 4-12. Hence, the series and shunt per-unit length immittances can be computed as,

$$Z_s = j\omega \frac{L_R}{2} \Delta z + \frac{R_R}{2} \Delta z + \frac{\Delta z}{j\omega 2C_L + 2G_L} \quad (4-25)$$

4. Modeling a Composite Right/Left-Handed TL in Matlab with Equivalent Circuits

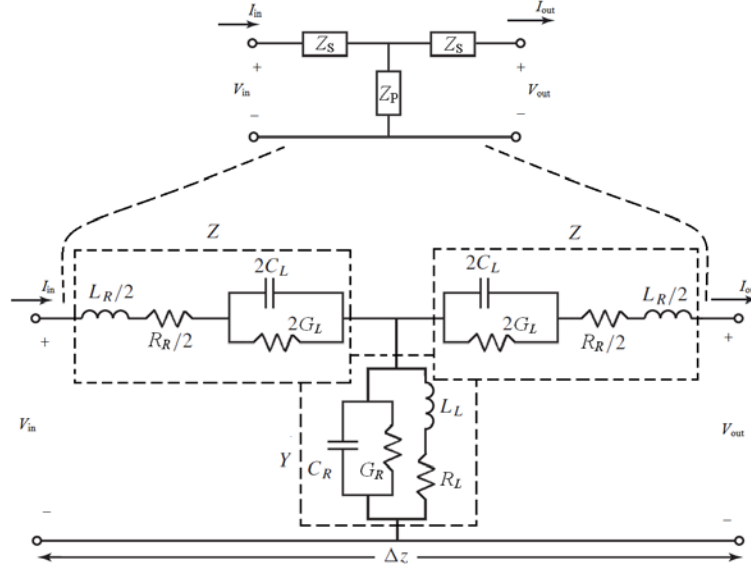


Fig. 4-12 Segment of a lossy CRLH TL. The series and parallel impedances, (Z_S and Z_P) representing the corresponding lumped elements of a CRLH TL symmetric model, with identical infinitesimal immitances as the asymmetric unit-cell.

$$Z_P = \frac{1}{j\omega C_R \Delta z + G_R \Delta z + \frac{\Delta z}{j\omega L_L + R_L}} \quad (4-26)$$

Having Z_S and Z_P using lossy parameters, a similar process to the Section 4.3 can be followed.

4.4.2 Matlab Implementation

As in the lossless case, the same script can be used (see Fig. 4-3) to compute the S-parameter response for the lossy case. Hence, for the lossy case our Matlab script uses: $l = 10$ m, $N = 10$, $\Delta z = 1$ m.

Fig. 4-13a shows the $|S_{21}|$ Matlab response obtained for the PRH lossy case with $R_S = 0$, $Z_L = \infty$, $R_R = 0.5$ Ω /m, $G_R = 0$, $L_R = 2.5$ nH/m, $C_R = 1$ pF/m. Although the -10 dB cutoff frequency is slightly affected, the transmission magnitude of S_{21} (see Fig. 4-13a) is more affected as R_R is increased. Fig. 4-13b shows the $|S_{21}|$ Matlab response obtained for the PRH lossy case with $R_S = 0$, $Z_L = \infty$, $R_R = 0$, $G_R = 0.001$ S/m, $L_R = 2.5$ nH/m, $C_R = 1$ pF/m. The RH conductance loss has a critical impact on the PRH response. The transmission parameter magnitude is decreased even with a small RH conductance loss (G_R) value.

4. Modeling a Composite Right/Left-Handed TL in Matlab with Equivalent Circuits

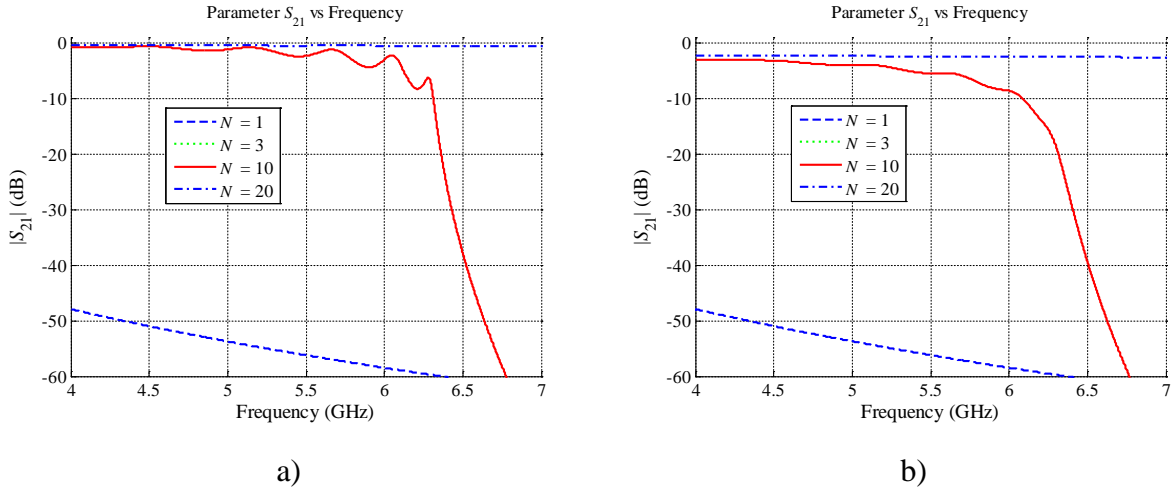


Fig. 4-13 Magnitude of S_{21} approximation, for the PRH case, from 4 GHz to 7 GHz using 1, 3, 10, and 20 lossy transmission line segments, when $R_S = 0$, $Z_L = \infty$, $L_R = 2.5$ nH/m, $C_R = 1$ pF/m, $Z_0 = 50 \Omega$, and $L_L = C_L = \infty$: a) $R_R = 0.5 \Omega/m$, $G_R = 0$, b) $R_R = 0$, $G_R = 0.001$ S/m.

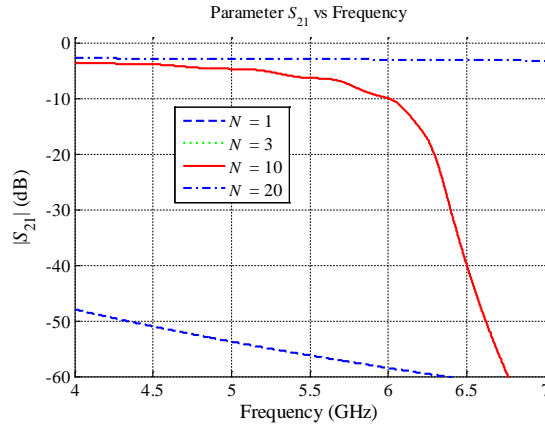


Fig. 4-14 Magnitude of S_{21} approximation, for the PRH case, from 4 GHz to 7 GHz using 1, 3, 10, and 20 lossy transmission line segments, when $R_S = 0$, $Z_L = \infty$, $R_R = 0.5 \Omega/m$, $G_R = 0.001$ S/m, $L_R = 2.5$ nH/m, $C_R = 1$ pF/m, $Z_0 = 50 \Omega$, and $L_L = C_L = \infty$.

As commented in Chapter 2, the bandwidth of the PRH circuit is reduced as R_R and G_R are increased. As shown in Fig. 4-14, the G_R loss has a larger impact, than R_R loss; the RH conductance loss moves the -10 dB cutoff frequency to lower frequencies, which reduces the PRH bandwidth. The RH resistive loss has less impact either on bandwidth or transmission parameter magnitudes. It is also observed that the peak responses are reduced.

Fig. 4-15a shows the $|S_{21}|$ Matlab response for the PLH lossy case with $R_S = 0$, $Z_L = \infty$, $R_L = 0.5 \Omega \times m$, $G_L = 0$, $L_L = 2.5$ nH \times m, $C_L = 1$ pF \times m. As observed, the -10 dB cutoff frequency is

4. Modeling a Composite Right/Left-Handed TL in Matlab with Equivalent Circuits

moved to higher frequencies, above 1.6 GHz. Similarly to Chapter 3, as we increase the LH resistive loss (RL), the cutoff frequency is moved to higher frequencies.

Fig. 4-15b shows the $|S_{21}|$ Matlab response for the PLH lossy case with $R_S = 0$, $Z_L = \infty$, $R_L = 0$, $G_L = 0.001 \text{ S}\times\text{m}$, $L_L = 2.5 \text{ nH}\times\text{m}$, $C_L = 1 \text{ pF}\times\text{m}$. As observed, the -10 dB cutoff frequency is moved to higher frequencies, above 1.95 GHz. The LH conductance loss has a critical impact on the PLH response. The magnitude of the transmission parameter, $|S_{21}|$, is decreased even with a small LH conductance loss value.

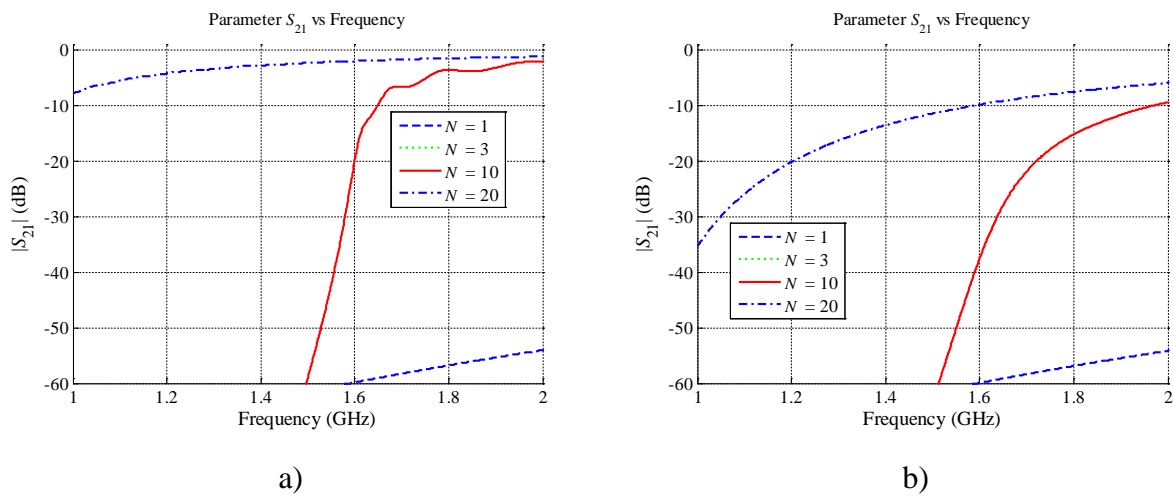


Fig. 4-15 Magnitude of S_{21} approximation, for the PLH case, from 1 GHz to 2 GHz using 1, 3, 10, and 20 lossy transmission line segments, when $R_S = 0$, $Z_L = \infty$, $L_R = C_R = 0$, $L_L = 2.5 \text{ nH}\times\text{m}$, $C_L = 1 \text{ pF}\times\text{m}$, and $Z_0 = 50 \text{ }\Omega$: a) $R_L = 0.5 \text{ }\Omega\times\text{m}$, $G_L = 0$, b) $R_L = 0$, $G_L = 0.001 \text{ S}\times\text{m}$.

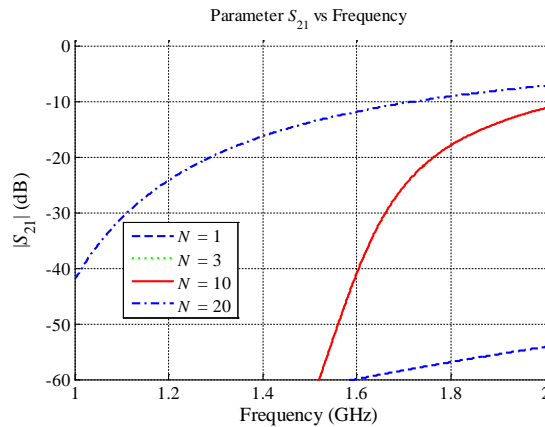


Fig. 4-16 Magnitude of S_{21} approximation for the PLH case, from 1 GHz to 2 GHz using 1, 3, 10, and 20 lossy TL segments, when: $R_S = 0$, $Z_L = \infty$, $L_R = C_R = 0$, $R_L = 0.5 \text{ }\Omega\times\text{m}$, $G_L = 0.001 \text{ S}\times\text{m}$, $L_L = 2.5 \text{ nH}\times\text{m}$, $C_L = 1 \text{ pF}\times\text{m}$, and $Z_0 = 50 \text{ }\Omega$.

4. Modeling a Composite Right/Left-Handed TL in Matlab with Equivalent Circuits

In general, as commented in Chapter 3, the PLH circuit bandwidth (from f_{cL} to ∞) is reduced as R_L and G_L are increased. As shown in Fig. 4-16, the G_L loss has a larger impact, than R_L loss; the LH conductance loss moves the -10 dB cutoff frequency to higher frequencies, which reduces the PLH bandwidth. The LH resistive loss has a lower impact either on bandwidth or transmission parameter magnitude. It is also observed that the peak responses are reduced.

Fig. 4-17a shows the $|S_{21}|$ Matlab response for the CRLH lossy balanced case with $R_S = 0$,

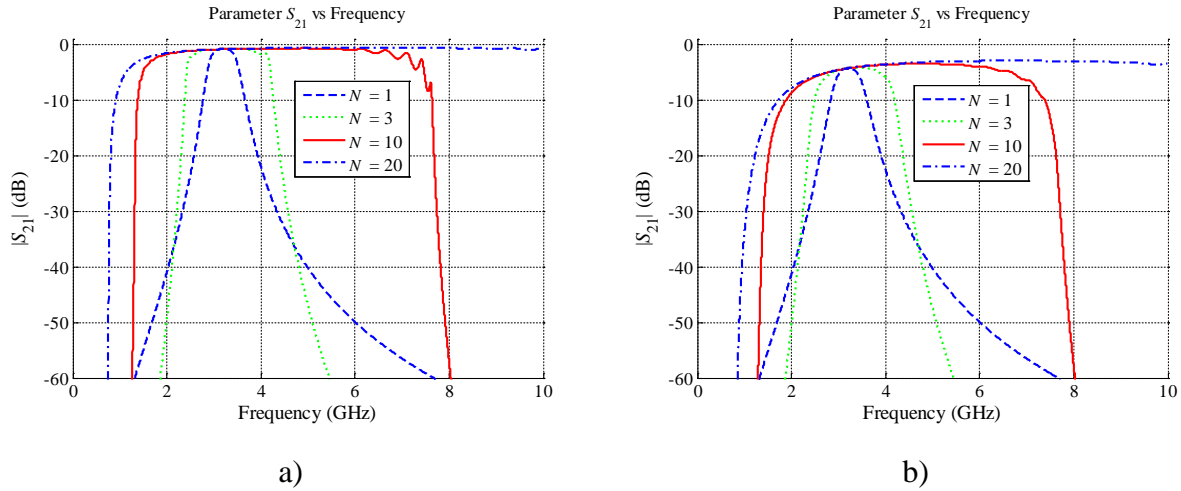


Fig. 4-17 Magnitude of S_{21} approximation for the CRLH balanced case, up to 10 GHz using 1, 3, 10, and 20 lossy TL segments, when $R_S = 0$, $Z_L = \infty$, $L_L = 2.5$ nH \times m, $C_L = 1$ pF \times m, $L_R = 2.5$ nH/m, $C_R = 1$ pF/m, and $Z_0 = 50$ Ω : a) $R_L = R_R = 0.5$, $G_L = G_R = 0$, b) $R_L = 0$, $G_L = G_R = 0.001$ S \times m.

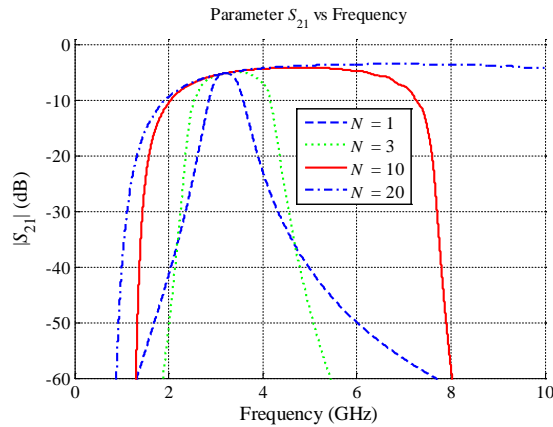


Fig. 4-18 Magnitude of S_{21} approximation, for the CRLH balanced case, up to 10 GHz using 1, 3, 10, and 20 lossy TL segments, when $R_S = 0$, $Z_L = \infty$, $R_L = 0.5$ $\Omega \times$ m, $G_L = 0.001$ S \times m, $L_L = 2.5$ nH \times m, $C_L = 1$ pF \times m, $R_R = 0.5$ Ω /m, $G_R = 0.001$ S/m, $L_R = 2.5$ nH/m, $C_R = 1$ pF/m, and $Z_0 = 50$ Ω .

4. Modeling a Composite Right/Left-Handed TL in Matlab with Equivalent Circuits

$Z_L = \infty$, $R_L = 0.5 \Omega \times m$, $G_L = 0$, $L_L = 2.5 \text{ nH} \times m$, $C_L = 1 \text{ pF} \times m$, $R_R = 0.5 \Omega/m$, $G_R = 0$, $L_R = 2.5 \text{ nH}/m$, $C_R = 1 \text{ pF}/m$.

Fig. 4-17b shows the $|S_{21}|$ Matlab response for the CRLH lossy balanced case with $R_S = 0$, $Z_L = \infty$, $R_L = 0$, $G_L = 0.001 \text{ S} \times m$, $L_L = 2.5 \text{ nH} \times m$, $C_L = 1 \text{ pF} \times m$, $R_R = 0$, $G_R = 0.001 \text{ S}/m$, $L_R = 2.5 \text{ nH}/m$, $C_R = 1 \text{ pF}/m$. The transmission parameter response, $|S_{21}|$, when only resistive loss is present (see Fig. 4-17a), the -10 dB cutoff frequency for the LH region has a larger impact than the RH region, as mentioned in the PLH and PRH previous cases. It is also observed that the peaks are reduced, and the total bandwidth is reduced due to the cutoff frequency displacement in the left-handed and right-handed regions. On the other hand, when only conductive loss is present (see Fig. 4-17b), the total bandwidth reduction is much larger. The conductive losses produce a larger effect on the LH and RH regions, by moving the -10 dB cutoff frequency to the right and left, respectively. It is also observed that $|S_{21}|$, at the transition frequency, is attenuated.

Fig. 4-18 shows the $|S_{21}|$ Matlab response for the CRLH lossy balanced case with $R_S = 0$, $Z_L = \infty$, $R_L = 0.5 \Omega \times m$, $G_L = 0.001 \text{ S} \times m$, $L_L = 2.5 \text{ nH} \times m$, $C_L = 1 \text{ pF} \times m$, $R_R = 0.5 \Omega/m$, $G_R = 0.001 \text{ S}/m$, $L_R = 2.5 \text{ nH}/m$, $C_R = 1 \text{ pF}/m$. The conductive loss has a larger effect on the CRLH lossy balanced case, as expected. The total bandwidth of the resulting band-pass structure is reduced as the losses increase; and the conductance losses (G_L , G_R) have greater impact than the resistive losses (R_L , R_R).

Fig. 4-19a shows the $|S_{21}|$ Matlab response for the CRLH lossy unbalanced case, where $L_R C_L \neq L_L C_R$, with $R_S = 0$, $Z_L = \infty$, $R_L = 0.5 \Omega \times m$, $G_L = 0$, $L_L = 2.5 \text{ nH} \times m$, $C_L = 0.75 \text{ pF} \times m$, $R_R = 0.5 \Omega/m$, $G_R = 0$, $L_R = 2 \text{ nH}/m$, $C_R = 1 \text{ pF}/m$.

Fig. 4-19b shows the $|S_{21}|$ Matlab response for the CRLH lossy unbalanced case with $R_S = 0$, $Z_L = \infty$, $R_L = 0$, $G_L = 0.001 \text{ S} \times m$, $L_L = 2.5 \text{ nH} \times m$, $C_L = 0.75 \text{ pF} \times m$, $R_R = 0$, $G_R = 0.001 \text{ S}/m$, $L_R = 2 \text{ nH}/m$, $C_R = 1 \text{ pF}/m$.

Fig. 4-20 shows the $|S_{21}|$ Matlab response for the CRLH lossy unbalanced case with $R_S = 0$, $Z_L = \infty$, $R_L = 0.5 \Omega \times m$, $G_L = 0.001 \text{ S} \times m$, $L_L = 2.5 \text{ nH} \times m$, $C_L = 0.75 \text{ pF} \times m$, $R_R = 0.5 \Omega/m$, $G_R = 0.001 \text{ S}/m$, $L_R = 2 \text{ nH}/m$, $C_R = 1 \text{ pF}/m$.

As shown in the balanced case, in the unbalanced case the conductive losses also produce larger effects than the resistive losses (using $l = 10 \text{ m}$). The resultant effect in the unbalanced case is more critical due to the difficulty to exactly satisfy the balanced condition ($L_R C_L = L_L C_R$).

4. Modeling a Composite Right/Left-Handed TL in Matlab with Equivalent Circuits

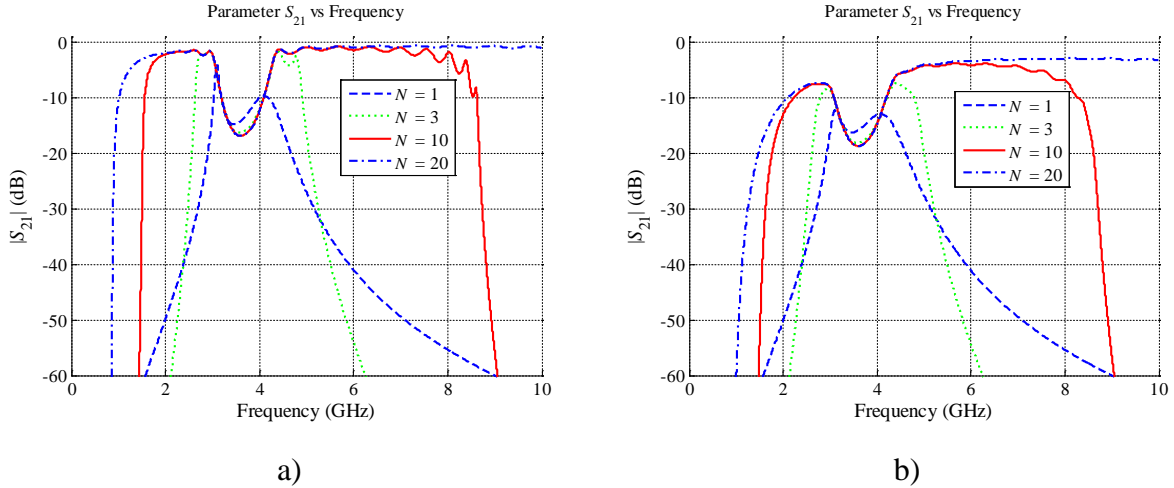


Fig. 4-19 Matlab response of $|S_{21}|$ for the CRLH unbalanced case up to 10 GHz, using 1, 3, 10, and 20 lossy TL segments, when $R_S = 0$, $Z_L = \infty$, $L_L = 2.5 \text{ nH} \times \text{m}$, $C_L = 0.75 \text{ pF} \times \text{m}$, $L_R = 2 \text{ nH/m}$, $C_R = 1 \text{ pF/m}$, and $Z_0 = 50 \Omega$: a) $R_L = 0.5 \Omega \times \text{m}$, $G_L = 0$, $R_R = 0.5 \Omega/\text{m}$, $G_R = 0$, b) $R_L = 0$, $R_R = 0$, $G_L = 0.001 \text{ S} \times \text{m}$, $G_R = 0.001 \text{ S/m}$.

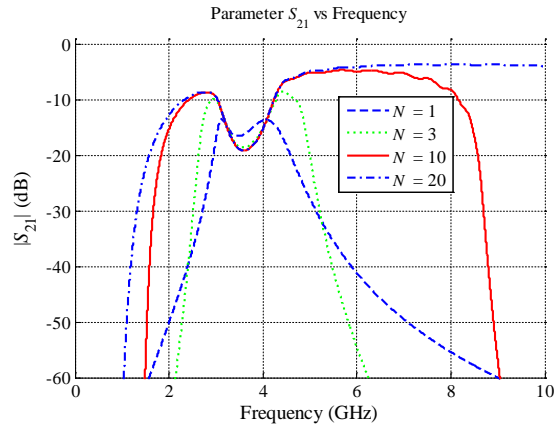


Fig. 4-20 Matlab response of $|S_{21}|$ for the CRLH unbalanced case up to 10 GHz using 1, 3, 10, and 20 lossy TL segments, when $R_S = 0$, $Z_L = \infty$, $R_L = 0.5 \Omega \times \text{m}$, $G_L = 0.001 \text{ S} \times \text{m}$, $L_L = 2.5 \text{ nH} \times \text{m}$, $C_L = 1 \text{ pF} \times \text{m}$, $R_R = 0.5 \Omega/\text{m}$, $G_R = 0.001 \text{ S/m}$, $L_R = 2.5 \text{ nH/m}$, $C_R = 1 \text{ pF/m}$, and $Z_0 = 50 \Omega$.

Since the CRLH parameters ($RGLC$, both LH and RH) are based on a particular interconnect shape, unavoidably unbalanced effects may exist on real structures, and a small attenuation may exist at ω_0 .

As observed on Fig. 4-20, it is important to maintain conductance and resistive losses reduced as much as possible. If such losses exist, the operation bandwidth will be reduced, for both the LH range and the RH range. The maximum allowed losses may depend on the required bandwidth and level of attenuation.

4. Modeling a Composite Right/Left-Handed TL in Matlab with Equivalent Circuits

4.5. Conclusions

Basic concepts of a CRLH transmission line were presented to develop a simple model of this component. The individual impact of the lossy parameters were observed, and analyzed. It was observed that the right/left-handed conductance losses have larger effects than the right/left-handed resistive losses in CRLH transmission lines.

It was demonstrated that simple right/left-handed transmission line approximations can be achieved by using the lumped element models in the low frequency range, where the *RGLC* transmission line model is still valid.

Similar circuit models will be used in the next chapter to perform a parameter extraction of 3D EM simulated structures, to finally approximate the L_L , C_L , L_R and C_R values, and obtain the LH and RH regions of operation of actual physical structure.

5. A Parameter Extraction Process for Equivalent Circuit Models of a PRH TL in Matlab

5.1. Introduction

Based on electromagnetic (EM) simulations of a 50-Ω microstrip line, it is explained in this Chapter a methodology to extract the per-unit length circuitual parameters (*RGLC*) of a purely right-handed (PRH) transmission line (TL) using our lumped element approximation described in Chapter 4. Initially, only the *LC* parameters are extracted for a lossless microstrip line, and finally the *RGLC* parameters are extracted for the lossy case.

In Section 5.2, it is briefly reviewed the parameter extraction (PE) problem, where a target EM response is obtained from Sonnet, while the approximating response is obtained from the PRH transmission line model implemented in Matlab. In Section 5.3, it is explained how the starting point for parameter extraction is selected based on theoretical equations found in common transmission line references [Pozar-05]. In Section 5.4, it is explained the parameter extraction methodology used for the lossless case, and the corresponding results obtained. Similarly, the parameter extraction methodology for the lossy case is presented in Section 5.5, including its results. Finally, the conclusions and future work description are presented in Section 5.6.

5.2. Formulation of Parameter Extraction (PE)

The problem of parameter extraction (PE) can be formulated as a nonlinear least-squares problem,

$$\mathbf{x}^* = \arg \min_{\mathbf{x}} \left\| \mathbf{R}(\mathbf{x}) - \mathbf{R}^t \right\|_2^2 \quad (5-1)$$

where \mathbf{x}^* contains the optimal extracted parameters that makes the approximating response $\mathbf{R}(\mathbf{x}^*)$ as close as possible to the target response \mathbf{R}^t . In a parameter extraction problem, we usually want the error between the approximating response and the target response to be zero,

5. A Parameter Extraction Process for Equivalent Circuit Models of a PRH TL in Matlab

$$\mathbf{e}(\mathbf{x}) = \mathbf{R}(\mathbf{x}) - \mathbf{R}' = \mathbf{0} \quad (5-2)$$

but this is not always possible, and a small error between both responses is allowed.

In this Chapter, the target response is obtained from a Sonnet electromagnetic simulation, which is also named as the fine model in the space mapping terminology [Koziel-08]. This response is regarded as very close to the real world behavior of the simulated structure. The approximating response is obtained from a lumped element model of a PRH transmission line implemented in Matlab (see Chapter 4). Similarly, this second model is named as the coarse model in the space mapping arena [Koziel-08].

The PE process in this chapter uses a classical optimization method, the Nelder-Mead method, available in `fminsearch` function in Matlab, to minimize a suitable norm of the error function (5-2).

In the particular case studied in this Chapter, this error is defined as the differences between the real and imaginary values of the S-parameter responses of Matlab (coarse) and Sonnet (fine) models at each frequency point,

$$e_1(\mathbf{x}) = \text{Re}\{S_{11}(f_k)_M\} - \text{Re}\{S_{11}(f_k)_S\} \quad (5-3)$$

$$e_2(\mathbf{x}) = \text{Im}\{S_{11}(f_k)_M\} - \text{Im}\{S_{11}(f_k)_S\} \quad (5-4)$$

$$e_3(\mathbf{x}) = \text{Re}\{S_{21}(f_k)_M\} - \text{Re}\{S_{21}(f_k)_S\} \quad (5-5)$$

$$e_4(\mathbf{x}) = \text{Im}\{S_{21}(f_k)_M\} - \text{Im}\{S_{21}(f_k)_S\} \quad (5-6)$$

where $\text{Re}\{S_{11}(f_k)_M\}$ represents the real part of the S_{11} obtained from Matlab at the k -th frequency point, $\text{Im}\{S_{21}(f_k)_S\}$ is the imaginary part of the S_{21} obtained from Sonnet at the same frequency point, etc. Finally, an error vector function $\mathbf{e}(\mathbf{x})$ is defined by concatenating the four errors (5-3)-(5-6), and the norm of the complete error vector is minimized,

$$\mathbf{x}^* = \arg \min_{\mathbf{x}} \|\mathbf{e}(\mathbf{x})\|_2^2 \quad (5-7)$$

where $\mathbf{e}(\mathbf{x}) = [e_1(\mathbf{x}) \ e_2(\mathbf{x}) \ e_3(\mathbf{x}) \ e_4(\mathbf{x})]^T$.

As in many optimization methods, the selected initial value is very important to avoid local minimizers. Hence, the starting point selection is also crucial for the PE process.

5. A Parameter Extraction Process for Equivalent Circuit Models of a PRH TL in Matlab

5.3. The Starting Point for Parameter Extraction

The starting point for the particular PE problem to be solved can be computed from two equations with two unknowns, L and C . The first equation is obtained from the lossless characteristic impedance [Pozar-05],

$$Z_0 = \sqrt{\frac{L}{C}} \quad (5-8)$$

The second equation is obtained from the phase velocity, v_p , of the TEM mode [Pozar-05],

$$v_p = \frac{1}{\sqrt{LC}} = \frac{c}{\sqrt{\epsilon_e}} \quad (5-9)$$

where ϵ_e is the effective dielectric constant of the microstrip line, and can be computed as follows [Pozar-05],

$$\epsilon_e = \frac{\epsilon_r + 1}{2} + \frac{\epsilon_r - 1}{2\sqrt{1 + 10(H/W)}} \quad (5-10)$$

where ϵ_r is the substrate relative dielectric constant, H is the substrate height, and W is the width of the microstrip trace.

An approximate 50- Ω microstrip trace is considered. The corresponding parameters [Estrada-11] are: $\epsilon_r = 3$, $H = 5$ mils (0.127 mm) and $W = 12$ mils (0.305 mm). Using these parameters in (5-10), the effective permittivity is $\epsilon_e = 2.44$, and using (5-9), the corresponding phase velocity is $v_p = 192.05$ m/s. Solving (5-8) and (5-9) simultaneously, we obtain $L = 260.3$ nH/m, and $C = 104.14$ pF/m. These values can be used as a good starting point for the parameter extraction process for both lossless and lossy cases.

5.4. Parameter Extraction for the Lossless Case

5.4.1 The Fine Model Using Sonnet

The fine model, based on the 50- Ω microstrip lossless line described earlier, has the following additional parameters: $l = 240$ mils (6.096 mm), the dielectric loss tangent is zero, and

5. A Parameter Extraction Process for Equivalent Circuit Models of a PRH TL in Matlab

also the metal used is lossless and infinitesimally thin. The S-parameter responses are obtained with 50Ω reference ports. The simulation was performed from 1 GHz to 20 GHz.

5.4.2 The Coarse Model Using Matlab

The coarse model, based on a lumped element model of a PRH transmission line (see Chapter 4), has the following parameters: $l = 6.096$ mm, $Z_S = 0$, $Z_L = \infty$, $R = 0$, $G = 0$, $N = 10000$, and it uses $L = 260$ nH/m, $C = 104$ pF/m at the starting point for PE. By making $Z_S = 0$ and $Z_L = \infty$, the complete interconnect circuit model (see Chapter 4) computes only the S-parameters of the transmission line segments.

5.4.3 Responses before Parameter Extraction

The S_{11} and S_{21} responses for both Sonnet and Matlab models are shown in Fig. 5-1 and Fig. 5-2, respectively.

Although the reflection response $|S_{11}|$ (see Fig. 5-1a) has a similar shape in both Sonnet and Matlab responses, there is a clear difference in the magnitude. It is expected the Matlab magnitude response to be smaller than Sonnet response, due the lossless ideally matched TL model used as the coarse model. Although the starting point meets the ideal characteristic

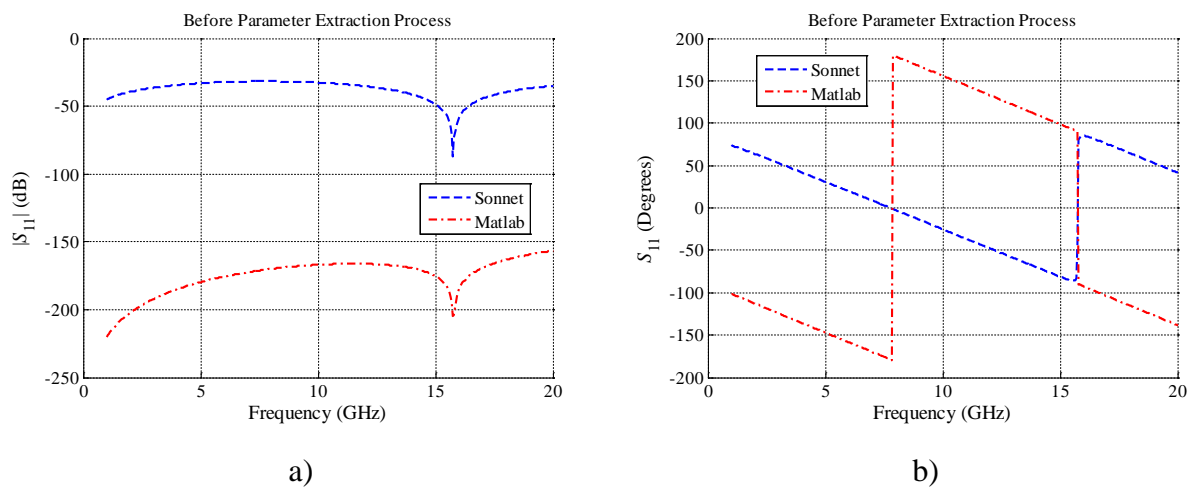


Fig. 5-1 S_{11} comparison before parameter extraction for the lossless case: a) magnitudes (dB) obtained in Sonnet and Matlab model, and b) phase (degrees) obtained in Sonnet and Matlab model.

5. A Parameter Extraction Process for Equivalent Circuit Models of a PRH TL in Matlab

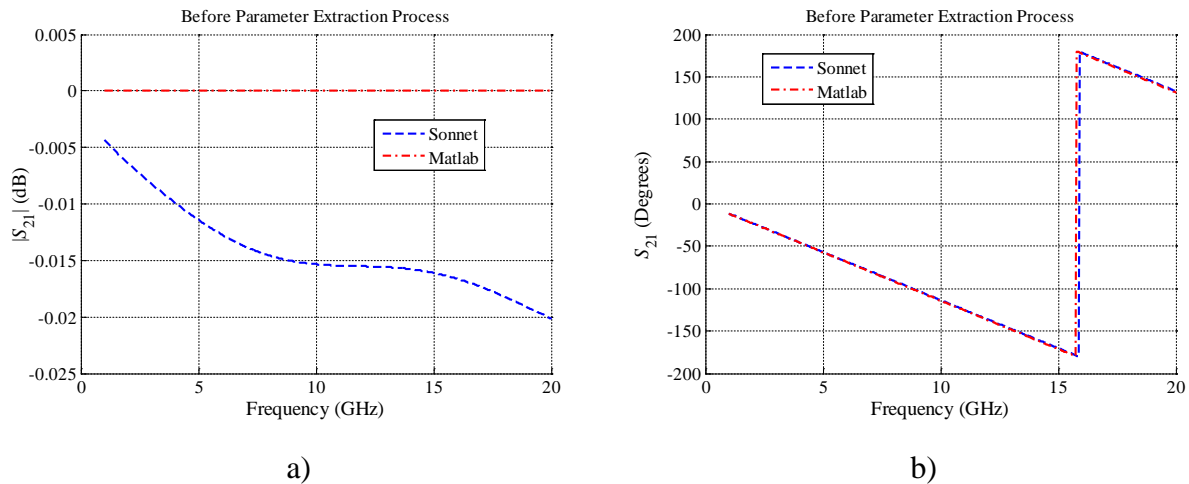


Fig. 5-2 S_{21} comparison before parameter extraction for the lossless case: a) magnitudes (dB) obtained in Sonnet and Matlab model, and b) phase (degrees) obtained in Sonnet and Matlab model.

impedance (5-8), this is not representing the real characteristic impedance that indirectly is computed by Sonnet. However, both models show very low reflection, as expected. In contrast, the phase of S_{11} (see Fig. 5-1b) shows a major difference between Sonnet and Matlab responses.

The transmission response $|S_{21}|$ (see Fig. 5-2a) shows a small relative difference between Sonnet and Matlab responses. The magnitude of the difference is less than 0.02 dB, which is a relatively good match. In this case, it is also expected to have $|S_{21}| = 0$ dB on the Matlab response, due the lossless ideally matched TL model used. The phase of S_{21} (see Fig. 5-2b) shows a good match between both models.

The Matlab responses in (see Fig. 5-1 and Fig. 5-2) show expected values: a very low reflection and a total transmission magnitude values. Sonnet responses, on the other hand, show a more realistic behavior, however, they are relatively close to Matlab responses. This confirms that we have selected a suitable starting point for optimization. In general, the above differences between both models indicate that the coarse model can be optimized to match the fine model with higher accuracy.

5.4.4 The LC Extracted Parameters

Once the PE process is completed at each frequency, the new LC values are shown in Fig. 5-3. The extracted L values are shown in Fig. 5-3a, and the average value is ~ 265 nH/m. The

5. A Parameter Extraction Process for Equivalent Circuit Models of a PRH TL in Matlab

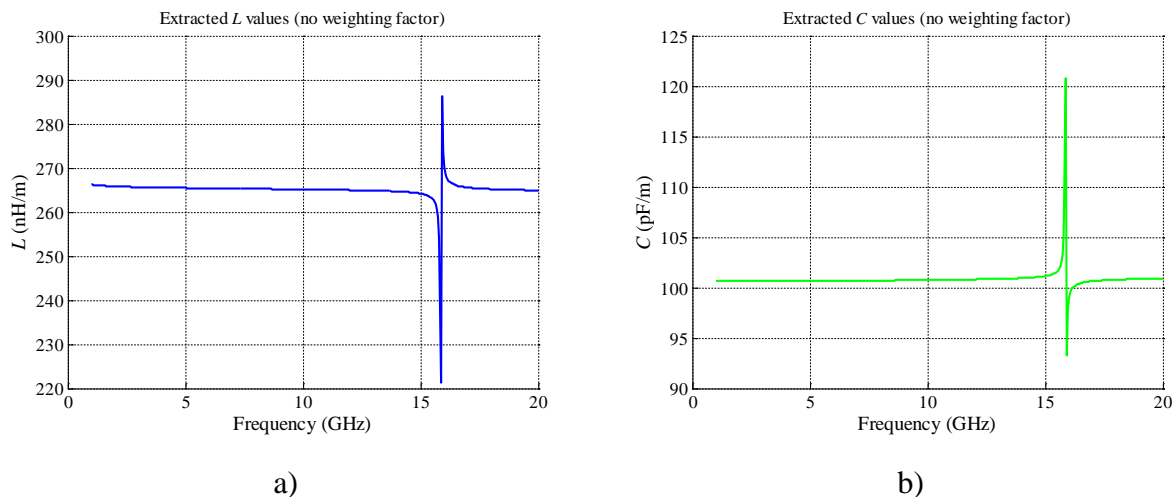


Fig. 5-3 Extracted values for the lossless case with no weighting factor in the parameter extraction algorithm: a) inductance values, and b) capacitance values.

extracted C values are shown in Fig. 5-3b, and the average value is ~ 101 pF/m.

As observed in both extracted values in Fig. 5-3, there are two peaks approximately at 16 GHz. According to the real and imaginary responses of Sonnet and Matlab models, shown in Fig. 5-4 and Fig. 5-5, three of the four responses are zero around 16 GHz. Only the real part of S_{21} is non-zero around 16 GHz, and hence the PE process is minimizing only the norm of e_3 around that frequency. Hence, we have more unknowns than equations at that particular frequency, and this problem becomes ill-conditioned. This causes the peaks in both plots of the LC extracted values.

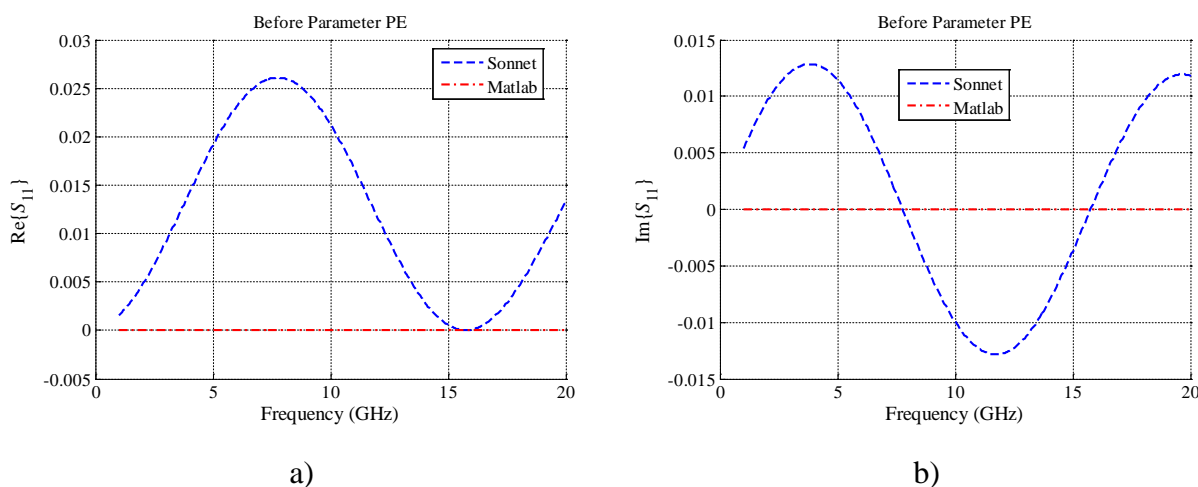


Fig. 5-4 S_{11} comparison before parameter extraction for the lossless case: a) real values obtained in Sonnet and the Matlab model, and b) imaginary values obtained in Sonnet and the Matlab model.

5. A Parameter Extraction Process for Equivalent Circuit Models of a PRH TL in Matlab

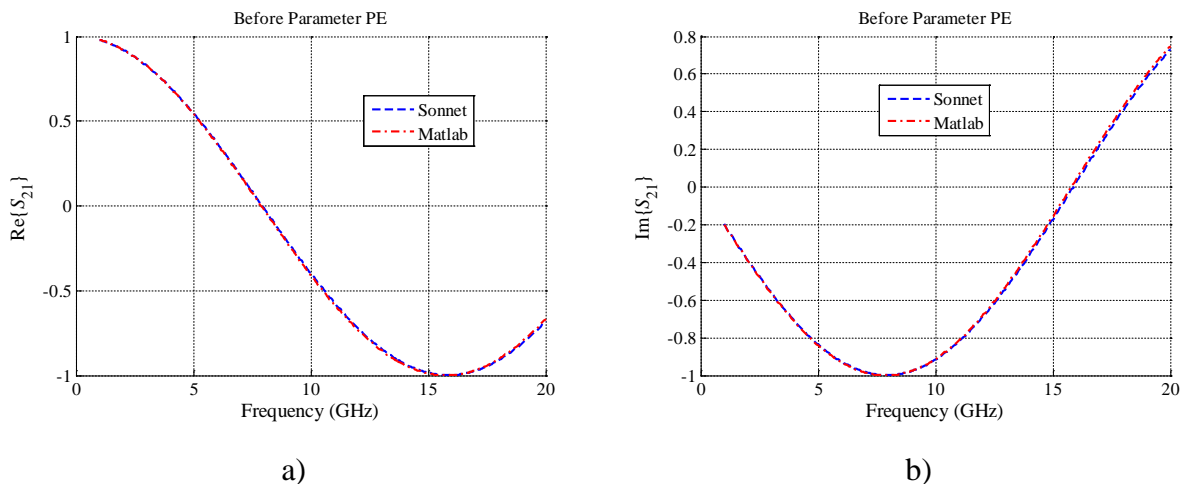


Fig. 5-5 S_{21} comparison before parameter extraction for the lossless case: a) real values obtained in Sonnet and Matlab model, and b) imaginary values obtained in Sonnet and Matlab model.

The above ill-conditioned problem can be avoided by introducing a penalty term in the objective function (5-7). This was implemented by defining the penalty term as a weighting factor applied to the norm of the difference between the extracted parameters and the previous optimal solution, obtained at the previous frequency point, such that when the extracted solution deviates too much from the previous optimal solution, the objective function is penalized (increased).

The Fig. 5-6 shows the new extracted LC values using the weighting factor to minimize the differences between the previous optimal solution and next extracted values. The new

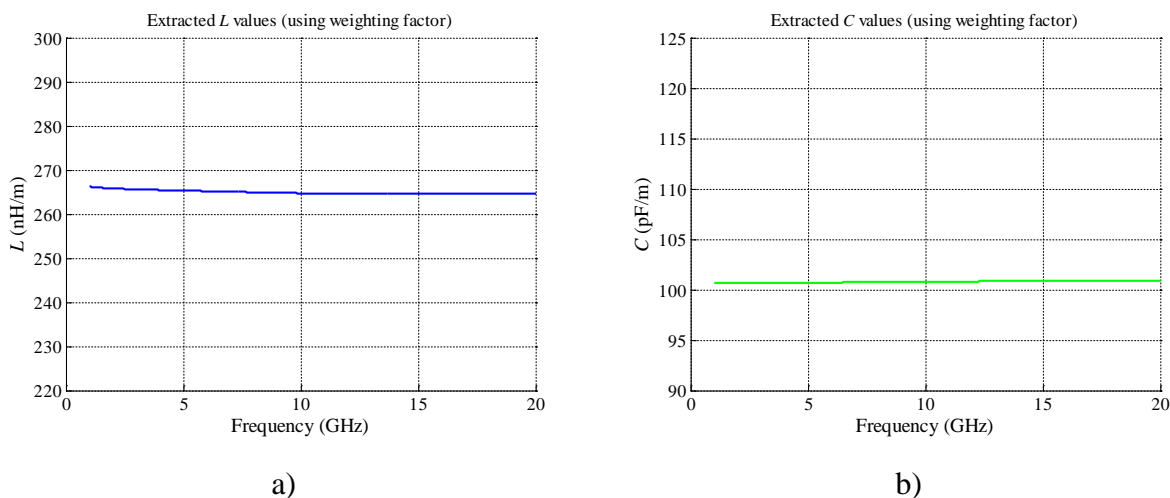


Fig. 5-6 Extracted values for the lossless case with weighting factor in the parameter extraction algorithm: a) inductance values, and b) capacitance values.

5. A Parameter Extraction Process for Equivalent Circuit Models of a PRH TL in Matlab

extracted L values with this weighting factor are in Fig. 5-6a, and the average value is ~ 265 nH/m. Similarly, the new extracted C values with this weighting factor are in Fig. 5-6b, and the average value is ~ 101 pF/m. It is confirmed that the peaks in both plots of the LC extracted values are practically eliminated by adding this penalty term in the original objective function.

5.4.5 Responses after Parameter Extraction

The extracted LC average values for the PRH lossless case are: $L = 265$ nH/m and $C = 101$ pF/m. The S_{11} and S_{21} responses, for both Sonnet and Matlab models, are shown in Fig. 5-7 and Fig. 5-8, respectively.

The Matlab model reflection response $|S_{11}|$ (see Fig. 5-7a) now shows an excellent match with Sonnet responses. Similarly, the phase of S_{11} (see Fig. 5-7b) also shows an excellent match with Sonnet responses. Although small differences are present, they exist because the coarse model is loaded with average values, and in the real world behavior, confirmed in our PE results, these values change with frequency.

The transmission response $|S_{21}|$ (see Fig. 5-8a) shows a better match between the Sonnet and Matlab responses than that one found in Fig. 5-2a. Similarly, the phase of S_{21} (see Fig. 5-8b) shows an excellent match between Sonnet and Matlab responses.

In general, it is confirmed that the responses with extracted LC parameters provide a

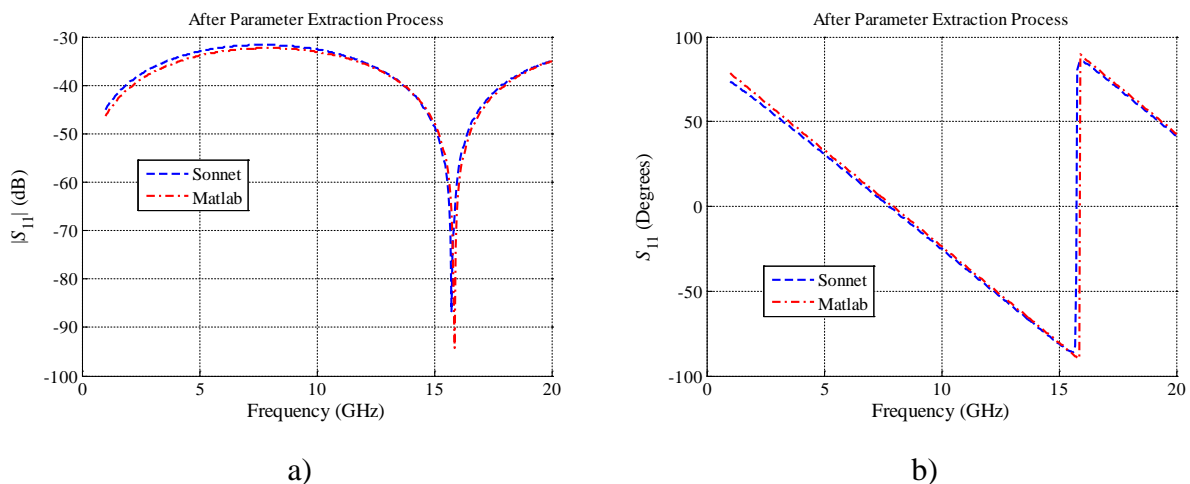


Fig. 5-7 S_{11} comparison after parameter extraction for the lossless case: a) magnitudes (dB) obtained in Sonnet and Matlab model, and b) phase (degrees) obtained in Sonnet and Matlab model.

5. A Parameter Extraction Process for Equivalent Circuit Models of a PRH TL in Matlab

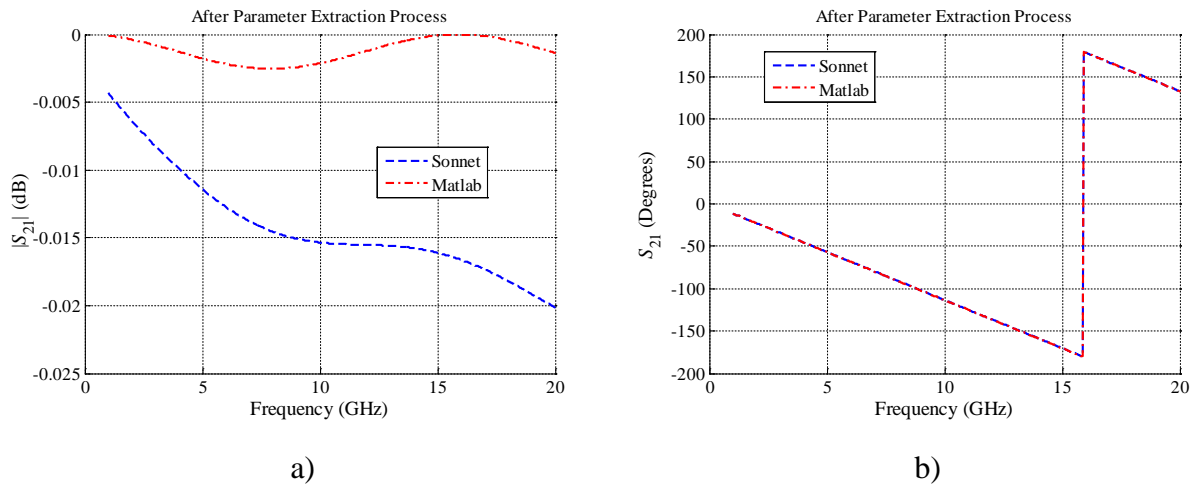


Fig. 5-8 S_{21} comparison after parameter extraction for the lossless case: a) magnitudes (dB) obtained in Sonnet and Matlab model, and b) phase (degrees) obtained in Sonnet and Matlab model.

better match between the coarse and fine models, in both magnitudes and angles.

5.5. Parameter Extraction for the Lossy Case

5.5.1 The Fine Model Using Sonnet

The fine model, based on the 50- Ω microstrip lossy line described earlier, has the following additional parameters: the dielectric loss tangent is 0.0013, the metal thickness is 0.65 mils (0.01651 mm), and the metal conductivity is 5.8×10^7 S/m. All the remaining settings in Sonnet are defined as in the lossless case.

5.5.2 The Coarse Model Using Matlab

The coarse model, based on a lumped element model of a PRH transmission line (see Chapter 4), has the same LC parameters as in the lossless case. But it uses $L = 260$ nH/m, $C = 104$ pF/m, $R = 0.001$ Ω /m, $G = 0.001$ S/m at the starting point for PE.

5. A Parameter Extraction Process for Equivalent Circuit Models of a PRH TL in Matlab

5.5.3 Responses before Parameter Extraction

The S_{11} and S_{21} responses for both Sonnet and Matlab models are shown in Fig. 5-9 and Fig. 5-10, respectively.

Similarly to the lossless case, $|S_{11}|$ (see Fig. 5-9a) has a similar shape in both Sonnet and Matlab responses, however, there is a clear difference in the magnitude. Again, it is expected the

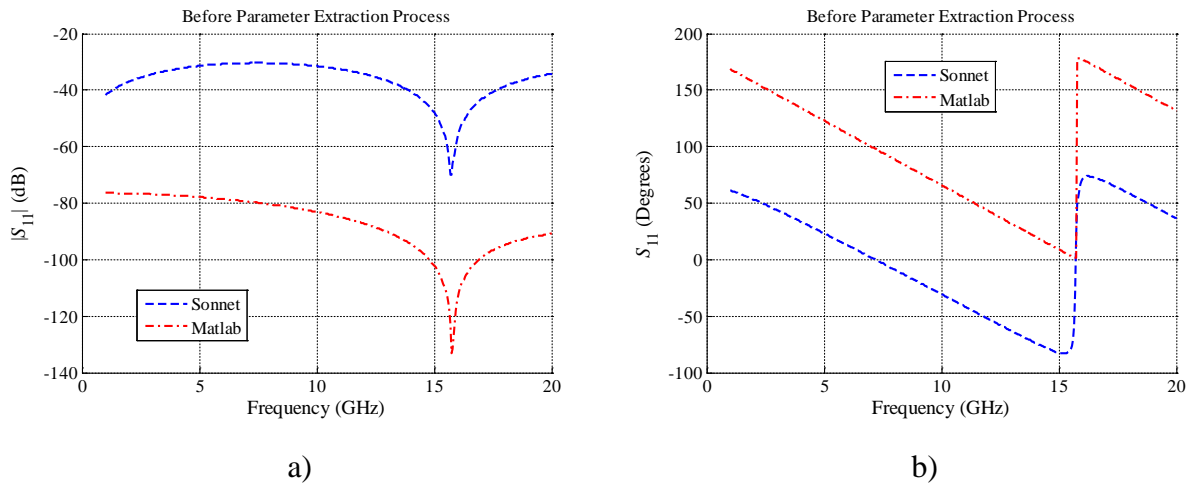


Fig. 5-9 S_{11} comparison before parameter extraction process for the lossy case: a) magnitudes (dB) obtained in Sonnet and Matlab model, and b) phase (degrees) obtained in Sonnet and Matlab model.

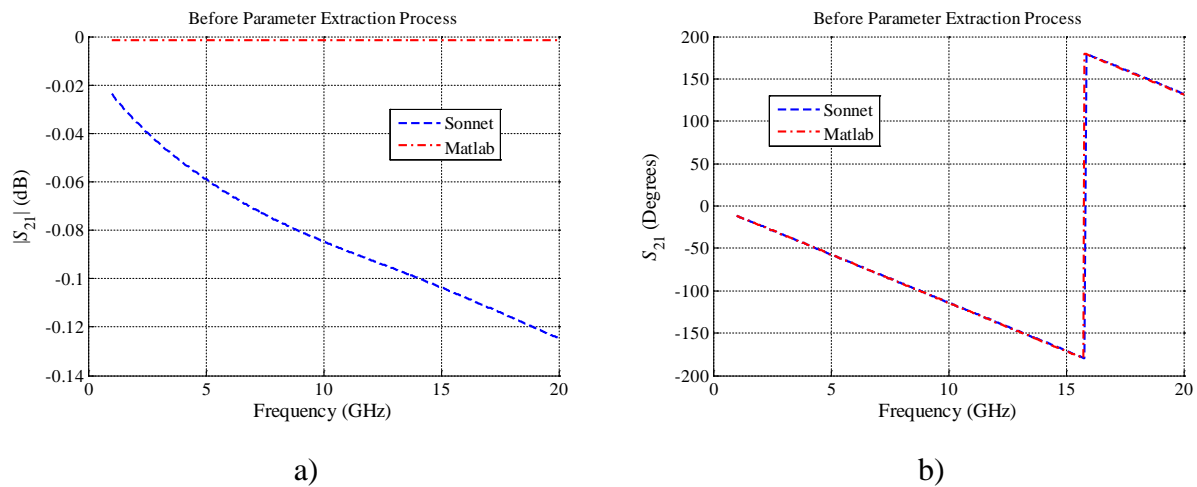


Fig. 5-10 S_{21} comparison before parameter extraction process for the lossy case: a) magnitudes (dB) obtained in Sonnet and Matlab model, and b) phase (degrees) obtained in Sonnet and Matlab model.

5. A Parameter Extraction Process for Equivalent Circuit Models of a PRH TL in Matlab

Matlab reflection to be smaller than Sonnet's, since the initial R and G parameters are very small and the line is ideally matched. However, both models show relatively low reflection, as expected. Additionally, as in the lossless case, the phase of S_{11} (see Fig. 5-9b) shows a major difference between Sonnet and Matlab.

The transmission response $|S_{21}|$ (see Fig. 5-10a) before PE shows a larger difference between Sonnet and Matlab responses than that one for the lossless case (see Fig. 5-2a). It is confirmed that the Matlab response has $|S_{21}| < 0$ dB due to the non-zero R and G parameter values. As in the lossless case, the phase of S_{21} (see Fig. 5-10b) shows a good match between both models before PE.

Again, Sonnet responses show a more realistic behavior than Matlab responses, however, overall they are similar, which confirms that we have selected a suitable starting point for optimization in the lossy case.

5.5.4 Initial RGLC Extracted Parameters

The PE process in this section is achieved with a weighting factor similar to that one used in previous section, to reduce the ill-conditioned problem around 16 GHz. The extracted $RGLC$ values are shown in Fig. 5-11 and Fig. 5-12. The extracted L values are shown in Fig. 5-11a, and the average value is ~ 267.4 nH/m. The extracted C values are shown in Fig. 5-11b, and the

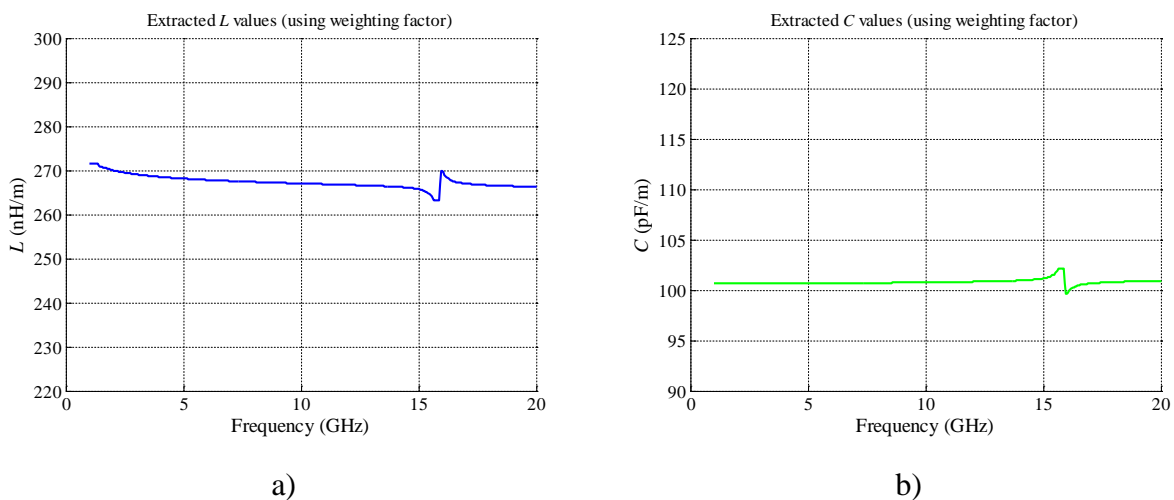


Fig. 5-11 Extracted values for the lossy case with a weighting factor in the parameter extraction algorithm: a) inductance values, and b) capacitance values.

5. A Parameter Extraction Process for Equivalent Circuit Models of a PRH TL in Matlab

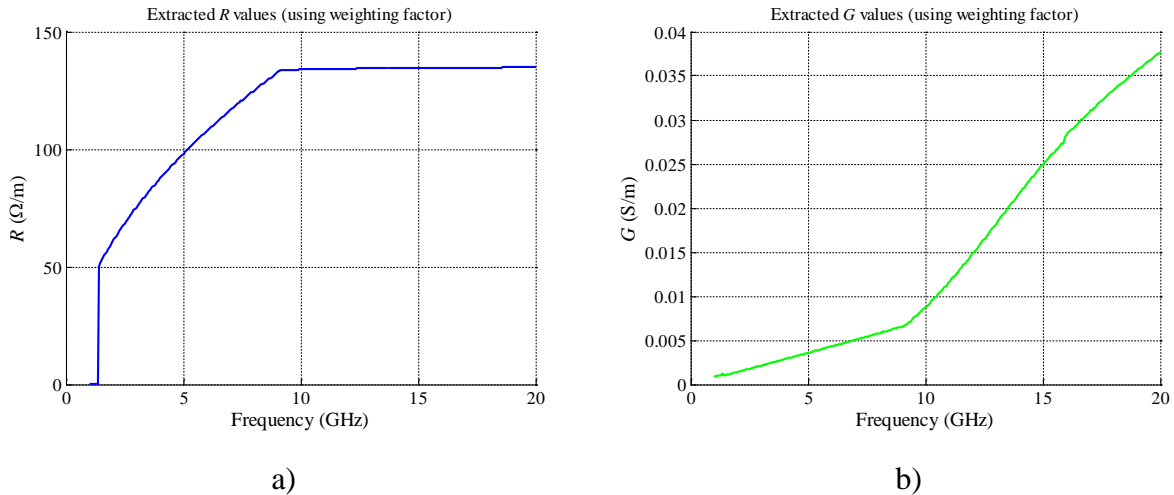


Fig. 5-12 Extracted values for the lossy case with a weighting factor in the parameter extraction algorithm: a) resistance values, and b) conductance values.

average value is ~ 100.7 pF/m. The extracted R values are shown in Fig. 5-12a, and the average value is ~ 120.19 Ω/m . The extracted G values are shown in Fig. 5-12b, and the average value is ~ 0.0138 S/m.

As observed in the L and C extracted values in Fig. 5-11, there are still two small peaks approximately at 16 GHz. These peaks were not completely removed as in the lossless case. When using a large value for the weighting factor, these peaks were decreased at the expense of a poorer overall matching. The selected weighting factor achieves a reasonable balance.

As observed in the extracted R values in Fig. 5-12a, they are approximately 50 Ω in the lower frequency ranges, and it changes as frequency is increased. This change can be explained by the skin effect indirectly computed in Sonnet EM response. Similarly, the extracted G values in Fig. 5-12b increase with frequency, as expected.

It is also important to notice that no peaks are observed in R and G extracted values around 16 GHz. This is due the penalty term added to the norm of the difference between the extracted parameters, and the previous optimal solution obtained in the previous frequency point.

5.5.5 Responses after Initial parameter Extraction

The extracted $RGLC$ average values for the PRH lossy case are: $L = 267.4$ nH/m, $C = 100.7$ pF/m, $R = 120.19$ Ω/m , and $G = 0.0138$ S/m. The S_{11} and S_{21} responses, for both Sonnet and Matlab models, are shown in Fig. 5-13 and Fig. 5-14 respectively.

5. A Parameter Extraction Process for Equivalent Circuit Models of a PRH TL in Matlab

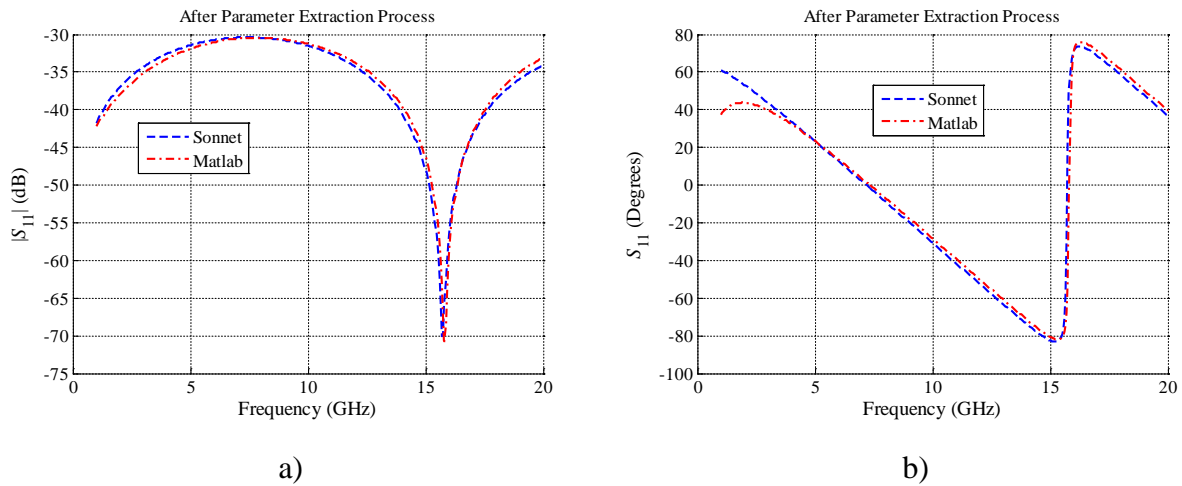


Fig. 5-13 S_{11} comparison after parameter extraction process for the lossy case: a) magnitudes (dB) obtained in Sonnet and Matlab model, and b) phase (degrees) obtained in Sonnet and Matlab model.

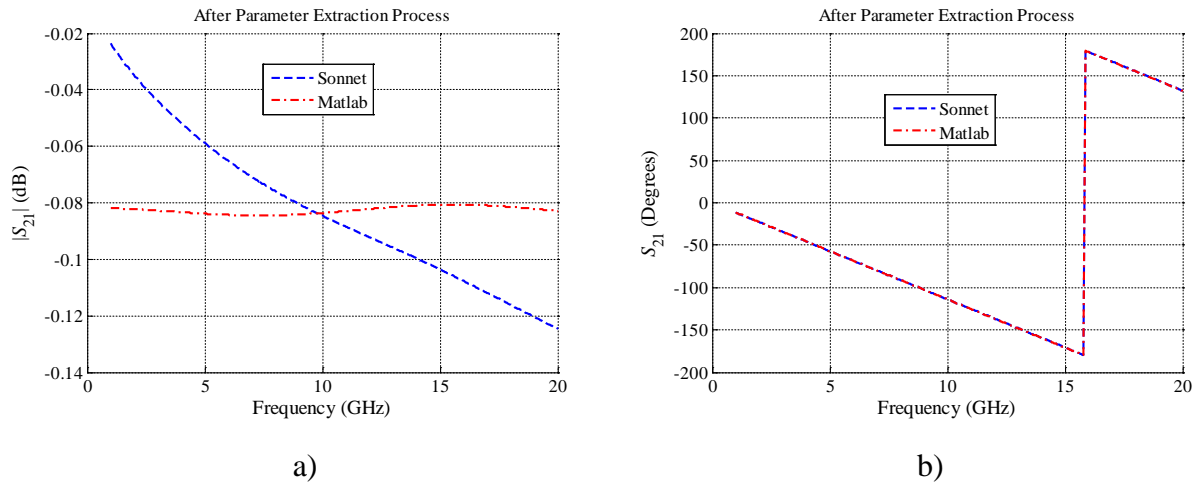


Fig. 5-14 S_{21} comparison after parameter extraction process for the lossy case: a) magnitudes (dB) obtained in Sonnet and Matlab model, and b) phase (degrees) obtained in Sonnet and Matlab model.

The Matlab model reflection responses $|S_{11}|$ (see Fig. 5-13a) now shows an excellent match with Sonnet responses. Similarly, the phase of S_{11} (see Fig. 5-13b) also shows an excellent match between Matlab and Sonnet responses above approximately 4 GHz.

The transmission response $|S_{21}|$ (see Fig. 5-14a) shows a better match between Sonnet and Matlab responses than that one found in Fig. 5-10a. The average value of the Matlab model response is closer to the average value of the Sonnet model response. Similarly, the phase of S_{21} (see Fig. 5-14b) shows an excellent exact match between Sonnet and Matlab responses.

5. A Parameter Extraction Process for Equivalent Circuit Models of a PRH TL in Matlab

In general, it is confirmed that the responses with extracted $RGLC$ parameters provide a better match between the coarse and fine models, in both magnitudes and angles, with the respect to the responses at the starting point.

5.5.6 An Enhanced PE for the Lossy Case

As seen in the previous results, the response of the Matlab model with extracted parameters show some poor matching in the low-frequency range, as well as some not-smooth behavior in the S-parameters using the extracted values for R and G . To improve the extracted responses, the ill-conditioned effect needs to be either removed or reduced; one way to reduce the ill-condition effect of an optimization problem is by reducing the number of the optimization variables. The best candidate to be removed from the optimization variables is the C parameter. By observing the lossless case (see Fig. 5-6b) and the lossy case (see Fig. 5-11b), it is seen that minor changes have occurred on the C average values. Hence, the C parameter is removed from the optimization variables and maintained fixed as in the lossless case, $C = 101$ pF/m. Finally, only the L , R , and G parameters are optimized.

The L extracted values are shown in Fig. 5-15a, and the average value is 267.14 nH/m. As it is observed the peaks have disappeared and a smooth response is obtained. The R extracted values are shown in Fig. 5-15b, and the average value is 151.49 Ω /m. It is seen that the flat

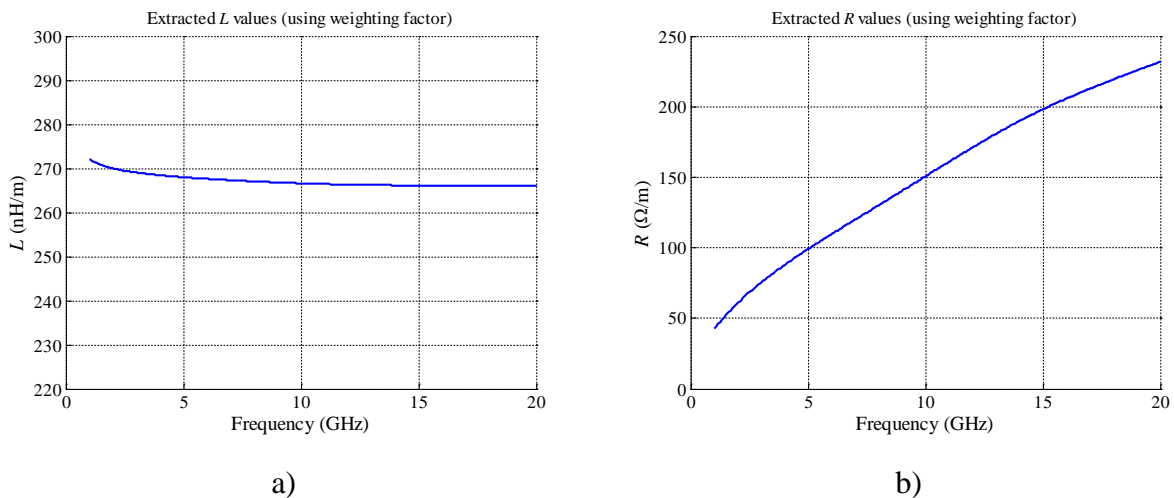


Fig. 5-15 Extracted values for the enhanced lossy case with a weighting factor in the parameter extraction algorithm: a) inductance values, and b) resistance values.

5. A Parameter Extraction Process for Equivalent Circuit Models of a PRH TL in Matlab

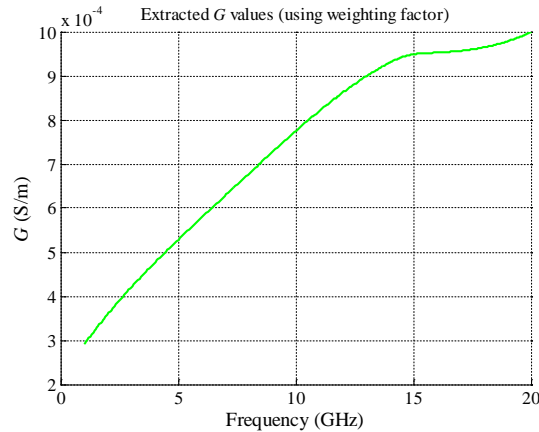


Fig. 5-16 Extracted values for the enhanced lossy case with a weighting factor in the parameter extraction algorithm: conductance values.

behavior in the previous response after 10 GHz (see Fig. 5-12a) is removed, and a smoother response is obtained. The smoother response provides confidence that it is a better approximation of the real physical behavior. The G extracted values are shown in Fig. 5-16, and the average value is 0.6562 mS/m. By comparing the enhanced response (see Fig. 5-16) with the previous response (see Fig. 5-12b), it is observed that a smoother response is obtained. Although small differences are obtained after 15 GHz, it is clearly observed a smooth trend before 15 GHz. In the case of the G extracted values, a smoother response also provides confidence that it is a better approximation of the real physical behavior.

The extracted $RGLC$ average values for the enhanced PRH lossy case are: $L = 267.14$ nH/m, $C = 101$ pF/m, $R = 151.49$ Ω /m, and $G = 0.6562$ mS/m. The S_{11} and S_{21} responses, for both Sonnet and Matlab models, are shown in Fig. 5-17 and Fig. 5-18, respectively.

The Matlab model reflection responses $|S_{11}|$ (see Fig. 5-17a) now shows a better match with Sonnet responses in the high frequency range than the one obtained in Fig. 5-13a, but equal or lower match in the low frequency range. Similarly, the phase of S_{11} (see Fig. 5-17b) also shows a better match with Sonnet in the high frequency range if compared with Fig. 5-13b, but worse match between Matlab and Sonnet responses below 10 GHz.

The transmission response $|S_{21}|$ (see Fig. 5-18a) now shows a larger match between Sonnet and Matlab responses than that one found in Fig. 5-14a. The average value of the Matlab model response apparently has a larger match to the average value of the Sonnet model response in the high frequency range, than the Matlab response obtained in Fig. 5-14a. The phase of S_{21} in Fig. 5-18b, now shows a poorer match between Sonnet and Matlab responses around 16 GHz,

5. A Parameter Extraction Process for Equivalent Circuit Models of a PRH TL in Matlab

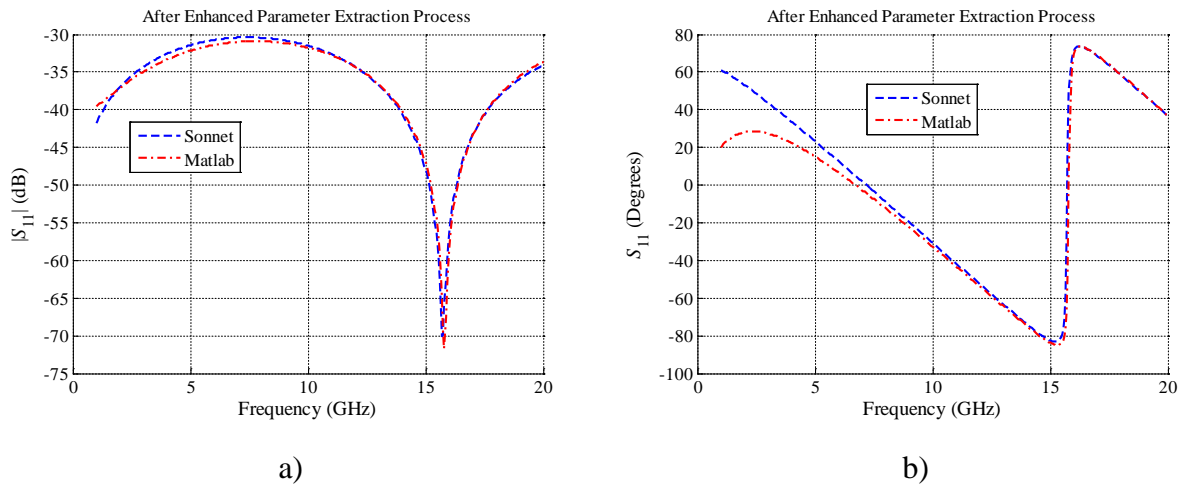


Fig. 5-17 S_{11} comparison after enhanced parameter extraction process for the lossy case: a) magnitudes (dB) obtained in Sonnet and Matlab model, and b) phase (degrees) obtained in Sonnet and Matlab model.

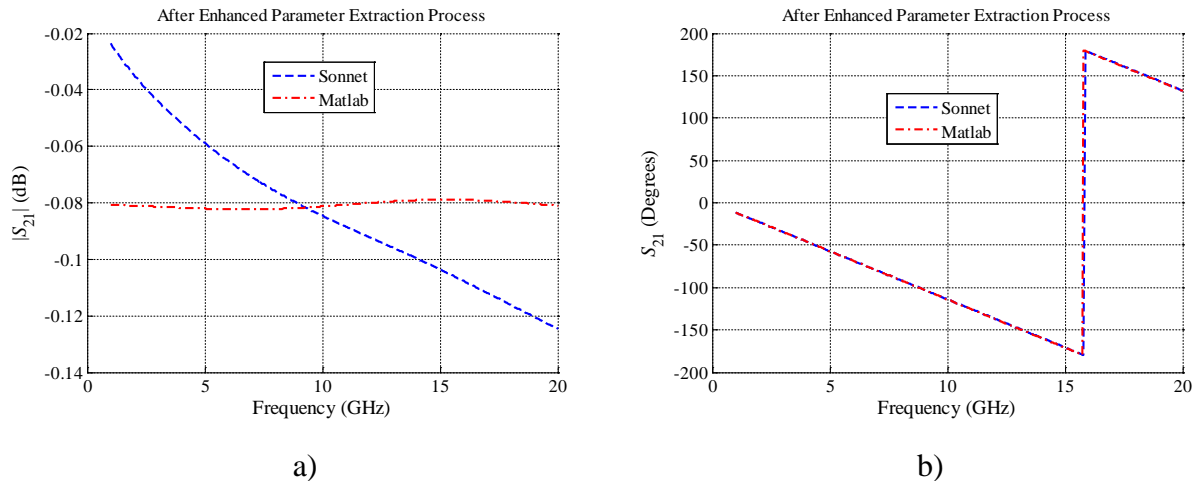


Fig. 5-18 S_{21} comparison after enhanced parameter extraction process for the lossy case: a) magnitudes (dB) obtained in Sonnet and Matlab model, and b) phase (degrees) obtained in Sonnet and Matlab model.

than that one perfectly matched in Fig. 5-14b.

In general, it is confirmed that the quality of the extracted responses are affected by the ill-conditioned effects on each PE problem. In this chapter it is observed that, by removing one optimization variables to attenuate the ill-conditioned effect, the extracted values have smoother responses. In this particular case, those smoother responses can be understood as a better approximation to the real physical behavior of a microstrip trace.

As expected, the differences shown in Fig. 5-17 and Fig. 5-18 are due to the inherent

5. A Parameter Extraction Process for Equivalent Circuit Models of a PRH TL in Matlab

differences of the coarse and fine model. In real world behavior the *RGLC* parameters change with frequency and the coarse model is using average values on the studied frequency range.

5.6. Conclusions

A procedure to extract the equivalent circuitual *RGLC* values of a purely right-handed (PRH) transmission line (TL) was presented in this Chapter. The parameter extraction (PE) process was based in the comparison of the real and imaginary values of the S-parameter responses of the fine model (50- Ω microstrip line electromagnetic simulation), and coarse model (PRH TL circuitual model in Matlab). The fine and coarse model responses were presented before and after the PE implementation and the expected results were shown.

It was demonstrated that simple direct parameter extraction process can be used to obtain the equivalent *RGLC* values of lumped element models from a target response, in the frequency range where the *RGLC* transmission line model is still valid. However, it was also demonstrated that these parameter extraction problems can be ill-conditioned at some frequency ranges, in which case a number of techniques can be applied to decrease the ill-condition effects, such as using penalty functions with suitable weighting factors, or reducing the number of optimization variables. Similar circuitual models will be used in following chapters to perform a parameter extraction of 3D electromagnetic simulated structures, to finally approximate the right/left-handed parameters L_L , C_L , L_R and C_R , and obtain the LH and RH regions of operation of actual physical structures.

6. Physical Implementation of Composite Right/Left-Handed Transmission Lines

6.1. Introduction

The physical implementation of composite right/left-handed (CRLH) transmission lines (TL) can be achieved in different manners (see Chapter 1). Such transmission line structures can be implemented using different technologies, as microstrip technology and discrete chip components in surface-mount technology (SMT). Several physical implementations of these structures are briefly described in this chapter. This compilation is restricted to one dimension (1D) physical structures only, such as planar transmission lines using microstrip technology and discrete chip components in SMT technology.

In Section 6.2, it is briefly explained several CRLH TL structures built with microstrip technology only, such structures are constituted mainly of interdigital capacitors. In Section 6.3, it is briefly explained several CRLH TL structures built with microstrip technology and discrete SMT components soldered over the microstrip structure. Finally, the conclusions and future work description are presented in Section 6.4.

6.2. Composite Right/Left-Handed TL with Distributed Implementation

There are several ways to implement high-speed interconnect structures with metamaterial behavior. Some of the important characteristic of such structures are, among others, the conductor's shape, the dielectric properties, the number of unit-cells, etc. The physical implementations described in this Section are built similarly, with microstrip technology only and without discrete SMT components.

6. Physical Implementation of Composite Right/Left-Handed Transmission Lines

6.2.1 Conventional CRLH TL with Interdigital Capacitors

A typical implementation of a composite right/left-handed transmission line is shown in Fig. 6-1. This structure is constituted by interdigital capacitors and stub inductors shorted to the ground plane by a via [Caloz-06]. The unit-cell is centered in the plane defined by the longitudinal axis of the stub, and represents a T-network constituted by two impedance branches with capacitance $2C_L$ and inductance $L_R/2$, and by an admittance branch with inductance L_L and capacitance C_R . The equivalent circuit for this implementation can be modeled by the T-network in Fig. 6-2. The left-handed contributions C_L and L_L are provided by the interdigital capacitors and stub inductors, and the right-handed contributions C_R and L_R exist from their parasitic reactances and have an increasing effect as the frequency is increased. The parasitic inductance

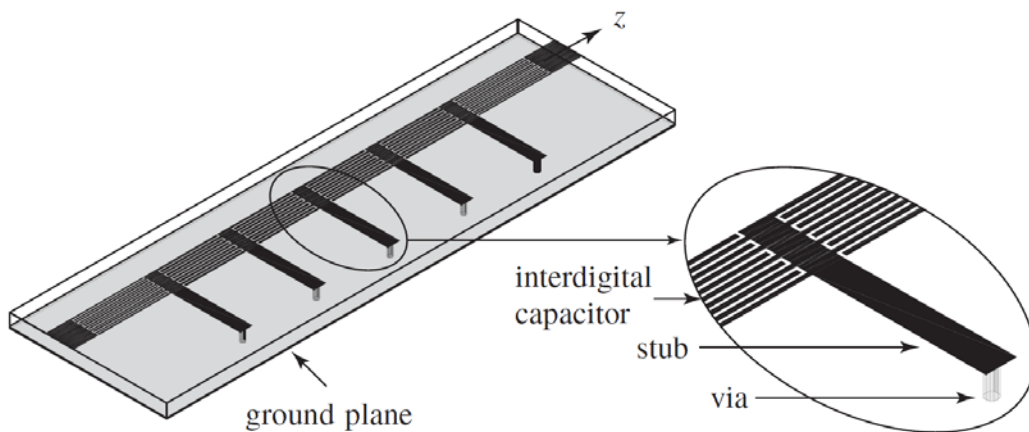


Fig. 6-1 Microstrip dual composite right/left-handed transmission line using interdigital capacitors and shorted stub inductors. Figure extracted from [Caloz-06].

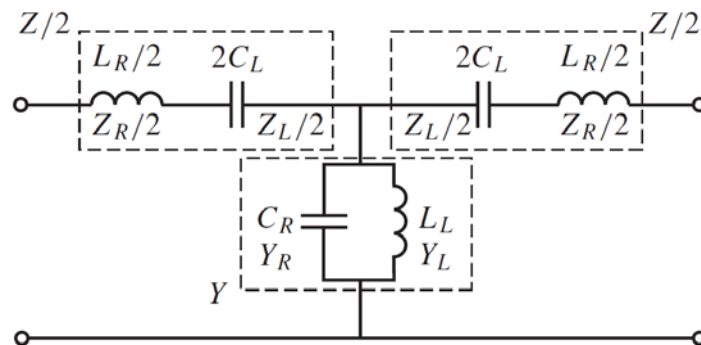


Fig. 6-2 Symmetric unit-cell of the LC composite right/left-handed TL implemented in Fig. 6-1. Impedance $Z/2$ represents half of the interdigital capacitor, while admittance Y represents the short-circuited stub. Figure extracted from [Caloz-06].

6. Physical Implementation of Composite Right/Left-Handed Transmission Lines

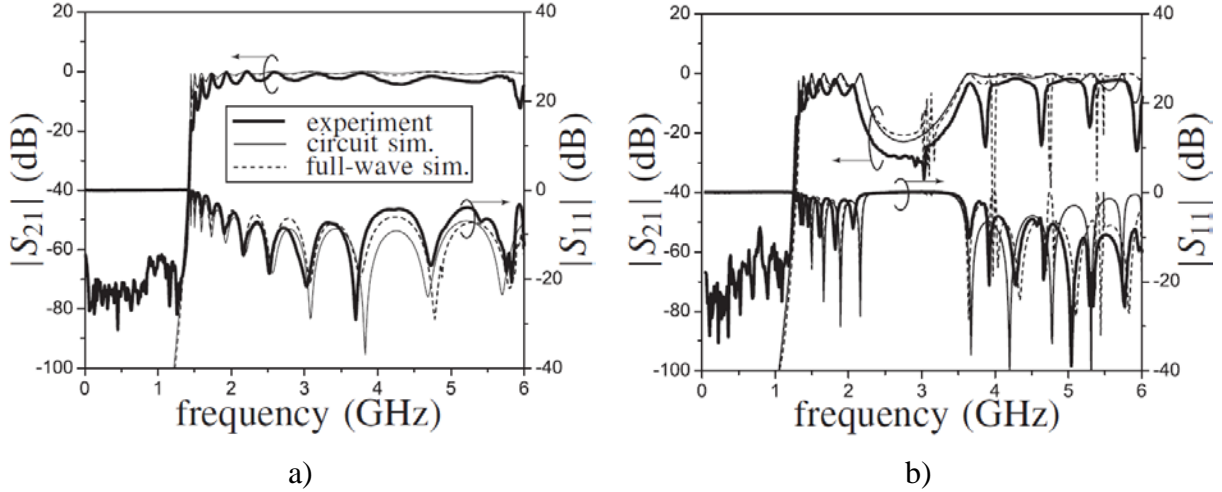


Fig. 6-3 Responses of the LC dual composite right/left-handed transmission line implemented in Fig. 6-1: a) the S parameter response of a D-CRLH TL with a 9 cells balanced design, b) the S parameter response of a D-CRLH TL with a 7 cells unbalanced design. Figure extracted from [Caloz-06].

L_R is due to the magnetic flux generated by the currents flowing along the digits of the capacitor and the parasitic capacitance C_R is due to the parallel-plate voltage gradients existing between the trace and the ground plane. The S -parameter response reported in [Caloz-06] for this CRLH transmission line implementation is shown in Fig. 6-3. The Fig. 6-3a shows the S -parameter response of a 9-cell balanced design, and no stop band is shown between the LH and RH propagation regions. The Fig. 6-3b shows the S -parameter response of a 7-cell unbalanced design, and a stop band is shown between the LH and the RH propagation regions. The geometric details of such implementations are described in [Caloz-06].

6.2.2 Simplified Extended CRLH TL with Interdigital Capacitors

Another physical implementation of a high-speed interconnect structure with metamaterial behavior is the simplified extended (SE) CRLH TL structure shown in Fig. 6-4a [Qiang-10]. The equivalent circuit of this implementation is shown in Fig. 6-4b. According to [Qiang-10], the capacitance C_D and the inductance L_D of the parallel resonance tank connected in series depend on the number of the interdigital fingers and/or their gap width, and its closed stub size, respectively. The capacitance C_S and inductance L_S of the series resonance tank connected in parallel depend on the dimension of the rectangular patch and the conjoint stub, respectively.

6. Physical Implementation of Composite Right/Left-Handed Transmission Lines

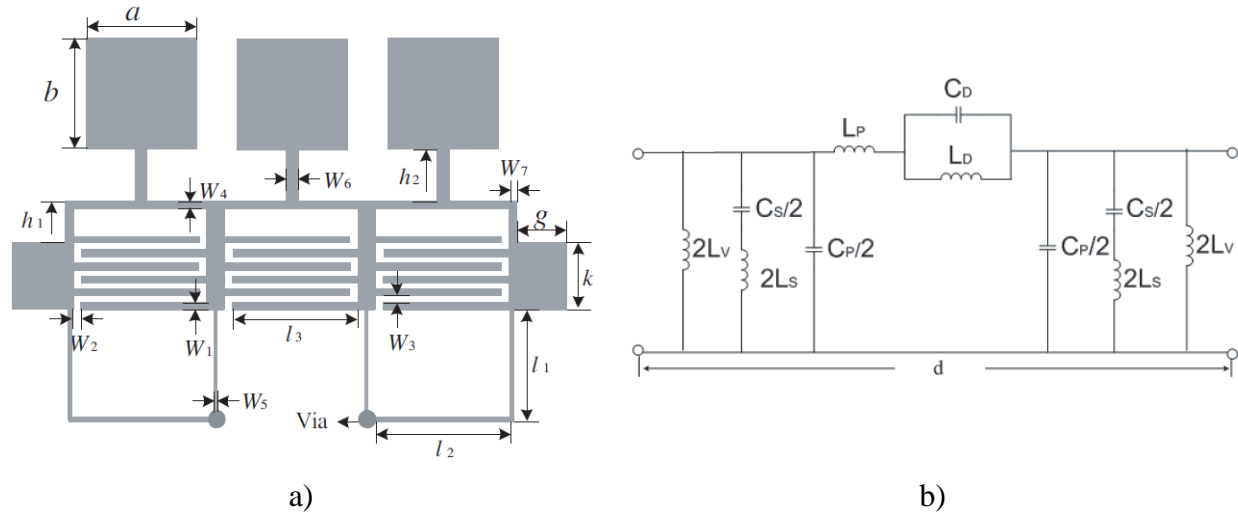


Fig. 6-4 The simplified extended CRLH TL using interdigital capacitors and short stub/series inductors: a) the microstrip physical implementation, b) the symmetric unit-cell model. Figure extracted from [Qiang-10].

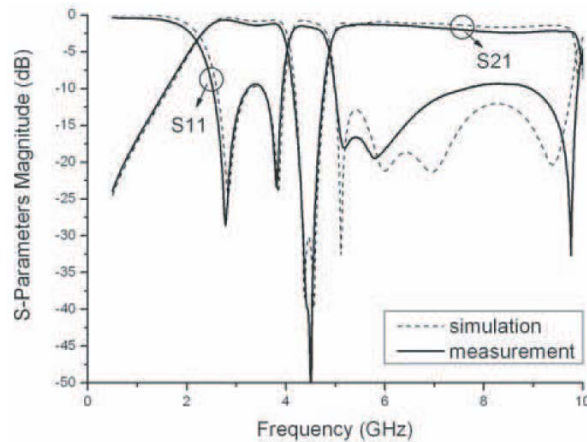


Fig. 6-5 Responses of the LC simplified extended composite right/left-handed TL implemented in Fig. 6-4a with a 3 stages design. Figure extracted from [Qiang-10].

The inductance L_V depends on the stub with metallic via hole. The series inductance L_P and shunt capacitance C_P are due to the inherent parasitic RH effect. To further reduce the size of the SE-CRLH structure, the grounded stub is bended and connected with the common metallic via as shown in Fig. 6-4a [Qiang-10].

The S-parameter response $|S_{21}|$ reported in [Qiang-10] for the physical implementation is shown in Fig. 6-5. The response shows two broadband balanced conditions [Qiang-10], although it is similar to the unbalanced CRLH case (see Fig. 6-3b), it also shows a stop band between the LH and RH propagation regions.

6. Physical Implementation of Composite Right/Left-Handed Transmission Lines

6.2.3 Composite Right/Left-Handed TL with Wire Bonded Interdigital Capacitors

An improvement of the conventional CRLH TL with interdigital capacitors (see Fig. 6-1), is the CRLH TL using wire bonded interdigital capacitors (WBIC) shown in Fig. 6-6 [Sanchez-09]. The use of the wire bonded interdigital capacitor (see Fig. 6-7b) eliminates the resonances due to the multiconductor nature of the interdigital capacitor [Sanchez-09]. The shunt inductance can also be implemented by an interdigital capacitor, operating at a frequency where is no longer a capacitor, but an inductor due to the usage of a row of vias connected to ground (see Fig. 6-6). The analytical model of such structure is shown in Fig. 6-8 [Sanchez-09], including one WBIC working as capacitor, and other WBIC working as inductor.

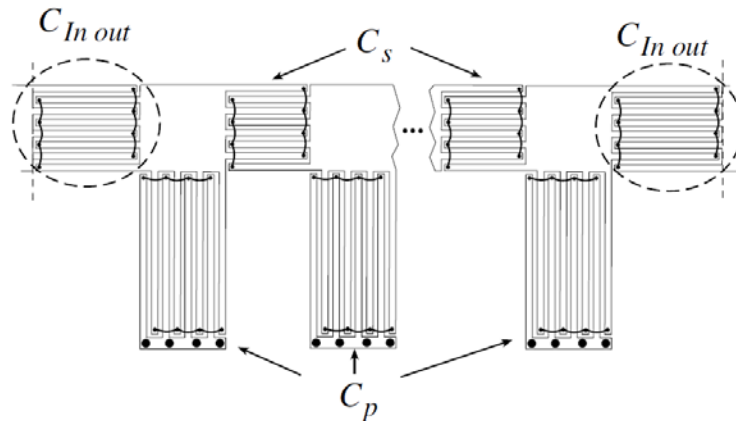


Fig. 6-6 Symmetric artificial transmission line using double-value wire bonded interdigital capacitors at both ends. Figure extracted from [Sanchez-09].

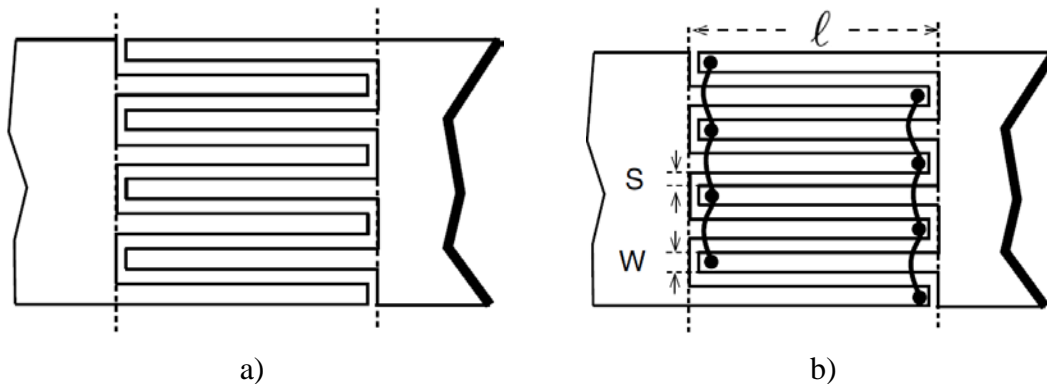


Fig. 6-7 Examples of interdigital capacitors used in microstrip CRLH TL: a) the conventional interdigital capacitor structure shown in Fig. 6-1, and b) the wire bonded interdigital capacitor. Figure extracted from [Sanchez-09].

6. Physical Implementation of Composite Right/Left-Handed Transmission Lines

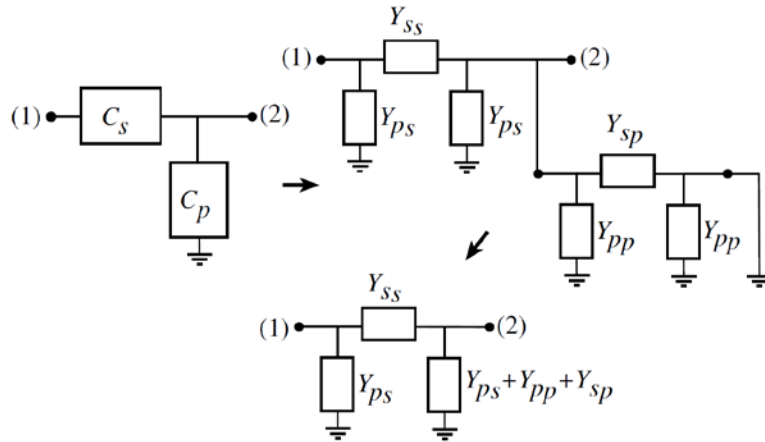


Fig. 6-8 Equivalent circuit of the two wire bonded interdigital capacitors, shown in Fig. 6-6. The series wire bonded interdigital capacitor connected to another wire bonded interdigital capacitor working as inductor in shunt connection to ground. Figure extracted from [Sanchez-09].

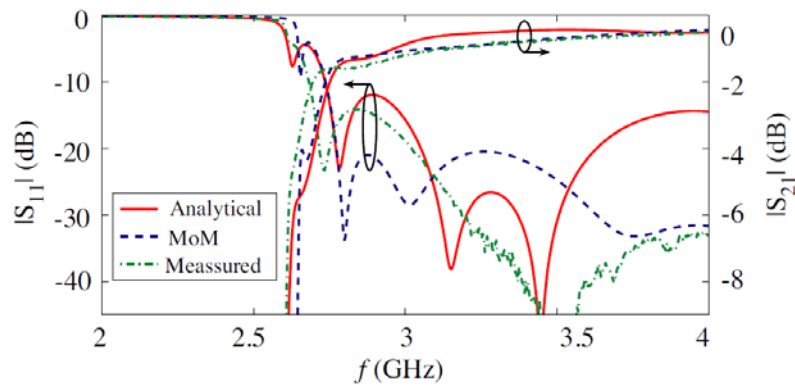


Fig. 6-9 Responses of the LC composite right/left-handed TL using wire bonded interdigital capacitors implemented in Fig. 6-6 with 3 unit-cells. Figure extracted from [Sanchez-09].

The S-parameter responses $|S_{11}|$ and $|S_{21}|$ reported in [Sanchez-09] for the physical implementation in Fig. 6-6, are shown in Fig. 6-9. Apparently the LH response starts at 2.7 GHz, and it has the expected high-pass nature. Unfortunately the analysis in [Sanchez-09] does not show any response after 4 GHz to identify the RH propagation region.

6. Physical Implementation of Composite Right/Left-Handed Transmission Lines

6.2.4 Another Composite Right/Left-Handed TL with Interdigital Capacitors

Another physical implementation of an artificial structure with metamaterial properties is shown in Fig. 6-10 [Li-08]. The equivalent circuit model of such physical implementation is shown in Fig. 6-11, and the equivalences between the physical implementation and the circuit model are shown in Fig. 6-10. In this case, not only the series interdigital capacitance exists, but also a small series inductance exists L_R (see Fig. 6-10).

The S-parameter responses $|S_{11}|$ and $|S_{21}|$ reported in [Li-08] for the physical implementation are shown in Fig. 6-12. As observed, a stopband exists at the transition between

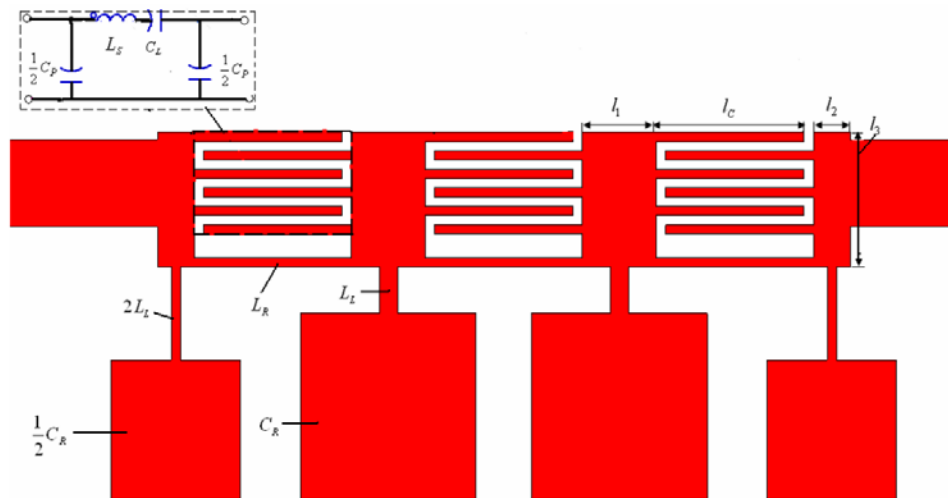


Fig. 6-10 Microstrip implementation of another composite right/left-handed transmission line using interdigital capacitors. Figure extracted from [Li-08].

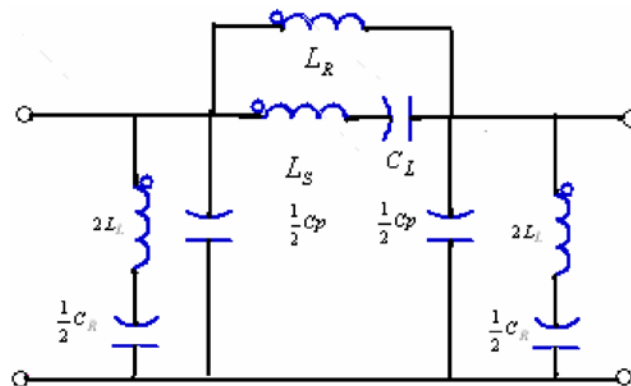


Fig. 6-11 Symmetrical circuit model of the composite right/left-handed transmission line unit cell shown in Fig. 6-10. Figure extracted from [Li-08].

6. Physical Implementation of Composite Right/Left-Handed Transmission Lines

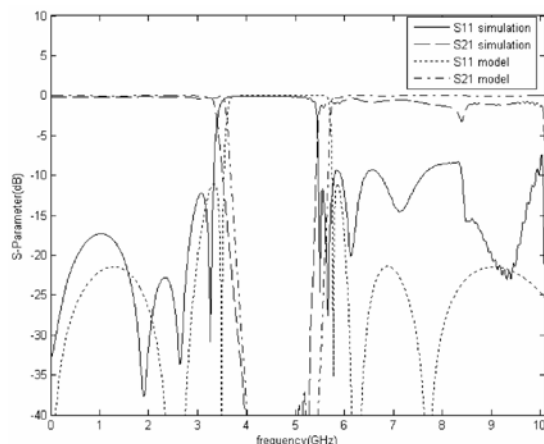


Fig. 6-12 S-parameter responses of another *LC* CRLH TL using interdigital capacitors implemented in Fig. 6-10 with three unit-cells. Figure extracted from [Li-08].

the LH and the RH propagation regions, approximately between 3.5 GHz and 5.5 GHz. In this case, the small series inductance L_R allows the physical structure to provide total transmission from DC to approximately 3.5 GHz, where the stopband starts to arise.

6.2.5 Composite Right/Left-Handed TL with Loading Series Capacitors

Another physical implementation of a CRLH TL can be achieved with loading series capacitors built in microstrip technology, and stubs shorted to ground plane, as shown in Fig. 6-13a [Kogure-10]. In this case the series capacitors are created by the proximity of one microstrip patch with the next one, and they are modeled ideally in Sonnet as indicated in Fig. 6-13b. The equivalent circuit for this implementation can be modeled by the network in Fig. 6-14. The left-

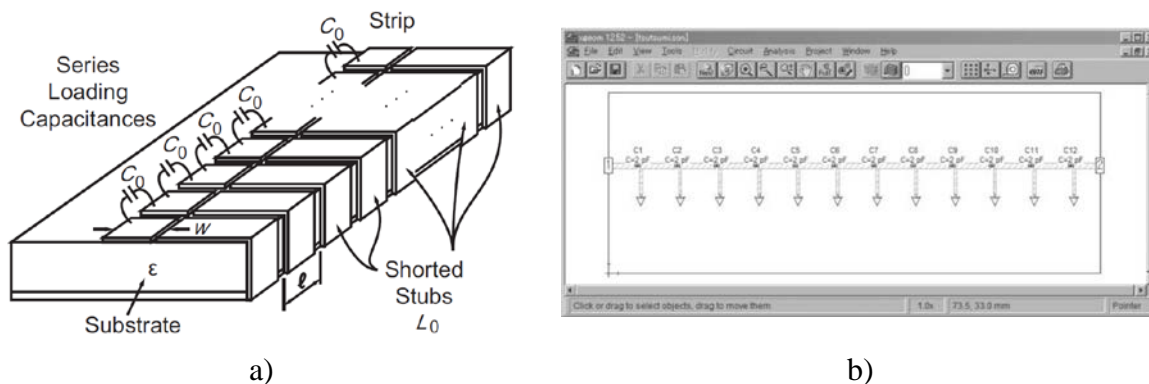


Fig. 6-13 A CRLH TL structure with discrete series capacitors in microstrip technology, and connected to ground plane using an inductive stub: a) LH TL designed for microwave band, b) specific example of a left-handed system. Figure extracted from [Kogure-10].

6. Physical Implementation of Composite Right/Left-Handed Transmission Lines

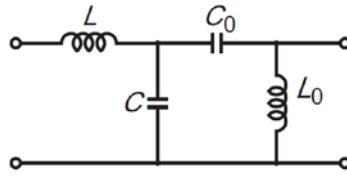


Fig. 6-14 Non-symmetric unit-cell of a lossless CRLH TL model as illustrated in Fig. 6-13. Figure extracted from [Kogure-10].

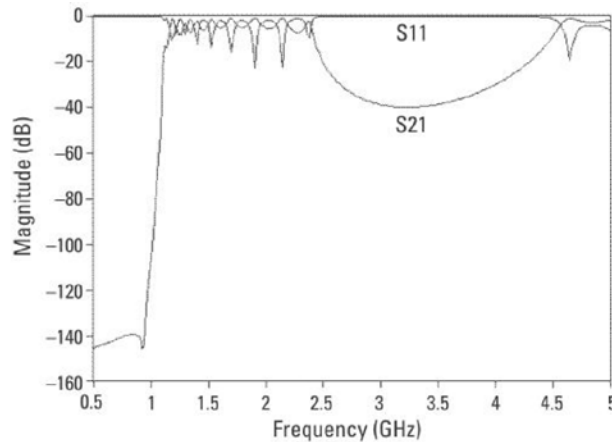


Fig. 6-15 S-parameter response of the LC composite right/left-handed TL implemented in Fig. 6-13. The LH nature emerges in the range 1 to 2.5 GHz. The RH nature emerges in the region above 4.5 GHz. The band between them is cut off and minimal transition occurs. Figure taken from [Kogure-10].

handed contributions C_0 and L_0 are provided by the loading series capacitors and stub inductors [Kogure-10]. The right-handed contributions C_R and L_R exist from their parasitic reactances and have an increasing effect as the frequency is increased.

The S-parameter responses $|S_{11}|$ and $|S_{21}|$ of this structure reported in [Kogure-10] are shown in Fig. 6-15, the LH nature emerges in the range from 1 GHz to 2.5 GHz [Kogure-10], and the RH nature emerges in the region above the 4.5 GHz. It is also observed that a stopband exists between the LH and the RH propagation regions, approximately between 2.5 GHz and 4.5 GHz.

6.3. Composite Right/Left-Handed Transmission Lines with Lumped Components.

The physical implementations described in this section are built similarly, using chip SMT lumped components soldered over microstrip structures.

6. Physical Implementation of Composite Right/Left-Handed Transmission Lines

6.3.1 Composite Right/Left-Handed TL with Discrete Series Capacitors

Another physical implementation of a CRLH TL can be achieved as the one shown in Fig. 6-16 [Wei-08]. This particular structure has periodically two or more different LC components in a single unit-cell. In [Wei-08], a unit cell consists of three chip capacitors in series (see Fig. 6-16a), soldered on the gaps of the microstrip lines and two chip inductors shunted to each capacitor by connecting the inductor between the microstrip line and the ground. The equivalent circuitual model of this physical implementation for one unit-cell can be modeled by the T-network shown in Fig. 6-17. The impedances Z_1 and Z_2 of the two series loops are constituted by a RH inductance L_R in series with a LH capacitance C_{L_i} ($i = 1$ or 2), respectively. The admittance Y is constituted by a RH capacitance C_R in parallel with a LH inductance L_L . The left-handed contributions C_{L1} , C_{L2} , and L_L are provided by the discrete series capacitors and the

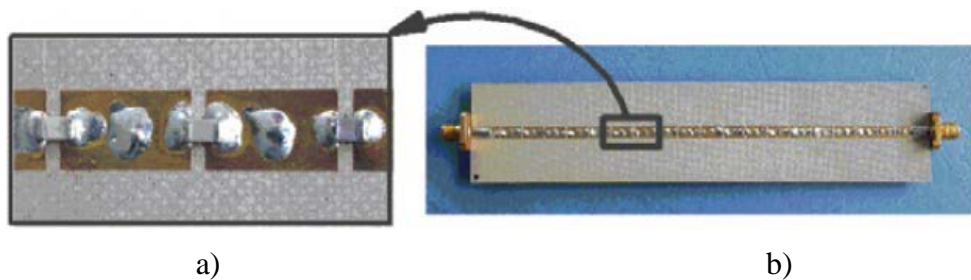


Fig. 6-16 Microstrip CRLH TL using discrete capacitors: a) each unit cell contains three chip capacitors in series, soldered on the gaps of the microstrip line, b) a 6 unit-cell inhomogeneous CRLH TL. Figure extracted from [Wei-08].

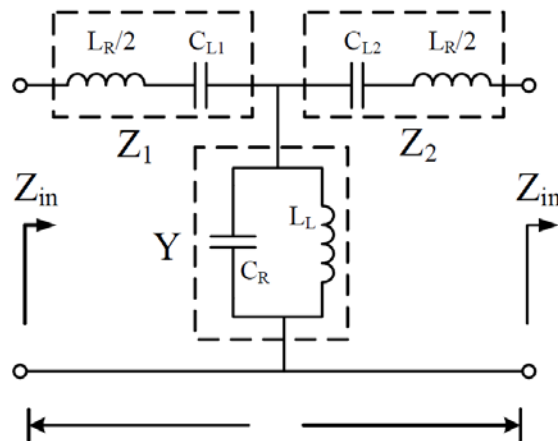


Fig. 6-17 Symmetric unit-cell of an LC composite right/left-handed TL implemented in Fig. 6-16a. Figure extracted from [Wei-08].

6. Physical Implementation of Composite Right/Left-Handed Transmission Lines

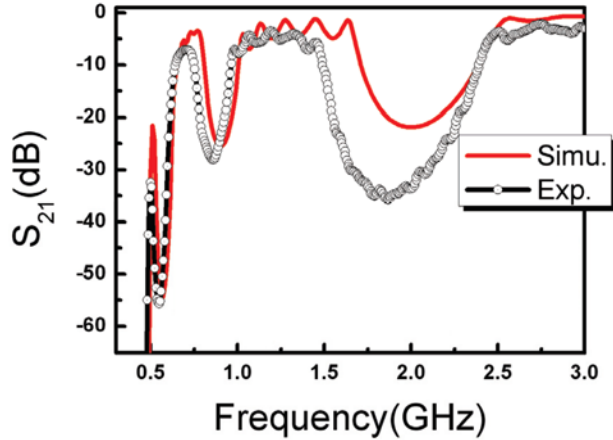


Fig. 6-18 S-parameter response of the LC composite right/left-handed TL implemented in Fig. 18b. There is a stop-band between the LH and the RH transition, at 1.8 GHz (measured value). The left-handed nature appears approximately from 0.5 GHz to 1.5 GHz (measured values), and it also has a stop-band around 0.8 GHz (measured value). The right-handed nature emerges in the region above 2.5 GHz. Figure extracted from [Wei-08].

chip inductor in stub connection to ground. The right-handed contributions C_R and L_R exist from their parasitic reactances and have an increasing effect as the frequency is increased.

The S-parameter response $|S_{21}|$ reported in [Wei-08] for this physical implementation is illustrated in Fig. 6-18. A stop-band exists in the transition between the LH and the RH propagation regions, approximately from 1.5 GHz to 2.5 GHz (measured values). There is also a stop-band in the conventional LH frequency region, centered at 0.8 GHz (measured values). This is caused due to the different capacitance values ($C_{L1} \neq C_{L2}$) (see Fig. 6-17) [Wei-08].

6.3.2 Coplanar Composite Right/Left-Handed TL with Discrete Series Capacitors

A different physical structure of a CRLH transmission line with lumped components can also be implemented as shown in the Fig. 6-19a [Siddiqui-03]. This particular structure is a coplanar waveguide periodically loaded with discrete SMT components. The equivalent circuit model of such implementation is shown in Fig. 6-19b. Apparently this model do not considers the RH shunt capacitance C_R as commonly shown in previous models (see Fig. 6-2 or Fig. 6-14).

The S-parameter responses $|S_{21}|$ and $\angle S_{21}$ reported in [Siddiqui-03], for this structure, are shown in Fig. 6-20. There are several responses depending on the stages of the structure, going

6. Physical Implementation of Composite Right/Left-Handed Transmission Lines

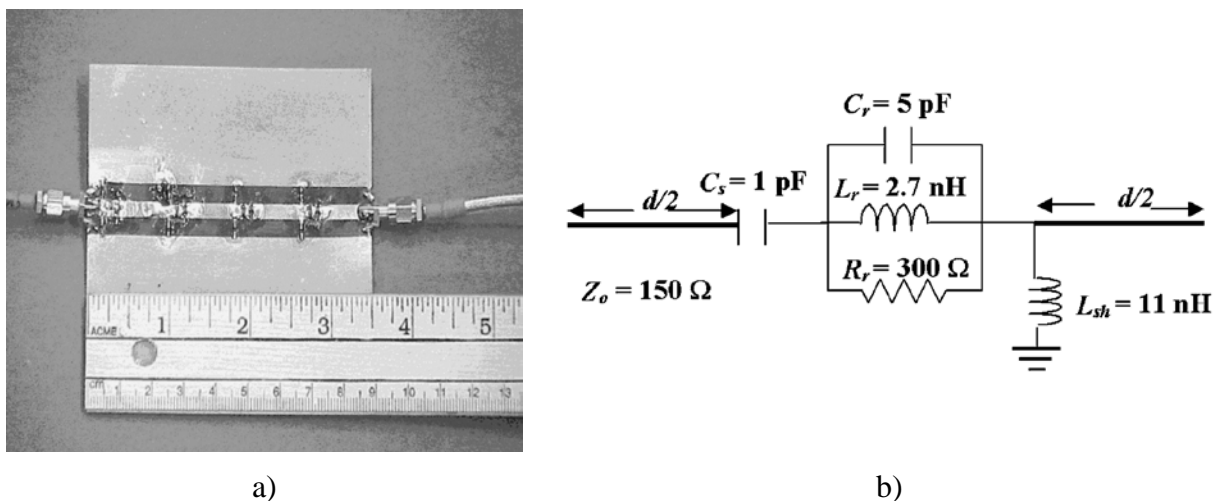


Fig. 6-19 A coplanar waveguide printed on a PCB, it is a CRLH TL using discrete capacitors: a) the microstrip 4-stage periodically loaded implementation, b) its asymmetric unit-cell. Figure extracted from [Siddiqui-03].

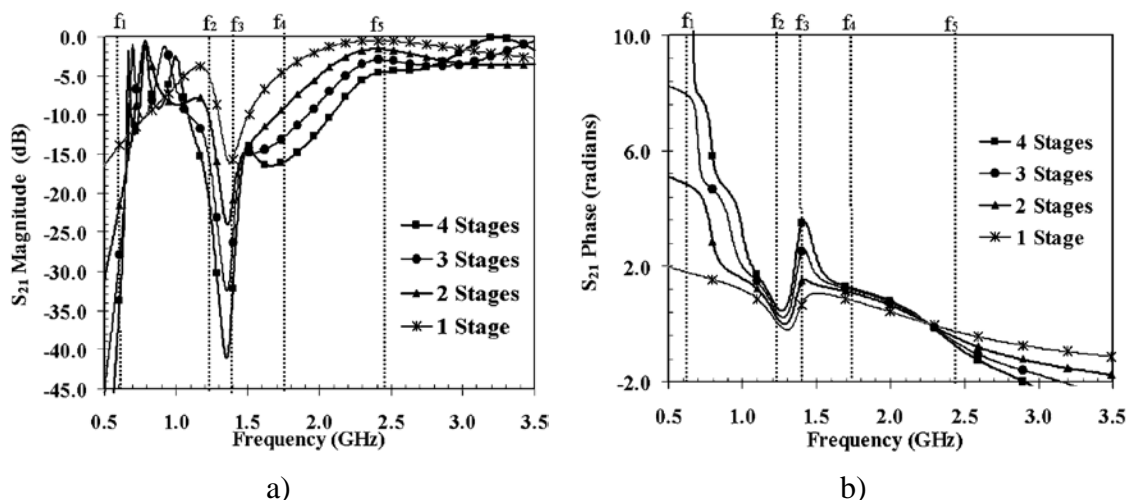


Fig. 6-20 S-parameter response of the composite right/left-handed transmission line implemented in Fig. 6-19a: a) magnitude of S_{21} parameter, and b) phase of the S_{21} parameter. Figure extracted from [Siddiqui-03].

from 1-stage structure to 4-stages structure.

The LH nature emerges from f_1 to f_4 (see Fig. 6-20), it is observed a stop-band between f_2 and f_3 [Siddiqui-03]. On the other hand, the RH nature emerges above f_4 [Siddiqui-03].

6. Physical Implementation of Composite Right/Left-Handed Transmission Lines

6.3.3 Composite Right/Left-Handed TL with discrete Series SMT Capacitors

Another physical structure of a CRLH transmission line can be achieved by using discrete series capacitors as shown in Fig. 6-21 [Suntives-07]. In this case, the capacitors are soldered between the metal microstrip patches in the structure, and the inductor is the connection to the ground plane through a via. The equivalent circuit model is shown in Fig. 6-22. As observed, this is a symmetric unit-cell and only the LH parameters are defined as lumped elements. The

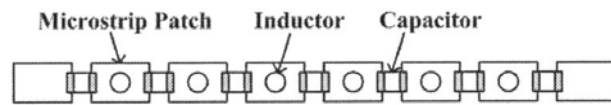


Fig. 6-21 A 6 cell composite right/left-handed transmission line using discrete capacitors soldered in microstrip rectangles. Figure extracted from [Suntives-07]

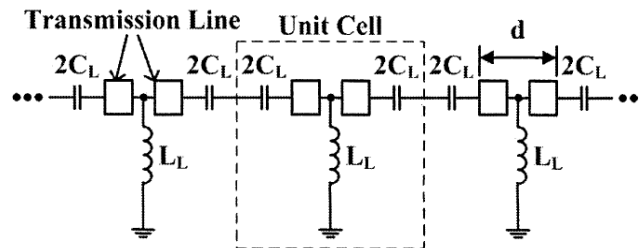


Fig. 6-22 Symmetric unit-cell of an CRLH lossless TL implemented in Fig. 6-21. Figure extracted from [Suntives-07].

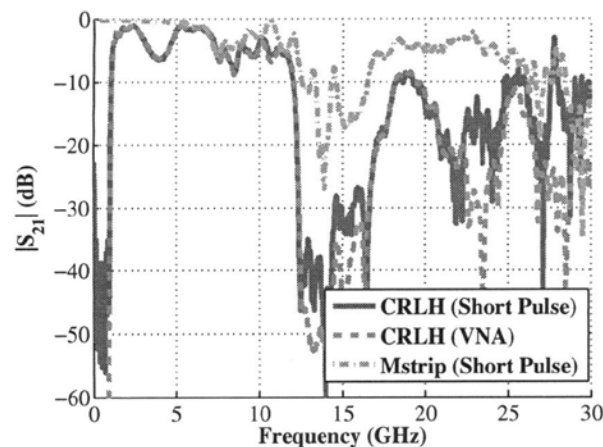


Fig. 6-23 S-parameter response of the *LC* CRLH TL implemented in Fig. 6-21. Figure extracted from [Suntives-07].

6. Physical Implementation of Composite Right/Left-Handed Transmission Lines

RH parameters are inherently defined by the conventional transmission line segments, as shown in Fig. 6-22. This is particularly useful to model the RH nature using conventional equations [Pozar-05], and model the LH nature by the lumped element models [Caloz-06].

The S-parameter responses $|S_{21}|$ are shown in Fig. 6-23. The responses labeled as “CRLH (Short Pulse)” and “CRLH (VNA)” represents the CRLH behavior, and they are measured differently [Suntives-07]. In both cases, the LH bandwidth goes from 1 GHz to 11 GHz, approximately. Apparently there is a stop-band in the transition between the LH and the RH propagation regions, approximately centered at 14 GHz. The right-handed response is apparently after 17 GHz and is below -10 dB, it seems that the RH response shows significant degradation (if compared with Fig. 6-3, for instance). The response labeled as “Mstrip (Short Pulse)” represents the transmission measured response $|S_{21}|$ of a conventional microstrip line with the same geometry as the microstrip patches in Fig. 6-21. Apparently, the response from DC to 5 GHz of this microstrip line has the maximum transmission effect. After 5 GHz, the measured transmission shows significant degradation.

In general, these structures with discrete components may have undesired effects if not properly modeled. The discrete capacitor is not equivalent to an ideal capacitor, since it has other parasitic elements which should be also modeled.

6.4. Conclusions

A compilation of several physical implementations of composite right/left-handed transmission line structures were briefly presented in this Chapter. Some of them are built using microstrip technology only, with no discrete SMT components. Other physical implementations are built using discrete SMT components soldered over the microstrip structure. The S-parameter responses of each structure were presented and briefly discussed to observe its metamaterial behavior, the left-handed and right-handed propagations regions.

In the next Chapter, one of the reviewed structures will be selected to perform a full wave electromagnetic simulation, and then perform a parameter extraction of its equivalent circuitual model.

7. A Parameter Extraction Process for Equivalent Circuit Models of a CRLH TL

7.1. Introduction

In a previous Chapter, several composite right/left-handed (CRLH) transmission line (TL) structures were briefly reviewed and analyzed. Here, one of them is selected and a parameter extraction methodology, similar to that one in Chapter 5, is applied to it.

However, in this Chapter, a decomposition approach is applied to gradually develop simple equivalent circuits to approximate individual segments of the complete CRLH transmission line structure. The initial parameter values of each simple equivalent circuit are obtained using well-known analytical expressions [Pozar-05]. Then, these parameter values are fine-tuned by optimization, that is, by applying a parameter extraction process to find their values that best approximate the corresponding full-wave EM responses. Finally, the simple equivalent circuits are connected all together to approximate the complete CRLH transmission line structure.

In Section 7.2, it is described the complete CRLH transmission line structure, its materials and properties. In Section 7.3, it is described the simplified microstrip sub-structures of the complete CRLH TL structure. In Section 7.4, the S-parameter responses of the EM lossless simulation in Sonnet, and its circuitual model approximation in Matlab, are presented and commented. In Section 7.5, the S-parameter responses of the EM lossy simulation in Sonnet, and its circuitual model approximation in Matlab, are also presented and commented. Finally, the conclusions are mentioned in Section 7.6

7.2. Composite Right/Left-Handed Transmission Line

The selected composite right/left-handed transmission line structure is shown in Fig. 6-13a. A highly accurate response of the structure is obtained from its full-wave electromagnetic (EM) simulation in Sonnet. Its implementation in Sonnet is illustrated in Fig. 7-1 [Kogure-10]. It

7. A Parameter Extraction Process for Equivalent Circuit Models of a CRLH TL

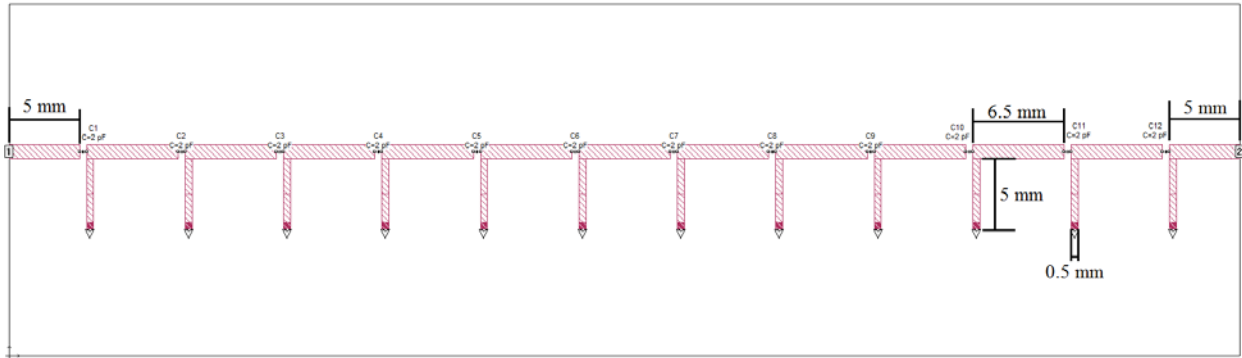


Fig. 7-1 2D view of the physical structure in Fig. 6-13b as implemented in Sonnet.

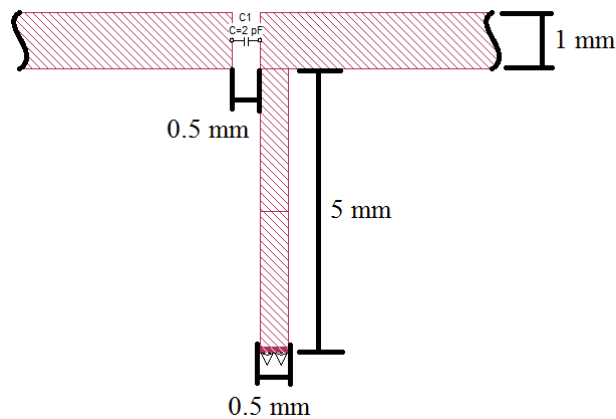


Fig. 7-2 Unit-cell of the CRLH structure in Fig. 7-1 as implemented in Sonnet.

uses a dielectric laminate with a dielectric constant $\epsilon_r = 2.6$, a substrate height $H = 0.4$ mm, and a dielectric loss tangent 0.0001. Thickness of the copper laminate is 0.003 mm. As observed in Fig. 7-1, the complete CRLH TL structure is built using 12 unit-cells similar to that one shown in Fig. 7-2.

A less accurate but much more computationally efficient circuitual model is implemented using Matlab.

7.3. Decomposing the CRLH Structure

The complete CRLH TL structure is divided into simpler conventional pure right-handed (PRH) microstrip structures, as follows.

7. A Parameter Extraction Process for Equivalent Circuit Models of a CRLH TL

7.3.1 Microstrip Line Segments

Two types of conventional PRH microstrip line segments in the direction of signal propagation are used in the CRLH TL (see Fig. 7-1). Both types of segments have a width of 1 mm. One microstrip line segment is 5 mm long, and it is located at the edges of the complete CRLH TL structure. Another microstrip line segment is 6.5 mm long, and interconnects each couple of unit-cells in the complete CRLH TL structure (see Fig. 7-1). A 3D view of the Sonnet implementation of these conventional microstrip line segments is shown in Fig. 7-3a, and its equivalent circuit model is illustrated in Fig. 7-3b.

7.3.2 Microstrip Grounded Stub

A conventional (PRH) microstrip grounded stub, transverse to the signal propagation direction, is shown in the unit-cell illustrated in Fig. 7-2. A 3D view of the Sonnet implementation is illustrated in Fig. 7-4a, and its equivalent circuit model is shown in Fig. 7-4b. The length and width of the grounded stub is 5 mm and 0.5 mm, respectively.

7.3.3 Two Microstrip Lines Separated by a Capacitor over a Gap

Two conventional microstrip lines separated by an ideal series capacitor above a gap or slot are shown in Fig. 7-5a. This structure corresponds to the original unit-cell when the

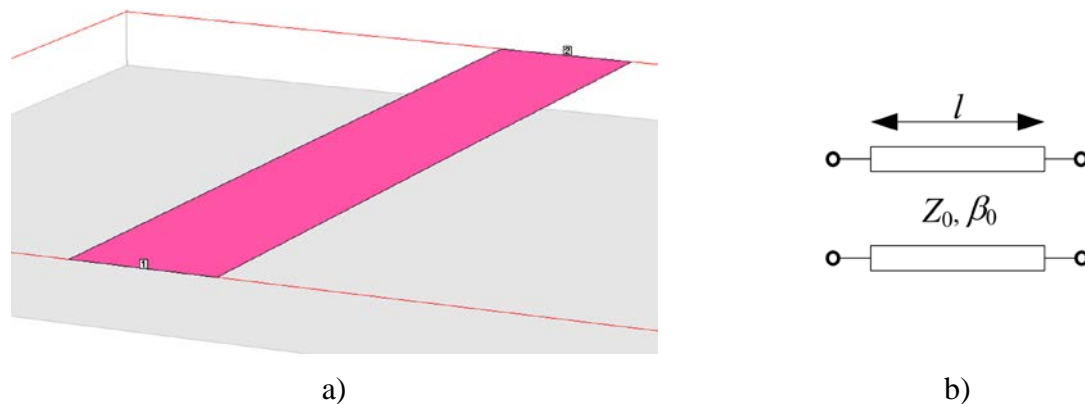


Fig. 7-3 Conventional (right-handed) microstrip line segment employed in Fig. 7-2 in the direction of signal propagation: a) Sonnet implementation; b) equivalent circuit.

7. A Parameter Extraction Process for Equivalent Circuit Models of a CRLH TL

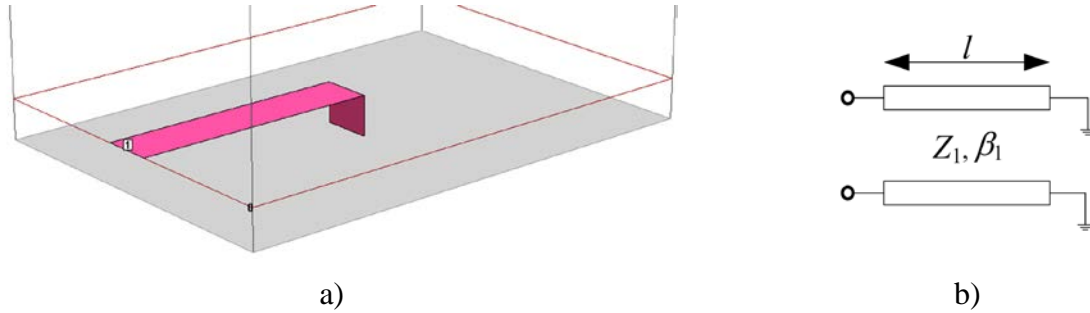


Fig. 7-4 Conventional microstrip grounded stub segment transverse to the signal propagation direction, employed in Fig. 7-2: a) Sonnet implementation; b) equivalent circuit.

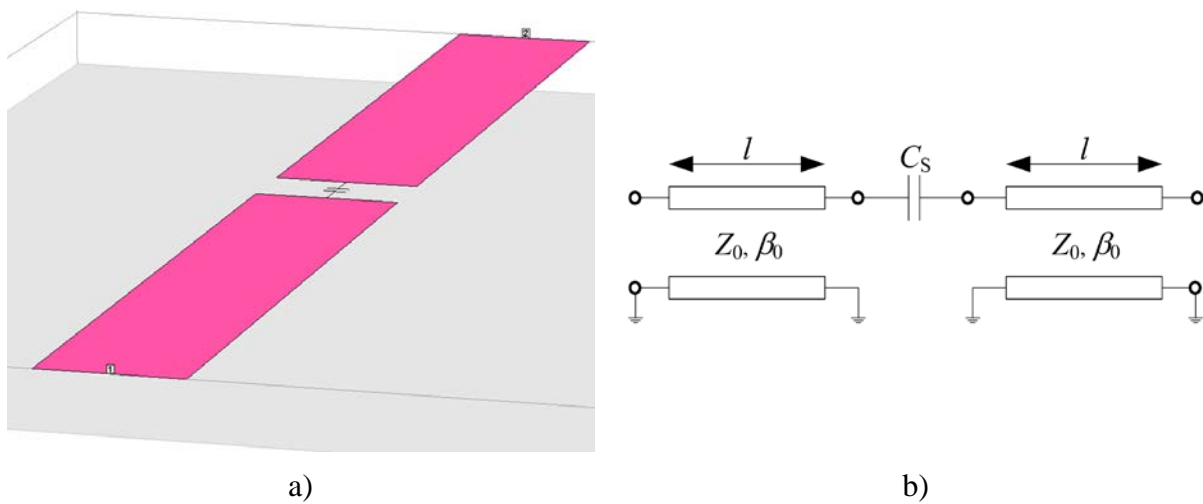


Fig. 7-5 Two conventional (right-handed) microstrip line segments, in the direction of signal propagation, with an ideal series capacitor over a slot of 0.5 mm long: a) Sonnet implementation; b) equivalent circuit neglecting the slot.

grounded stubs are removed (see Fig. 7-2). The dimensions of each microstrip line is 5 mm in length and 1 mm in width. The slot length is 0.5 mm, such that the total length is 10.5 mm. The equivalent circuit is shown in Fig. 7-5b. Notice that, in this case, $C_s = 2$ pF in both the EM model and the circuit model.

7.3.4 Microstrip Line Connected to a Grounded stub by a Right-Angle Bend

A conventional PRH microstrip line is connected to a grounded stub structure by a right angle bend discontinuity, as illustrated in Fig. 7-6a. The length of the microstrip line in the direction of signal propagation is 5 mm. The dimensions of the grounded stub sub-structure,

7. A Parameter Extraction Process for Equivalent Circuit Models of a CRLH TL

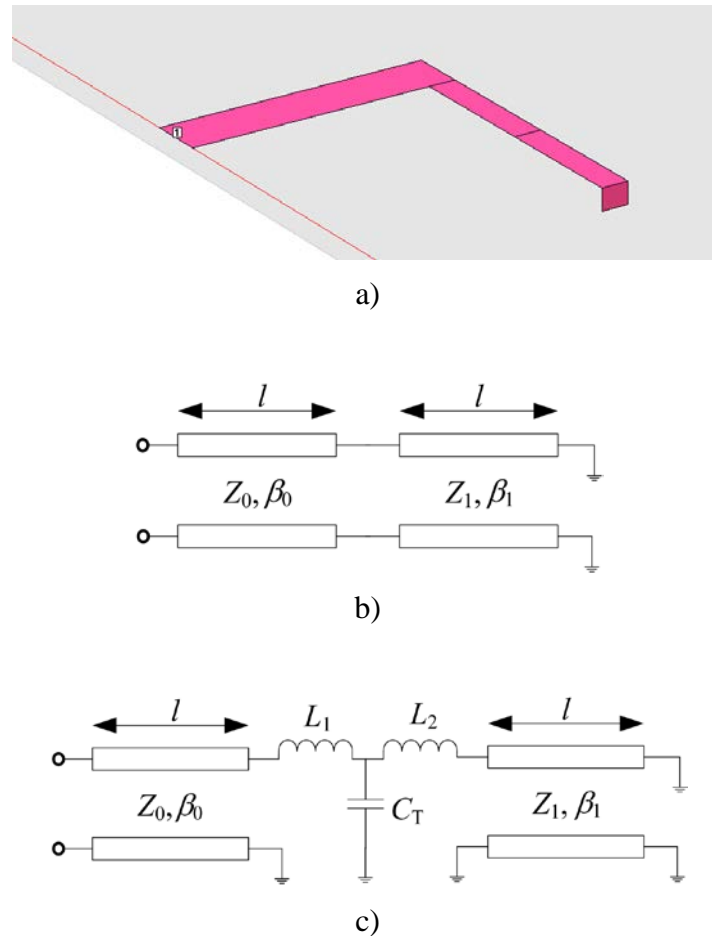


Fig. 7-6 Conventional microstrip line segment with dimensions 5 mm x 1 mm, and a conventional grounded stub with dimensions 5 mm x 0.5 mm connected by a right-angle bend: a) Sonnet implementation; b) equivalent circuit neglecting the bend; c) equivalent circuit with bend modeled [Gupta-96].

transverse to the signal propagation direction, are the same as those in Section 7.3.2. Two equivalent circuits of this sub-structure are shown: Fig. 7-6b (neglecting the right-angle bend) and Fig. 7-6c (modeling the right-angle bend).

7.3.5 Complete Unit-Cell of the CRLH Structure

The complete unit-cell of the CRLH TL structure (see Fig. 7-2) as implemented in Sonnet is illustrated in Fig. 7-7a. The dimensions of this unit-cell are the same as those in Fig. 7-2, using a 5 mm length for all the microstrip lines. Two equivalent circuits to model the complete unit-cell are shown: Fig. 7-7b (ignoring the right-angle effect) and Fig. 7-7c (considering the right-angle bend discontinuity).

7. A Parameter Extraction Process for Equivalent Circuit Models of a CRLH TL

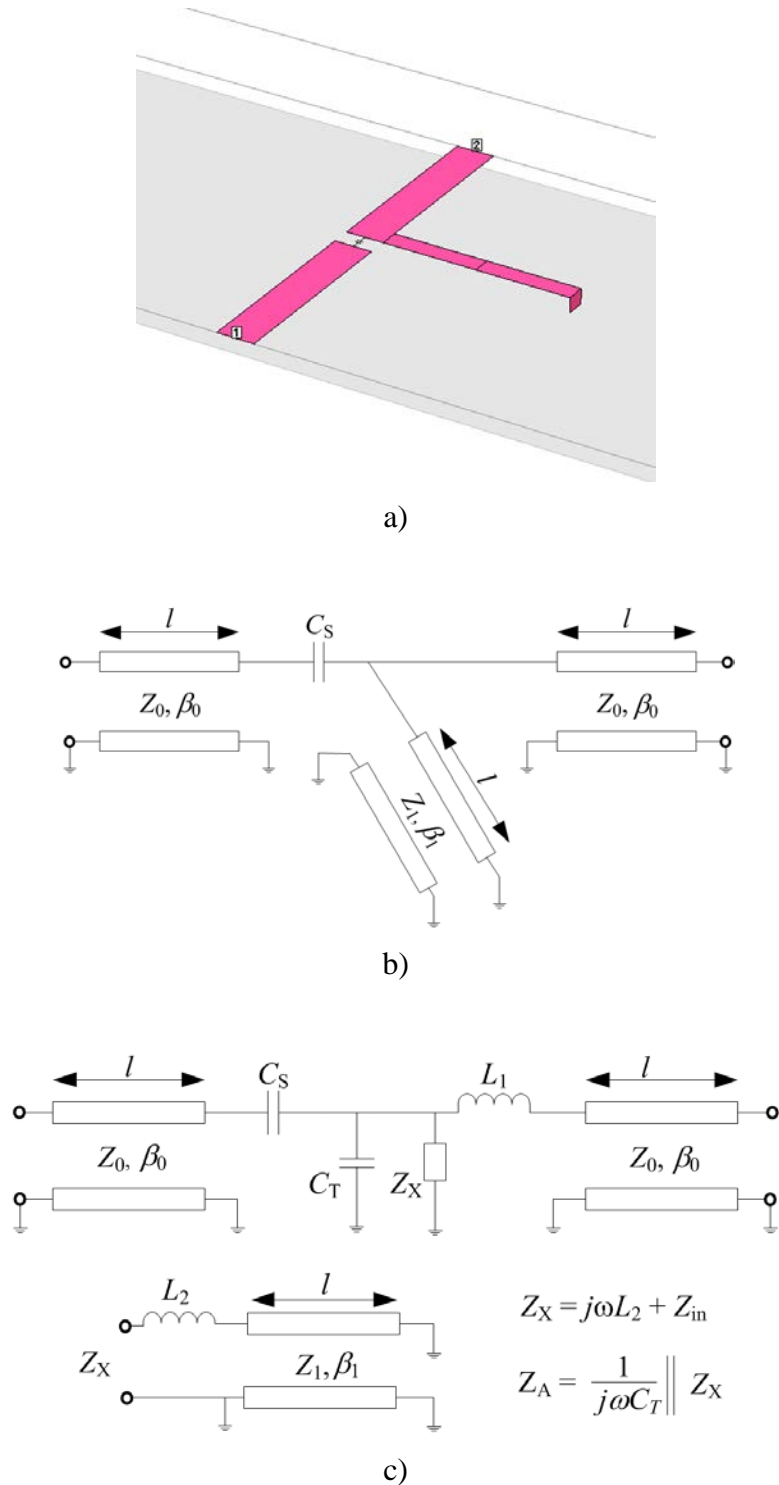


Fig. 7-7 Complete unit-cell of the CRLH structure is formed by two conventional (right-handed) microstrip line segments, in direction of signal propagation, with an ideal series capacitor over a slot of 0.5 mm long, and a grounded stub: a) Sonnet implementation; b) equivalent circuit neglecting the bend and the slot; c) equivalent circuit considering the bend, and neglecting the slot.

7. A Parameter Extraction Process for Equivalent Circuit Models of a CRLH TL

7.4. Proposed Methodology for Parameter Extraction of the Equivalent Circuits

For the sake of simplicity, we will initially neglect losses, both dielectric and metallic. The circuitual model of each individual segment is implemented in Matlab. Each individual structure is simulated in order to extract, by optimization, the equivalent purely right-handed (*RGLC*) per-unit length parameters (see Chapter 5). The complete CRLH unit-cell structure is also implemented in Matlab by assembling the individually approximated models, to finally approach the response of the complete CRLH transmission line structure shown in Fig. 7-1.

The parameters required to obtain an approximation of TL structures are: physical length (l), characteristic impedance (Z_0), and propagation constant (β). The propagation velocity (v_p) of each structure is required to compute the initial circuit parameter values for the PE procedure. Based on well-known analytical expressions [Pozar-05] and the dimensions of each sub-structure, such TL parameters can be computed. Having calculated Z_0 and v_p , we calculate its equivalent per unit-length parameters L and C . Following this procedure, the initial LC values for the PE procedure of the microstrip line segment, shown in Fig. 7-3a, are: $L_{\text{seg}} \approx 260$ nH/m, and $C_{\text{seg}} \approx 92$ pF/m. The initial LC values for the PE procedure of the PRH grounded stub illustrated in Fig. 7-4a, are: $L_{\text{stub}} \approx 380$ nH/m, and $C_{\text{stub}} \approx 60$ pF/m.

Similarly to Chapter 5, the optimization algorithm uses the Nelder-Mead method, available in `fminsearch` function in Matlab, and minimizes the norm of the error between Sonnet and Matlab S-parameter responses at each frequency point. Then, a list of per-unit length parameter values are extracted over the working frequency band. For simplicity, when comparing EM simulation responses versus Matlab circuitual responses, we use per-unit length average values for the circuitual approximations.

7.4.1 PE of the Conventional Microstrip Line 6.5 mm Long

After the optimization process, the per-unit length LC values are: $L_{\text{seg}} \approx 261.879$ nH/m, and $C_{\text{seg}} \approx 90.697$ pF/m.

The magnitude and phase of the reflection response, $|S_{11}|$ and $\angle S_{11}$, are shown in the Fig. 7-8a and Fig. 7-8b, respectively. It is seen that there is an excellent match between Sonnet and

7. A Parameter Extraction Process for Equivalent Circuit Models of a CRLH TL

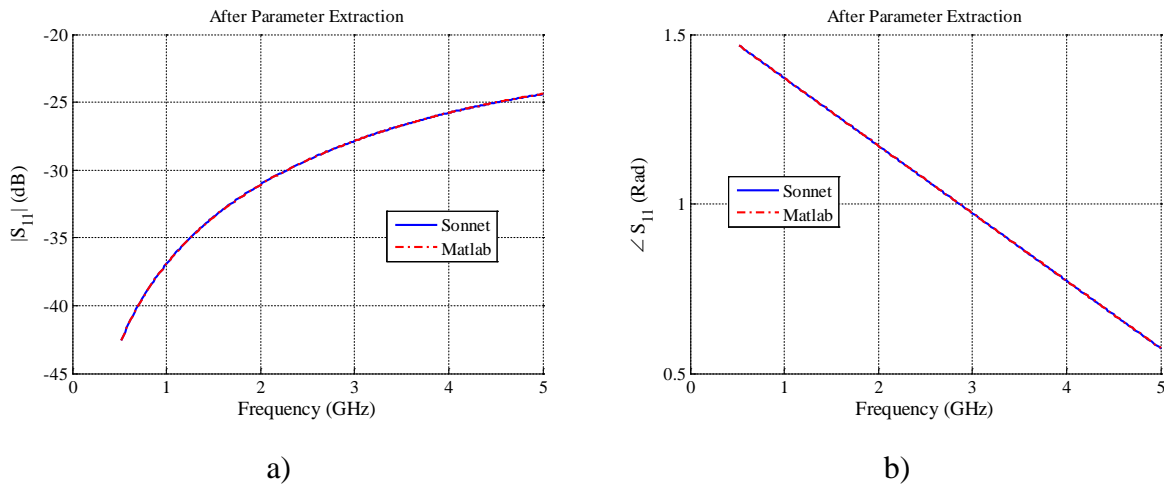


Fig. 7-8 S_{11} parameter response comparison between Matlab and Sonnet after the PE of the 6.5 mm TL long illustrated in Fig. 7-3a (lossless case): a) magnitude, b) phase.

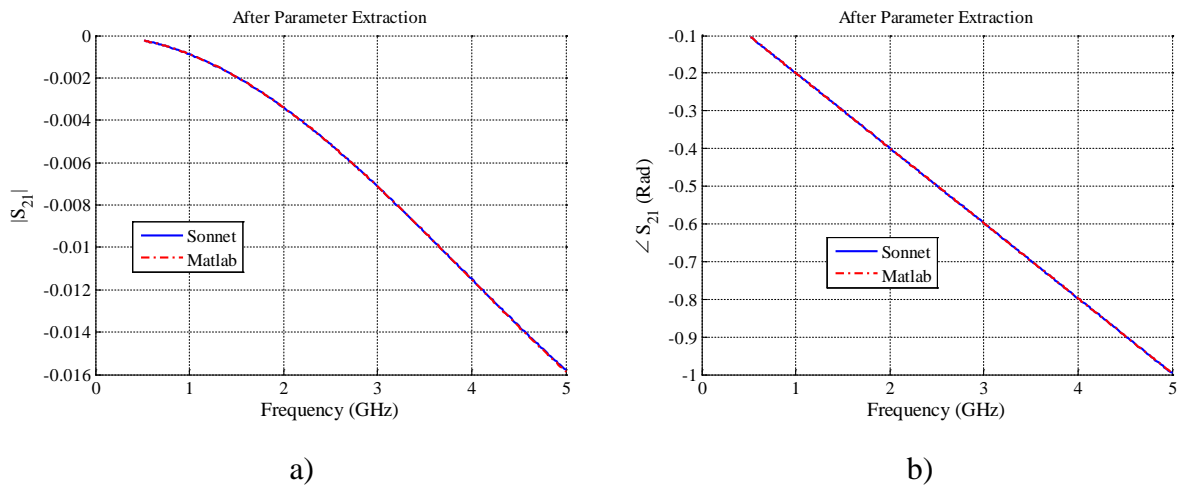


Fig. 7-9 S_{21} parameter response comparison between Matlab and Sonnet after the PE of the 6.5 mm TL long illustrated in Fig. 7-3a (lossless case): a) magnitude, b) phase.

Matlab responses for S_{11} .

The transmission responses, $|S_{21}|$ and $\angle S_{21}$, are shown in the Fig. 7-9a and Fig. 7-9b, respectively. There is also very good match in the magnitude responses, although slight differences arise above 4.5 GHz. The phase of S_{21} shows an excellent match between both responses.

It is confirmed that the EM response of this lossless microstrip line segment can be modeled with circuitual transmission line models up to 5 GHz with high accuracy.

7. A Parameter Extraction Process for Equivalent Circuit Models of a CRLH TL

7.4.2 PE of the Conventional Microstrip Line 5 mm Long

Since this microstrip line has the same cross-sectional properties (dimensions and materials) as those used in the previous section, we could use the same values for L_{seg} and C_{seg} obtained in previous section. However, since we are using average per-unit length values in the Matlab circuitual models over the complete frequency band of interest, and the current structure is shorter than the previous one, better results are obtained by fine tuning these per-unit length values for this particular length.

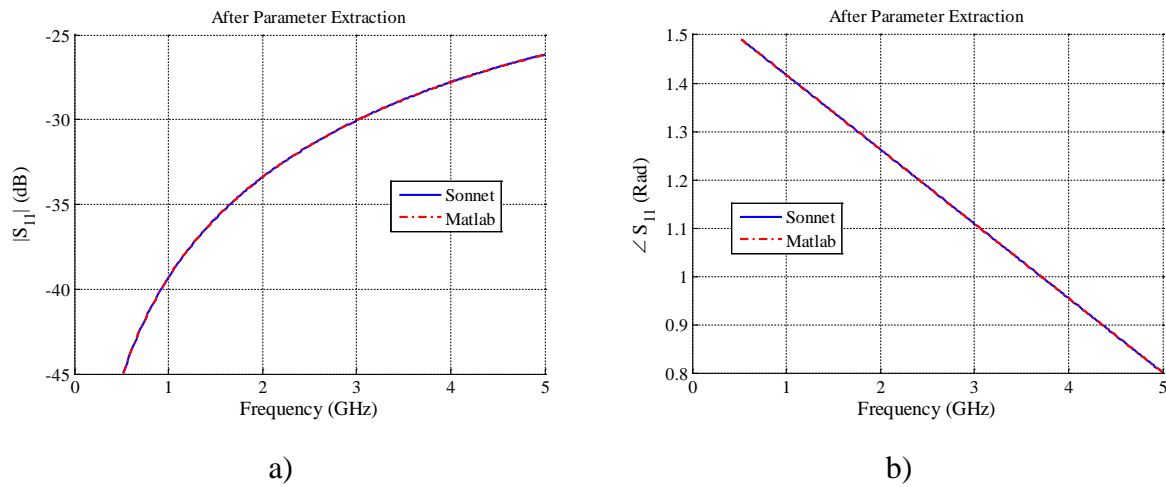


Fig. 7-10 S_{11} parameter response comparison between Matlab and Sonnet after the PE of the 5 mm TL long illustrated in Fig. 7-3a (lossless case): a) magnitude, b) phase.

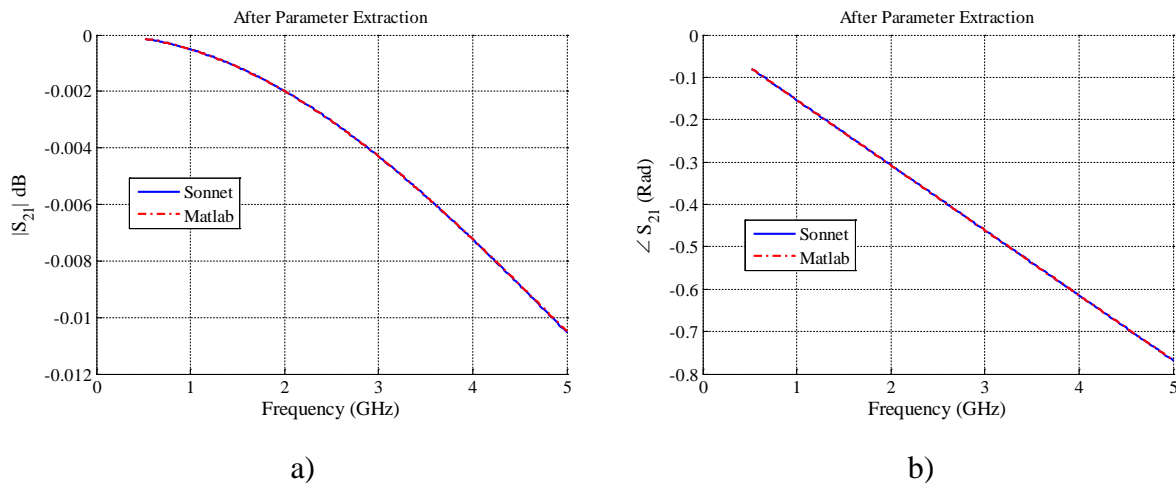


Fig. 7-11 S_{21} parameter response comparison between Matlab and Sonnet after the PE of the 5 mm TL long illustrated in Fig. 7-3a (lossless case): a) magnitude, b) phase.

7. A Parameter Extraction Process for Equivalent Circuit Models of a CRLH TL

After the optimization process, the per-unit length LC values are: $L_{\text{seg}} \approx 261.921$ nH/m, $C_{\text{seg}} \approx 90.927$ pF/m.

The magnitude and phase of the reflection response, $|S_{11}|$ and $\angle S_{11}$, are shown in the Fig. 7-10a and Fig. 7-10b, respectively. There is an excellent match between Sonnet and Matlab for both magnitude and phase of S_{11} , over the working frequency band.

The transmission responses, $|S_{21}|$ and $\angle S_{21}$, are shown in the Fig. 7-11a and Fig. 7-11b, respectively. There is also an excellent match in the magnitude responses. The phase of S_{21} shows an excellent match between both EM and circuital models.

It is confirmed that the EM response of this lossless microstrip line segment can be modeled with circuital transmission line models up to 5 GHz with high accuracy.

7.4.3 PE of the Conventional Microstrip Grounded Stub

After the optimization process, the per-unit length LC values are: $L_{\text{stub}} \approx 388.63$ nH/m, $C_{\text{stub}} \approx 60.48$ pF/m for the TL model in Fig. 7-4b.

The magnitude and phase of the reflection response, $|S_{11}|$ and $\angle S_{11}$, are shown in Fig. 7-12a and Fig. 7-12b, respectively. It is seen that there is an excellent match between Sonnet and Matlab responses for S_{11} , confirming that the EM response of this lossless microstrip grounded stub can be modeled with circuital transmission line models up to 5 GHz with high accuracy.

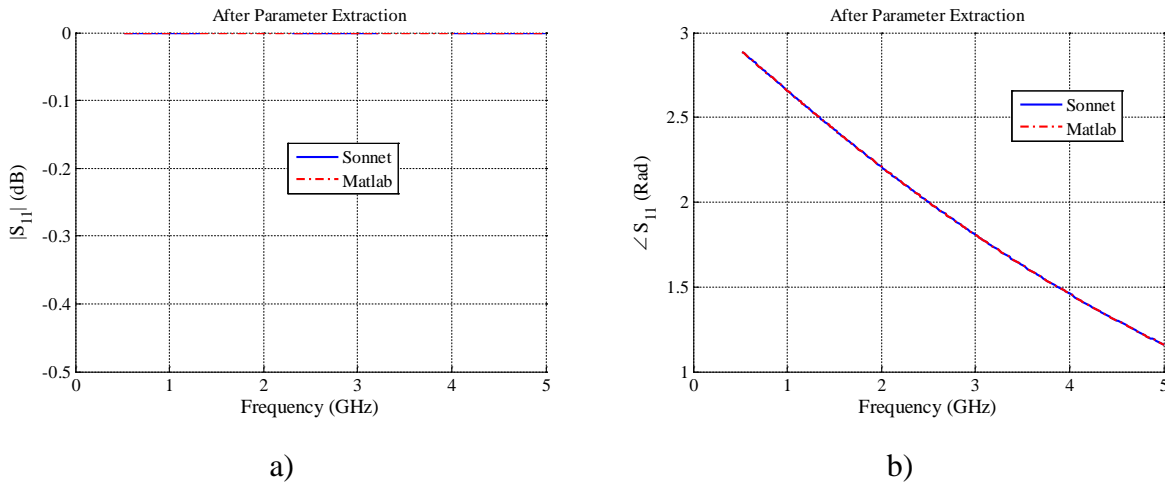


Fig. 7-12 S_{11} parameter response comparison between Matlab and Sonnet after the PE of the microstrip grounded stub shown in Fig. 7-4a (lossless case): a) magnitude, b) phase.

7. A Parameter Extraction Process for Equivalent Circuit Models of a CRLH TL

7.4.4 PE of the Two Microstrip Lines Separated by a Capacitor over a Gap

The per-unit length LC values of each TL separated by the capacitor over a gap (see Fig. 7-5b), are the same as those in Section 7.4.2.

The magnitude and phase of the reflection response, $|S_{11}|$ and $\angle S_{11}$, are shown in Fig. 7-13a and Fig. 7-13b, respectively. Although there is an excellent match in the low frequency

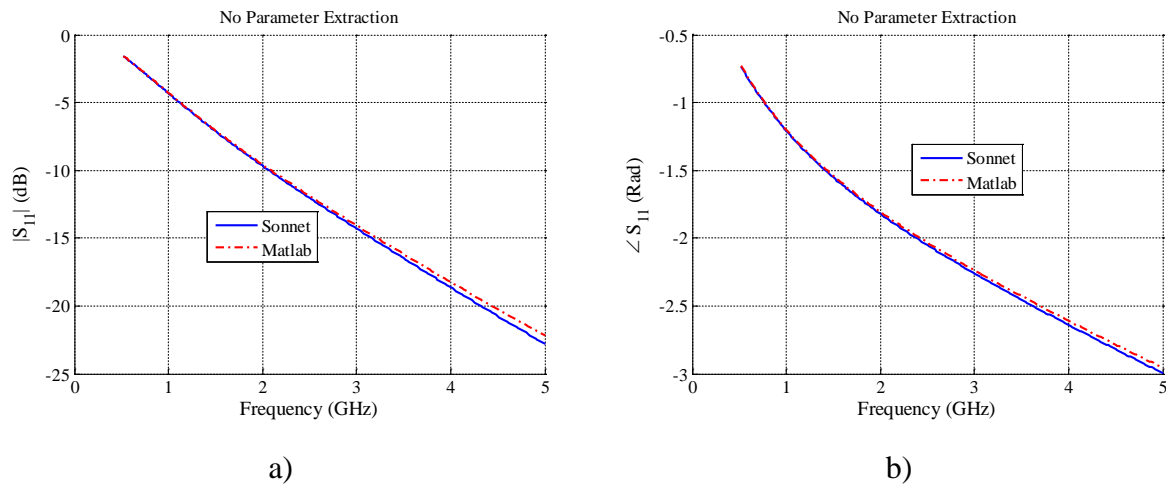


Fig. 7-13 S_{11} parameter response comparison between Matlab and Sonnet with no PE of the two 5 mm TL long, and series capacitor over a gap, illustrated in Fig. 7-5a (lossless case): a) magnitude, b) phase.

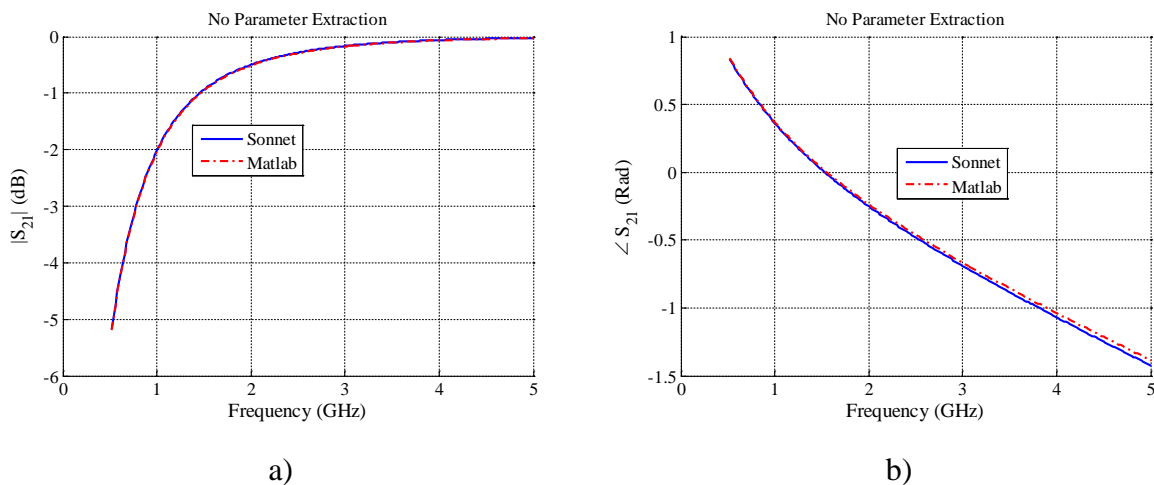


Fig. 7-14 S_{21} parameter response comparison between Matlab and Sonnet with no PE of the two 5 mm TL long, and series capacitor over a gap, illustrated in Fig. 7-5a (lossless case): a) magnitude, b) phase.

7. A Parameter Extraction Process for Equivalent Circuit Models of a CRLH TL

range below 2 GHz, the difference between Matlab and Sonnet arises as frequency is increased, as expected.

The transmission responses, $|S_{21}|$ and $\angle S_{21}$, are shown in Fig. 7-14a and Fig. 7-14b, respectively. It is seen an excellent match in $|S_{21}|$ up to 5 GHz. There is also an excellent match below 2 GHz in the phase of S_{21} , however, the error between Matlab and Sonnet responses for the phase of S_{21} arises as frequency is increased.

As expected for this particular sub-structure, there is not an excellent match between Matlab and Sonnet responses over the complete frequency band. It seems that such mismatch is generated by the slot illustrated in Fig. 7-5a. Apparently, the effect of the series capacitor (C_S) dominates over the slot effect below 2 GHz. As frequency is increased, the slot effect arises and makes some influence over the series capacitor (C_S) effect. This additional effect is not considered in the circuital model, because here C_S is constant.

For simplicity, and the fact that such difference is relatively low up to 5 GHz, the slot is not modeled by a more complex equivalent circuit in the present work.

7.4.5 PE of the Microstrip Line Connected to a Grounded Stub by a Right-Angle Bend

The per-unit length LC values for the TL circuital model of the microstrip line and the grounded stub illustrated in Fig. 7-6a, are the same as those in Section 7.4.2 and Section 7.4.3, respectively. Initially, the bend is neglected and the equivalent circuital model used is that one shown in Fig. 7-6b.

The magnitude and phase of the reflection response, $|S_{11}|$ and $\angle S_{11}$, are shown in Fig. 7-15a and Fig. 7-15b, respectively. It is seen that the mismatch is too large. This large error is due to the discontinuity existing between the two conventional microstrip lines, forming a right-angle bend structure, as shown next.

The circuital model of the microstrip line connected to a grounded stub, considering the right-angle bend lumped model, is illustrated in Fig. 7-6c. In this T-network, L_1 and L_2 correspond to the inductance calculations for T-junctions [Gupta-96], due to the different width values of each microstrip structure. Similarly, C_T corresponds to the capacitance calculations for T-junctions, due to the excess of capacitance in the bend [Gupta-96].

7. A Parameter Extraction Process for Equivalent Circuit Models of a CRLH TL

A new parameter extraction process is performed for the bend structure only, and the average extracted values of the right-angle bend lumped model are: $L_1 \approx 2.09$ nH, $L_2 \approx 5.73$ nH, and $C_T \approx 40.26$ nF.

The magnitude and phase of the reflection response, $|S_{11}|$ and $\angle S_{11}$, are shown in Fig. 7-16a and Fig. 7-16b, respectively. It is seen that there is an excellent match between Matlab and Sonnet responses for $|S_{11}|$. The phase of S_{11} shows a small mismatch between both responses.

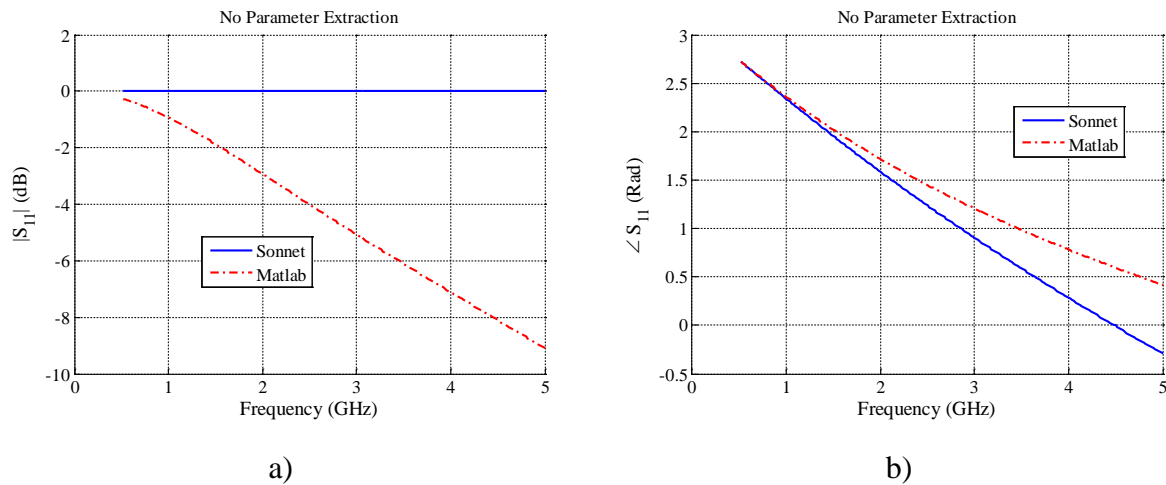


Fig. 7-15 S_{11} parameter response comparison between Matlab and Sonnet with no PE of the microstrip grounded stub, and neglecting the right-angle bend, illustrated in Fig. 7-6a (lossless case): a) magnitude, b) phase.

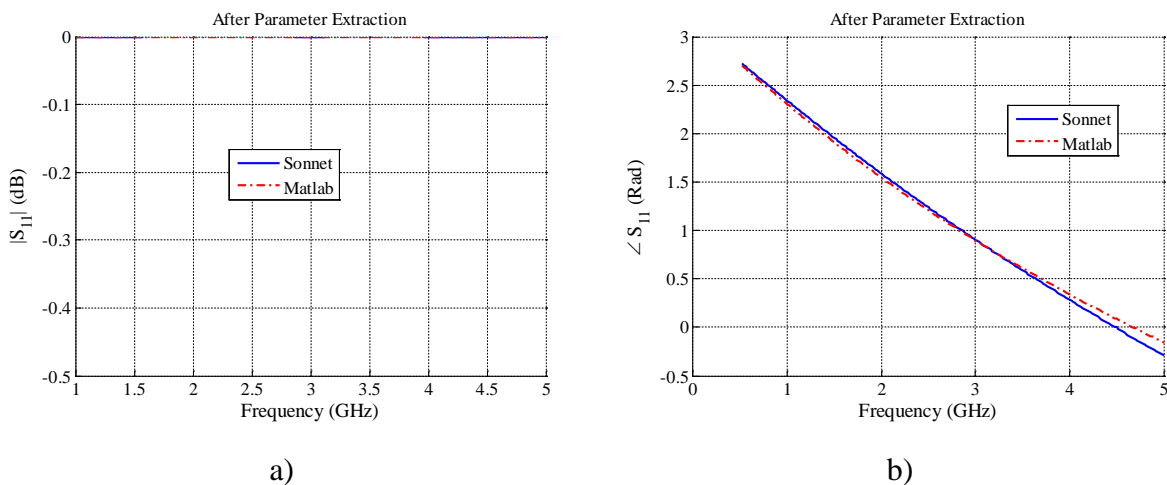


Fig. 7-16 S_{21} parameter response comparison between Matlab and Sonnet with no PE of the microstrip grounded stub, and considering a right-angle bend, illustrated in Fig. 7-6a (lossless case): a) magnitude, b) phase.

7. A Parameter Extraction Process for Equivalent Circuit Models of a CRLH TL

It is confirmed that the EM response of this lossless microstrip line connected to a grounded stub by a right-angle bend discontinuity, can be modeled using circuitual TL models (for the microstrip lines) and lumped circuitual models (for the bend), up to 5 GHz.

7.4.6 PE of the Complete Unit-Cell of the CRLH Structure

The per-unit length LC values of the TL model for microstrip lines in the direction of signal propagation, as shown in Fig. 7-7a, are the same as those in Section 7.4.2. Similarly, the per-unit length LC values of the TL model for the grounded stub illustrated in Fig. 7-7a, are the same as those in Section 7.4.3. Initially the bend is neglected; hence, the circuitual model of the complete unit-cell is that one in Fig. 7-7b.

The magnitude and phase of the reflection response, $|S_{11}|$ and $\angle S_{11}$, are shown in the Fig. 7-17a and Fig. 7-17b, respectively. It is seen an excellent match between Matlab and Sonnet below 1.25 GHz and above 4.9 GHz for $|S_{11}|$, although the differences between EM and circuitual responses arises in the middle frequency band. The phase of S_{11} shows an excellent match between both responses below 2 GHz. It is seen that the circuitual response is displaced a few MHz to higher frequencies.

The transmission responses, $|S_{21}|$ and $\angle S_{21}$, are shown in the Fig. 7-18a and Fig. 7-18b, respectively. It is seen that there is a very good match between Matlab and Sonnet for S_{21} over

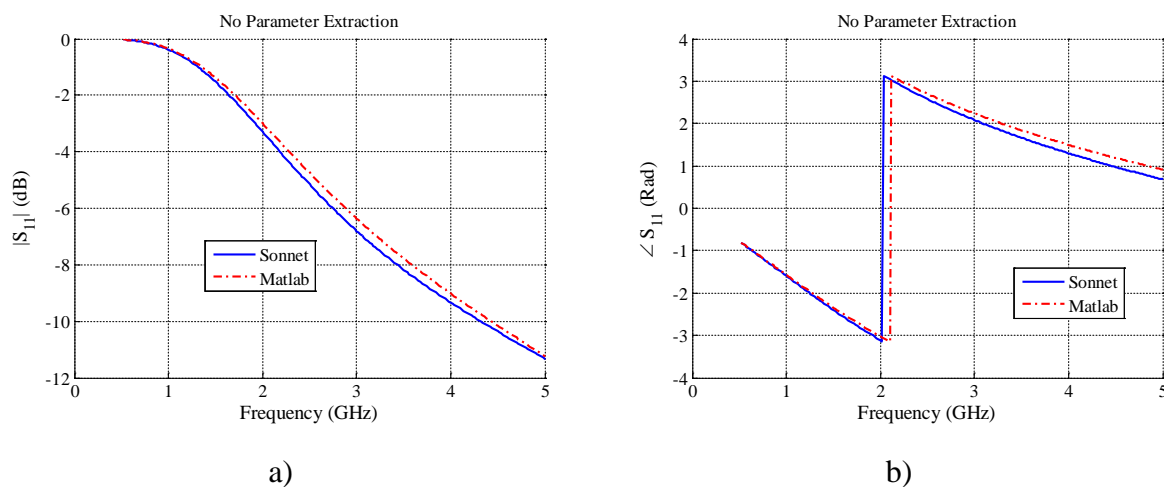


Fig. 7-17 S_{11} parameter response comparison between Matlab and Sonnet with no PE of the CRLH unit-cell, illustrated in Fig. 7-7a, using the Matlab circuitual model shown in Fig. 7-7b (lossless case): a) magnitude, b) phase.

7. A Parameter Extraction Process for Equivalent Circuit Models of a CRLH TL

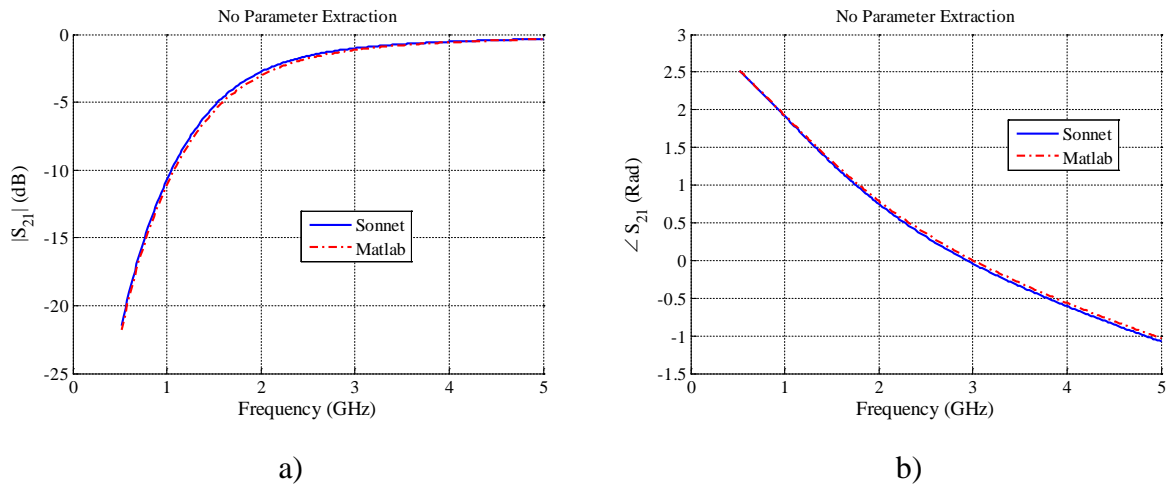


Fig. 7-18 S_{21} parameter response comparison between Matlab and Sonnet with no PE of the CRLH unit-cell, illustrated in Fig. 7-7a, using the Matlab circuitual model shown in Fig. 7-7b (lossless case): a) magnitude, b) phase.

the complete frequency band.

We now consider the equivalent circuit for the complete unit-cell of the CRLH structure modeling the bend (Fig. 7-7c). A new parameter extraction process is performed for the lumped elements of the right-angle bend only. The average extracted values are: $L_1 \approx 0.603$ fH, $L_2 \approx 140.74$ pH, and $C_T \approx 16.39$ fF.

The magnitude and phase of the reflection response, $|S_{11}|$ and $\angle S_{11}$, are shown in the Fig. 7-19a and Fig. 7-19b, respectively. There is an excellent match for both magnitude and phase of

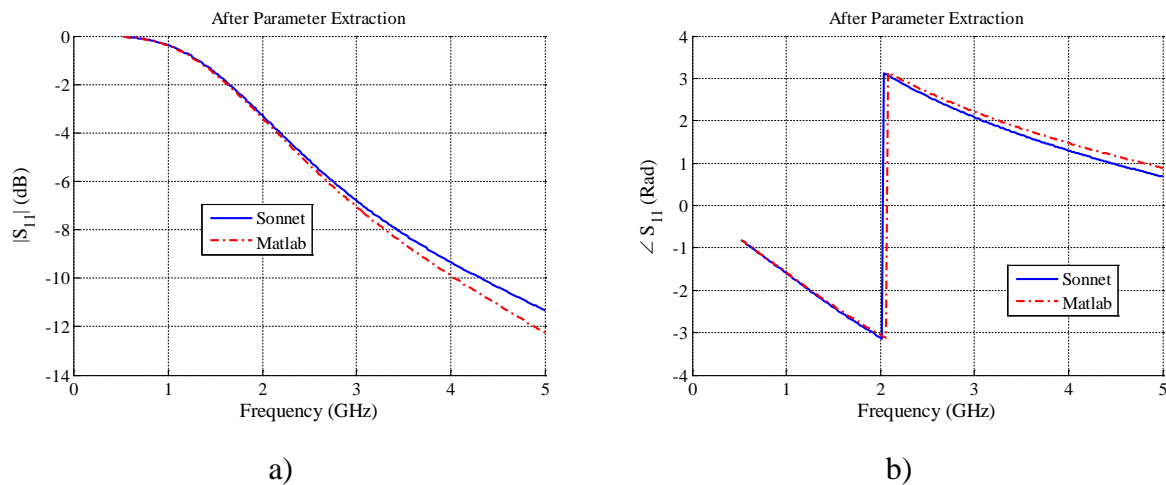


Fig. 7-19 S_{11} parameter response comparison between Matlab and Sonnet after PE of the CRLH unit-cell, illustrated in Fig. 7-7a, using the Matlab circuitual model shown in Fig. 7-7c (lossless case): a) magnitude, b) phase.

7. A Parameter Extraction Process for Equivalent Circuit Models of a CRLH TL

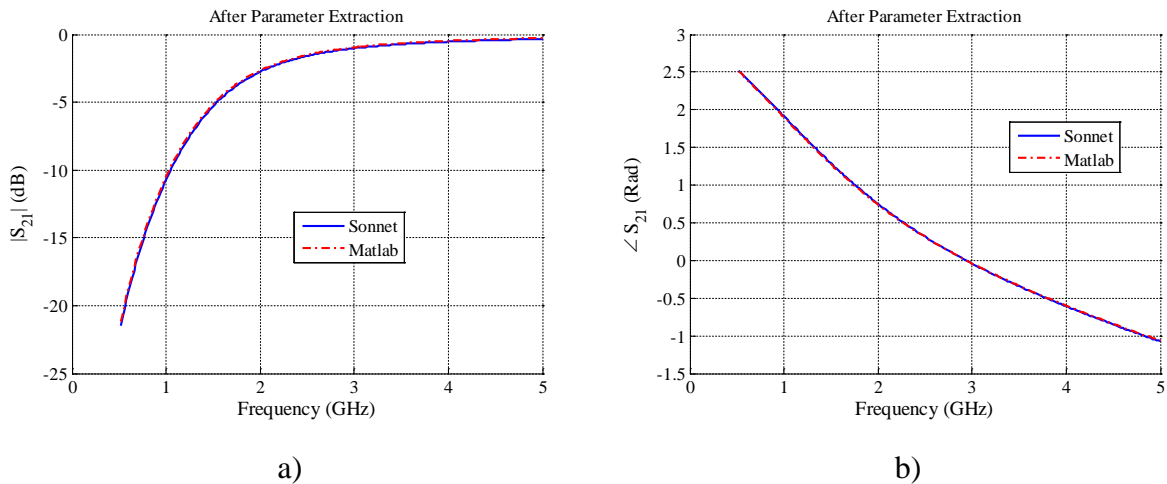


Fig. 7-20 S_{21} parameter response comparison between Matlab and Sonnet after PE of the CRLH unit-cell, illustrated in Fig. 7-7a, using the Matlab circuitual model shown in Fig. 7-7c (lossless case): a) magnitude, b) phase.

S_{11} below 2 GHz and an overall acceptable match over the complete frequency band.

The transmission responses, $|S_{21}|$ and $\angle S_{21}$, are shown in the Fig. 7-20a and Fig. 7-20b, respectively. It is observed an excellent match for both magnitude and phase of S_{21} in the working frequency band.

By comparing Fig. 7-17 with Fig. 7-19 and Fig. 7-18 with Fig. 7-20, it is confirmed that circuit in Fig. 7-7c is a better model for the complete unit-cell than that in Fig. 7-7b, as expected. It seems that the existing error in S_{11} (see Fig. 7-19a) is due to the slot effect. This difference is also observed in Section 7.4.4 (see Fig. 7-13-Fig. 7-14), the mismatch between EM and circuitual responses arises as frequency is increased above 3 GHz. For the sake of simplicity, and the fact that the error between Sonnet and Matlab is relatively small and present in $|S_{11}|$ above 3 GHz only, the slot is not modeled in this thesis.

In general it is confirmed that the EM response of the complete CRLH unit-cell structure, can be modeled with high accuracy using circuitual TL models and lumped circuitual models (for the bend), up to around 3.5 GHz.

7.4.7 PE of the Complete CRLH TL Structure

The per-unit length LC values of TL segments for the microstrip lines in the complete CRLH TL structure, illustrated in Fig. 7-1, are the same as those in Sections 7.4.1, 7.4.2, and

7. A Parameter Extraction Process for Equivalent Circuit Models of a CRLH TL

7.4.3. For illustrative purposes, initially the bend is neglected in the equivalent circuit model.

The magnitude and phase of the reflection response, $|S_{11}|$ and $\angle S_{11}$, are shown in Fig. 7-21a and Fig. 7-21b, respectively. It is seen a small mismatch between Sonnet and Matlab for S_{11} around 1.25 GHz. Matlab responses are displaced a few MHz to higher frequencies.

The magnitude and phase of the transmission response, $|S_{21}|$ and $\angle S_{21}$, are shown in Fig. 7-22a and Fig. 7-22b, respectively. It is seen also a small mismatch between Matlab and Sonnet

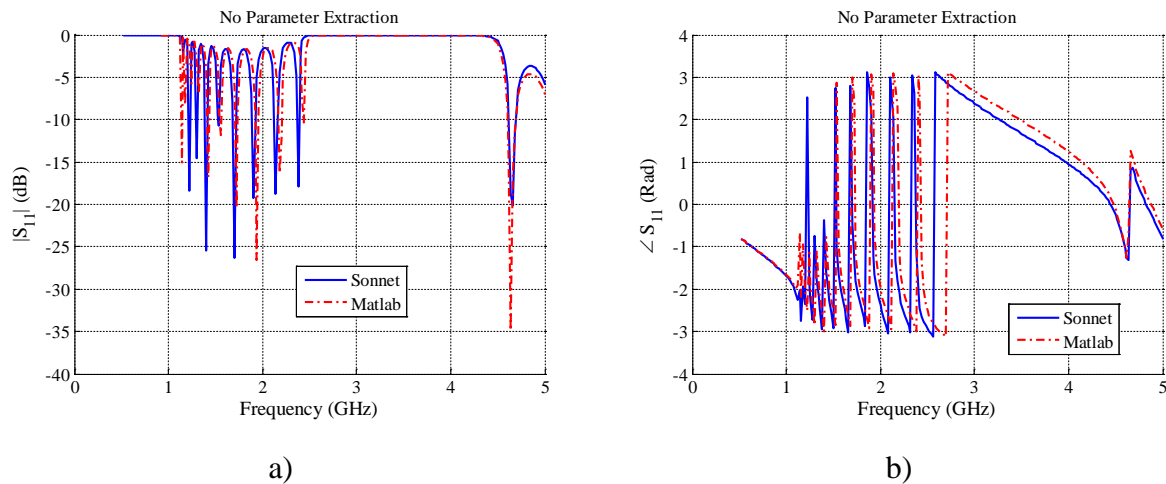


Fig. 7-21 S_{11} parameter response comparison between Matlab and Sonnet with no PE of the complete CRLH TL structure, illustrated in Fig. 7-1 (lossless case and neglecting the bend and slot): a) magnitude, b) phase.

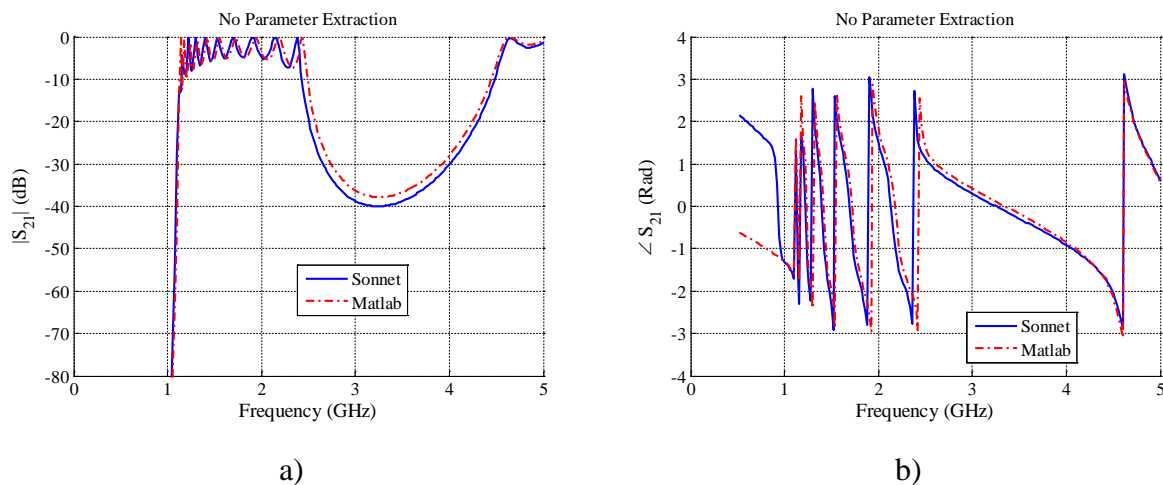


Fig. 7-22 S_{21} parameter response comparison between Matlab and Sonnet with no PE of the complete CRLH TL structure, illustrated in Fig. 7-1 (lossless case and neglecting the bend and slot): a) magnitude, b) phase.

7. A Parameter Extraction Process for Equivalent Circuit Models of a CRLH TL

for S_{21} around 1.25 GHz. The phase of S_{21} shows a particularly large mismatch below 1 GHz. Again, Matlab response is displaced a few MHz to higher frequencies.

We now consider the equivalent circuit for the complete unit-cell of the CRLH structure modeling the bend (Fig. 7-7c). The width of the microstrip line segments in the unit-cell, illustrated in Fig. 8a, is the same in all the unit-cells illustrated in Fig. 7-1. The EM interaction for each unit-cell is expected to be the same as that one in Section 7.4.6. Hence, the same

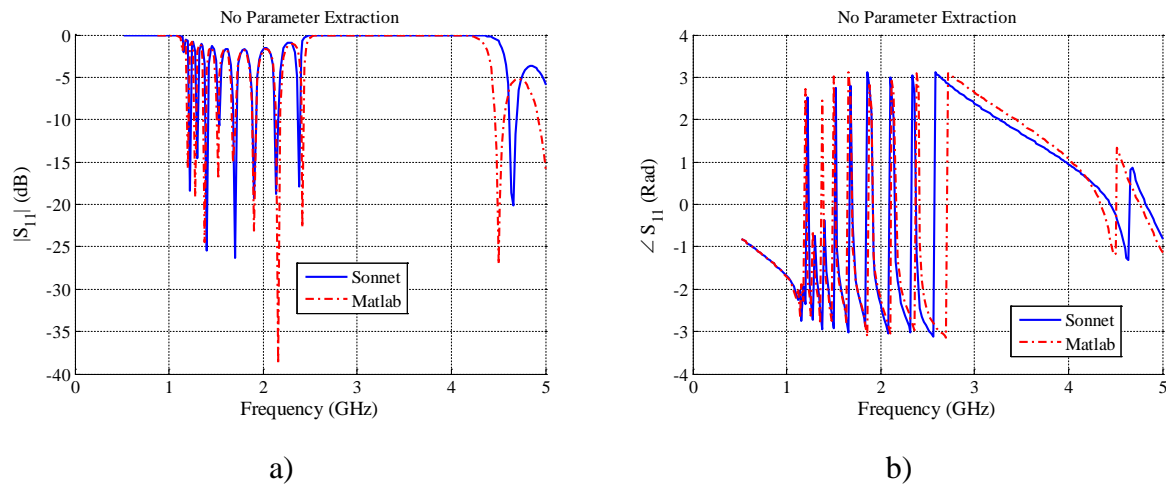


Fig. 7-23 S_{11} parameter response comparison between Matlab and Sonnet with no PE of the complete CRLH TL structure, illustrated in Fig. 7-1 (lossless case with bend and neglecting the slot): a) magnitude, b) phase.

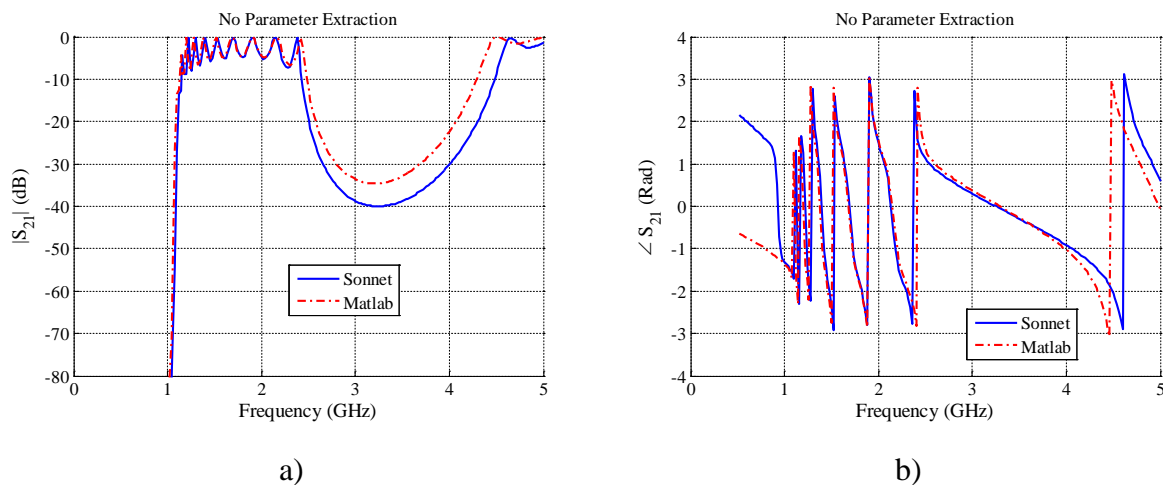


Fig. 7-24 S_{21} parameter response comparison between Matlab and Sonnet with no PE of the complete CRLH TL structure, illustrated in Fig. 7-1 (lossless case with bend and neglecting the slot): a) magnitude, b) phase.

7. A Parameter Extraction Process for Equivalent Circuit Models of a CRLH TL

average extracted values, for the bend circuital model, are used in this case.

The magnitude and phase of the reflection response, $|S_{11}|$ and $\angle S_{11}$, are shown in Fig. 7-23a and Fig. 7-23b, respectively. It is observed a very good match between Matlab and Sonnet for S_{11} below 2 GHz. The differences between the EM and circuital responses are increased above ~2.25 GHz.

The magnitude and phase of the transmission response, $|S_{21}|$ and $\angle S_{21}$, are shown in Fig. 7-24a and Fig. 7-24b, respectively. It is seen an excellent match between Sonnet and Matlab for S_{21} , between 1 GHz and 2.25 GHz. The phase of S_{21} shows a particularly large mismatch below 1 GHz. Again, the differences between the EM and circuital responses are increased above ~2.25 GHz.

By comparing Fig. 7-21 with Fig. 7-23, and Fig. 7-22 with Fig. 7-24, it is confirmed that circuit in Fig. 7-7c is a better model (below ~2.25 GHz), than that one in Fig. 7-7b. Apparently, the error between EM and circuital responses above 2.25 GHz, is due to the cumulative effect of all the slots not being modeled in the assembled circuital approximation. Notice that this error is also observed in Section 7.4.6 (see Fig. 7-19a).

Finally, it is seen from Fig. 7-23-Fig. 7-24 that the EM response of the complete CRLH TL structure, can be modeled using circuital TL models and lumped circuital models (for the bend), up to 2.25 GHz with high accuracy.

7.5. Parameter Extraction Considering Losses

7.5.1 PE of the Lossy Microstrip Line 6.5 mm Long

After the optimization process, the per-unit length RGLC values are: $L_{\text{seg}} \approx 263.16$ nH/m, $C_{\text{seg}} \approx 90.69$ pF/m, $R_{\text{seg}} \approx 19.67$ Ω /m, and $G_{\text{seg}} \approx 0.147$ mS/m.

The magnitude and phase of the reflection response, $|S_{11}|$ and $\angle S_{11}$, are shown in the Fig. 7-25a and Fig. 7-25b, respectively. There is an excellent match between Sonnet and Matlab responses for $|S_{11}|$. The phase of S_{11} shows some errors between EM and circuital responses below 1.5 GHz, although there is an excellent match above 2 GHz.

The transmission responses, $|S_{21}|$ and $\angle S_{21}$, are shown in the Fig. 7-26a and Fig. 7-26b,

7. A Parameter Extraction Process for Equivalent Circuit Models of a CRLH TL

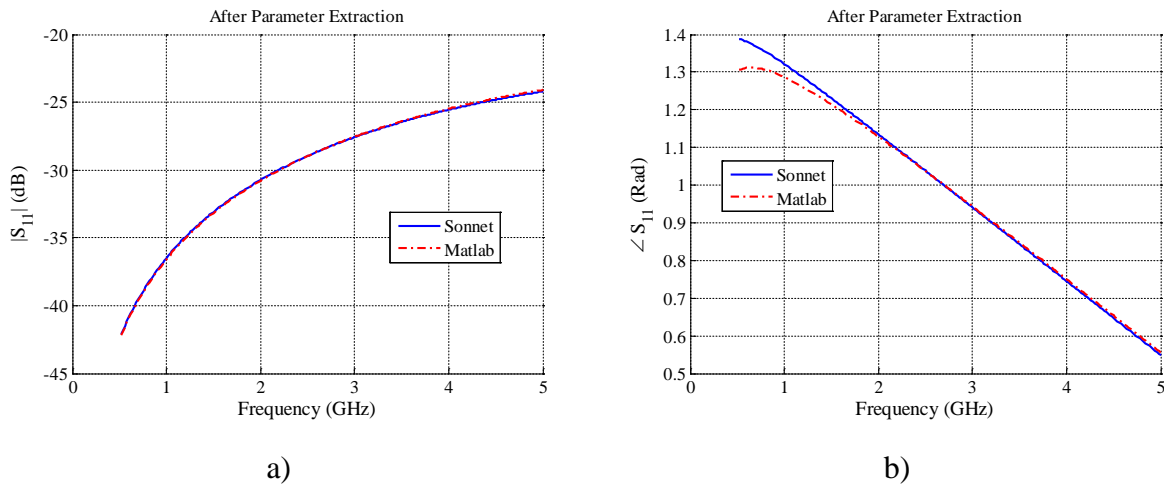


Fig. 7-25 S_{11} parameter response comparison between Matlab and Sonnet after the PE of the 6.5 mm TL long illustrated in Fig. 7-3a (lossy case): a) magnitude, b) phase.

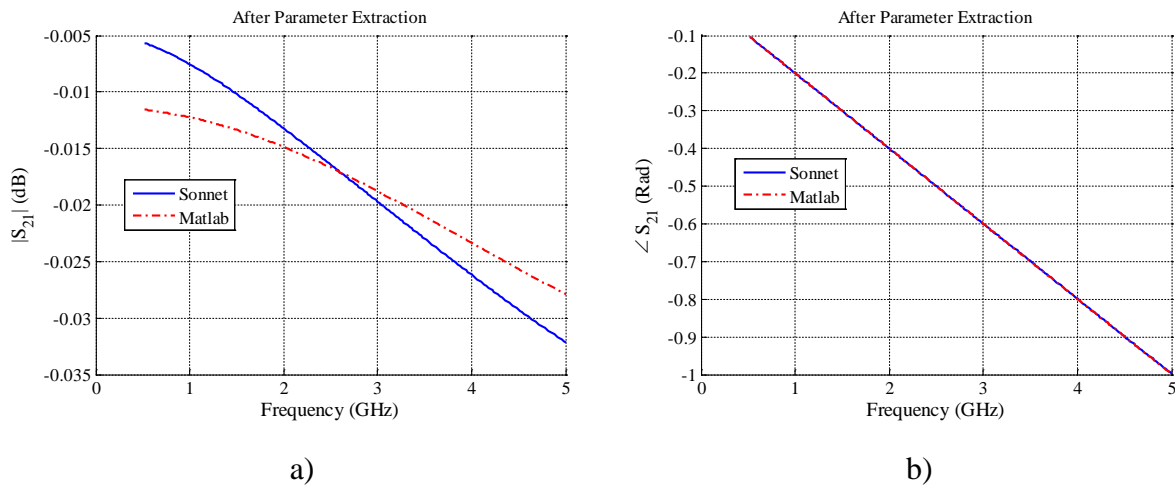


Fig. 7-26 S_{21} parameter response comparison between Matlab and Sonnet after the PE of the 6.5 mm TL long illustrated in Fig. 7-3a (lossy case): a) magnitude, b) phase.

respectively. It is seen some mismatch between Sonnet and Matlab responses for $|S_{21}|$, although this mismatch is very small (<0.006 dB). The phase of S_{21} shows an excellent match between both EM and circuitual models.

It is confirmed that the EM response of this lossy microstrip line segment can be modeled with circuitual lossy transmission line models up to 5 GHz with good accuracy.

7. A Parameter Extraction Process for Equivalent Circuit Models of a CRLH TL

7.5.2 PE of the Lossy Microstrip Line 5 mm Long

After the optimization process, the per-unit length $RGLC$ values are: $L_{\text{seg}} \approx 259.05$ nH/m, $C_{\text{seg}} \approx 91.22$ pF/m, $R_{\text{seg}} \approx 19.50$ Ω /m, and $G_{\text{seg}} \approx 0.145$ mS/m.

The magnitude and phase of the reflection response, $|S_{11}|$ and $\angle S_{11}$ are shown in the Fig. 7-27a and Fig. 7-27b, respectively. It is seen that there is an excellent match between Sonnet and Matlab for $|S_{11}|$. The phase of S_{11} shows a small error below 1.5 GHz, although also shows an excellent match above around 1.8 GHz.

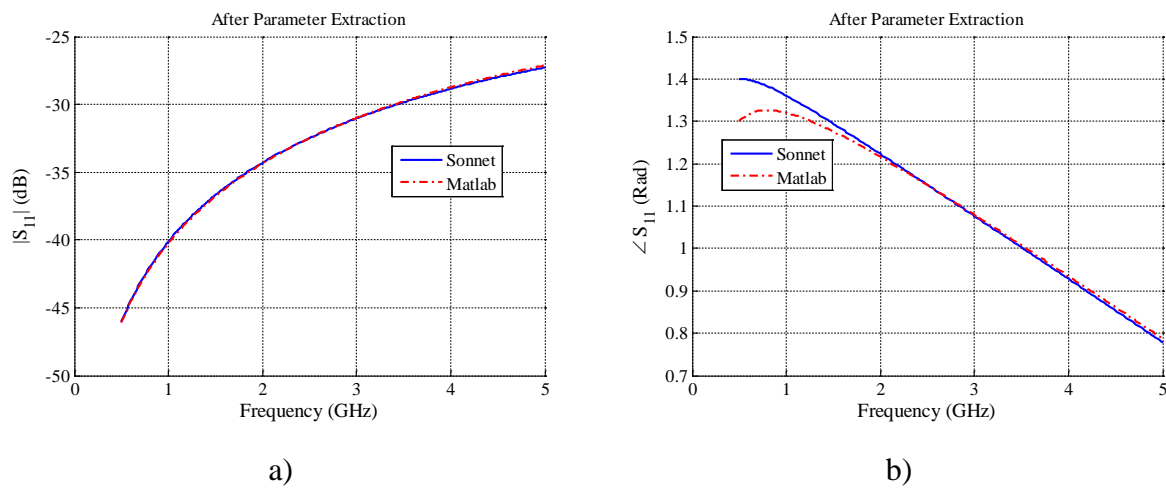


Fig. 7-27 S_{11} parameter response comparison between Matlab and Sonnet after the PE of the 5 mm TL long illustrated in Fig. 7-3a (lossy case): a) magnitude, b) phase.

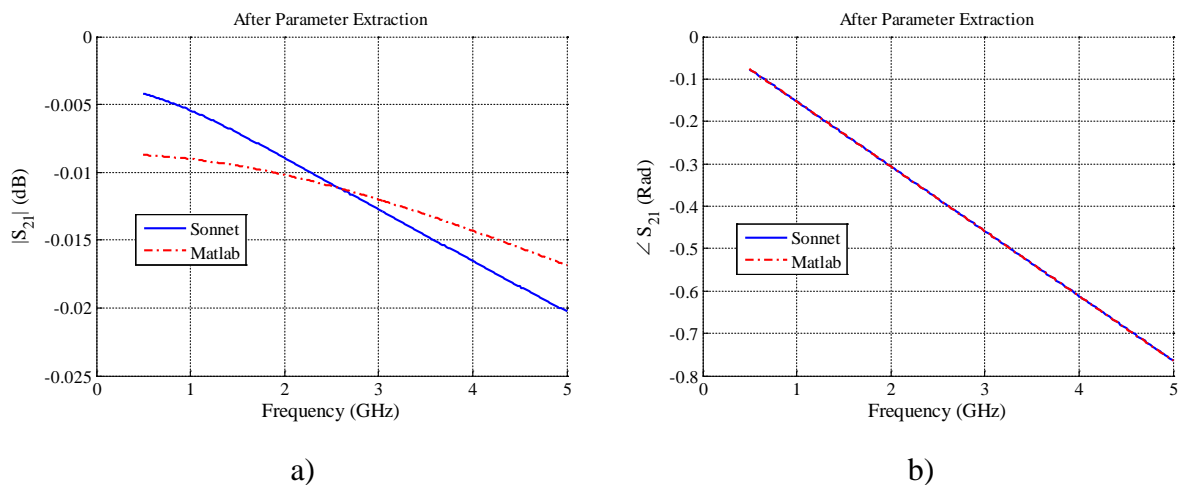


Fig. 7-28 S_{21} parameter response comparison between Matlab and Sonnet after the PE of the 5 mm TL long illustrated in Fig. 7-3a (lossy case): a) magnitude, b) phase.

7. A Parameter Extraction Process for Equivalent Circuit Models of a CRLH TL

The transmission responses, $|S_{21}|$ and $\angle S_{21}$, are shown in the Fig. 7-28a and Fig. 7-28b, respectively. It is seen a small mismatch between Sonnet and Matlab for $|S_{21}|$. Again, this mismatch between Sonnet and Matlab is very small (< 0.005 dB). The phase of S_{21} shows an excellent match between the EM and circuital responses.

The mismatch between Sonnet and Matlab responses, in Sections 7.5.1 and 7.5.2, is apparently due to the fact that the circuital models are using per-unit length average values in the complete frequency band. As frequency is increased the skin effect arises, and the resistive losses can no longer be represented as per-unit length average values (see Chapter 5) in the complete frequency band. The accuracy of the circuital model could be enhanced by using frequency dependent per-unit length lossy parameters, but we preferred to keep the circuital model simple.

It is confirmed that the EM response of this lossy microstrip line segment can be modeled with circuital lossy transmission line models up to 5 GHz with good accuracy.

7.5.3 PE of the Lossy Microstrip Grounded Stub

After the optimization process, the per-unit length RGLC values are: $L_{\text{stub}} \approx 384.56$ nH/m, $C_{\text{stub}} \approx 73.58$ pF/m, $R_{\text{stub}} \approx 35.74$ Ω /m, and $G_{\text{stub}} \approx 0.039$ mS/m.

The magnitude and phase of the reflection response, $|S_{11}|$ and $\angle S_{11}$, are shown in Fig. 7-

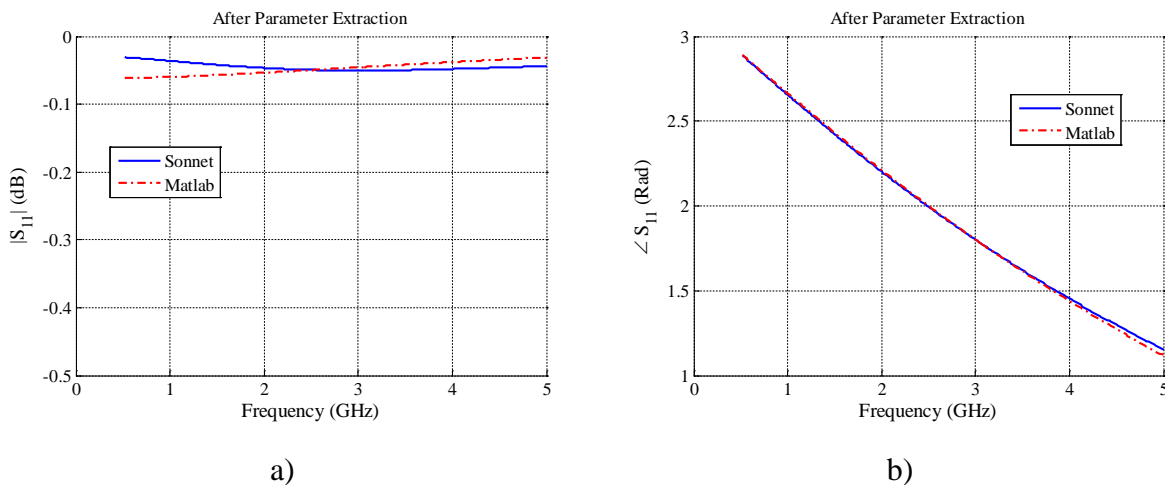


Fig. 7-29 S_{11} parameter response comparison between Matlab and Sonnet after the PE of the microstrip grounded stub shown in Fig. 7-4a (lossy case): a) magnitude, b) phase.

7. A Parameter Extraction Process for Equivalent Circuit Models of a CRLH TL

29a and Fig. 7-29b, respectively. It is seen a small error between Matlab and Sonnet for $|S_{11}|$, although the mismatch between the EM and circuital responses is small (< 0.03 dB). The phase of S_{11} shows an excellent match up to 4 GHz, confirming that the EM response of this lossy microstrip grounded stub can be modeled with circuital lossy transmission line models up to 5 GHz with good accuracy.

7.5.4 PE of the Two Lossy Microstrip Lines Separated by a Capacitor over a Gap

The per-unit length *RGLC* values of each TL separated by the capacitor over a gap (see Fig. 7-5b), are the same as those in Section 7.5.2.

The magnitude and phase of the reflection response, $|S_{11}|$ and $\angle S_{11}$, are shown in Fig. 7-30a and Fig. 7-30b, respectively. Although there is an excellent match in the low frequency band, below 2 GHz, the difference between Matlab and Sonnet arises as frequency is increased.

The transmission responses, $|S_{11}|$ and $\angle S_{11}$, are shown in Fig. 7-31a and Fig. 7-31b, respectively. There is an excellent match in $|S_{11}|$ up to 5 GHz. The phase of S_{11} shows an excellent match below 2 GHz, however, the error arises as frequency is increased.

In general, it is observed a similar behavior for this sub-structure to that one for the lossless case, confirming that the existing error is due to the slot not being modeled.

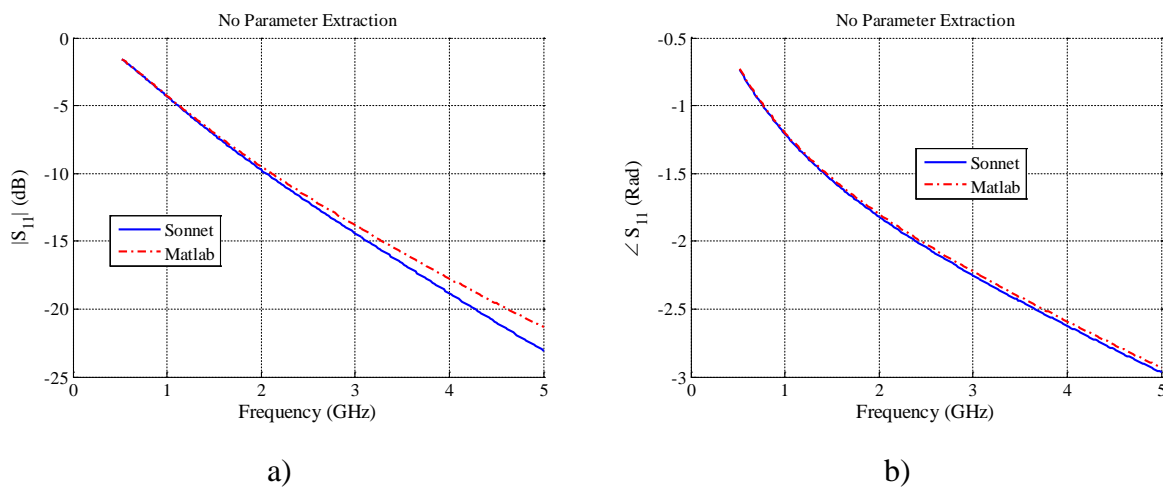


Fig. 7-30 S_{11} parameter response comparison between Matlab and Sonnet with no PE of the two 5 mm TL long, and series capacitor over a gap, illustrated in Fig. 7-5a (lossy case): a) magnitude, b) phase.

7. A Parameter Extraction Process for Equivalent Circuit Models of a CRLH TL

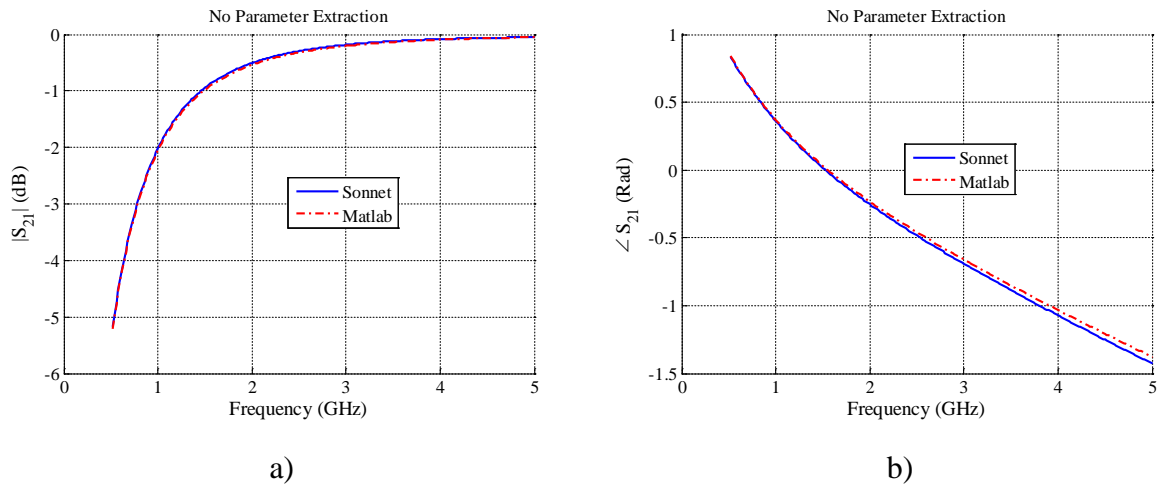


Fig. 7-31 S_{21} parameter response comparison between Matlab and Sonnet with no PE of the two 5 mm TL long, and series capacitor over a gap, illustrated in Fig. 7-5a (lossy case): a) magnitude, b) phase.

7.5.5 PE of the Complete Lossy Unit-Cell of the CRLH Structure

The per-unit length $RGLC$ values of the TL model for microstrip lines in the direction of signal propagation (see Fig. 8a), are the same as those in 7.5.2. Similarly, the per-unit length $RGLC$ values of the TL model for the grounded stub, illustrated in Fig. 8a, are the same as those in Section 7.5.3. The bend is considered and its average extracted values are: $L_1 \approx 0.190$ aH, $L_2 \approx$

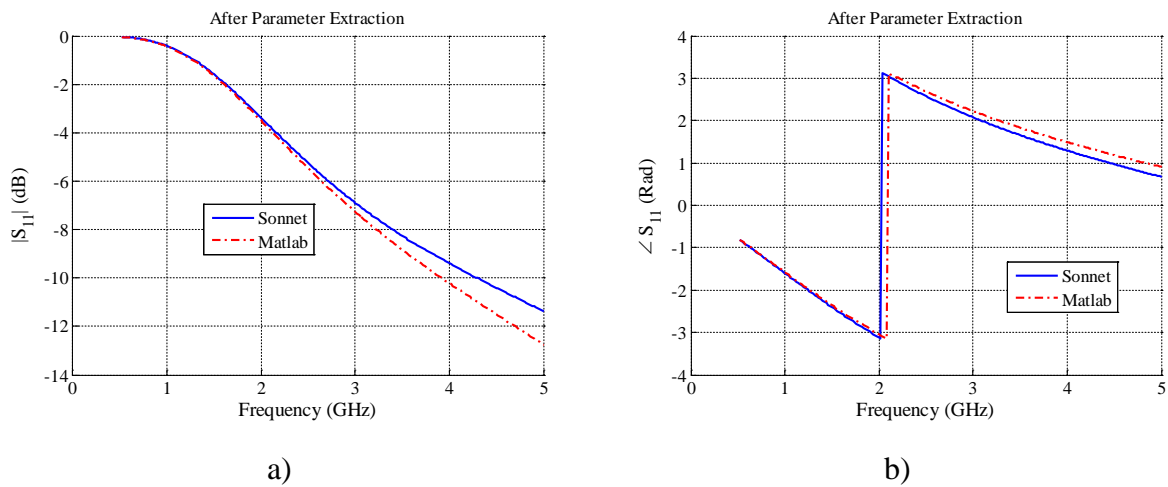


Fig. 7-32 S_{11} parameter response comparison between Matlab and Sonnet after PE of the CRLH unit-cell, illustrated in Fig. 7-7a, using the Matlab circuital model shown in Fig. 7-7c (lossy case): a) magnitude, b) phase.

7. A Parameter Extraction Process for Equivalent Circuit Models of a CRLH TL

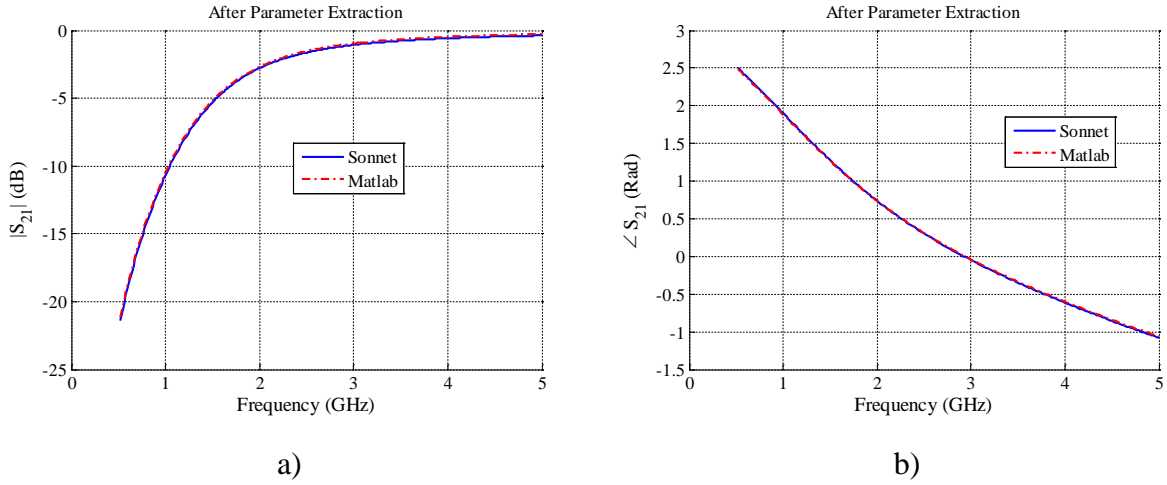


Fig. 7-33 S_{21} parameter response comparison between Matlab and Sonnet with no PE of the CRLH unit-cell, illustrated in Fig. 7-7a, using the Matlab circuitual model shown in Fig. 7-7c (lossy case): a) magnitude, b) phase.

177.49 pH, and $C_T \approx 0.938$ aF.

The magnitude and phase of the reflection response, $|S_{11}|$ and $\angle S_{11}$, are shown in the Fig. 7-32a and Fig. 7-32b, respectively. There is an excellent match for S_{11} below 2 GHz, and an overall acceptable match over the complete frequency band.

The transmission responses, $|S_{21}|$ and $\angle S_{21}$, are shown in the Fig. 7-33a and Fig. 7-33b, respectively. It is observed an excellent match for S_{21} in the working frequency band. It is observed a similar behavior as that one for the lossless case, as expected.

7.5.6 PE of the Complete Lossy CRLH TL Structure

The per-unit length *RGLC* values of the TL segments for the microstrip lines, illustrated in Fig. 7-1, are the same as those in Sections 7.5.1, 7.5.2, and 7.5.3. Similarly, the extracted values of the bend's circuitual approximation are the same as those in Section 7.5.5.

The magnitude and phase of the reflection response, $|S_{11}|$ and $\angle S_{11}$, are shown in Fig. 7-34a and Fig. 7-34b, respectively. It is observed a relatively good match between Matlab and Sonnet responses for S_{11} below 2 GHz.

The magnitude and phase of the transmission response, $|S_{21}|$ and $\angle S_{21}$, are shown in Fig. 7-35a and Fig. 7-35b, respectively. It is seen a relatively good match between Sonnet and Matlab for S_{21} , between 1.1 GHz and 2.25 GHz. The phase of S_{21} shows a particularly large mismatch

7. A Parameter Extraction Process for Equivalent Circuit Models of a CRLH TL

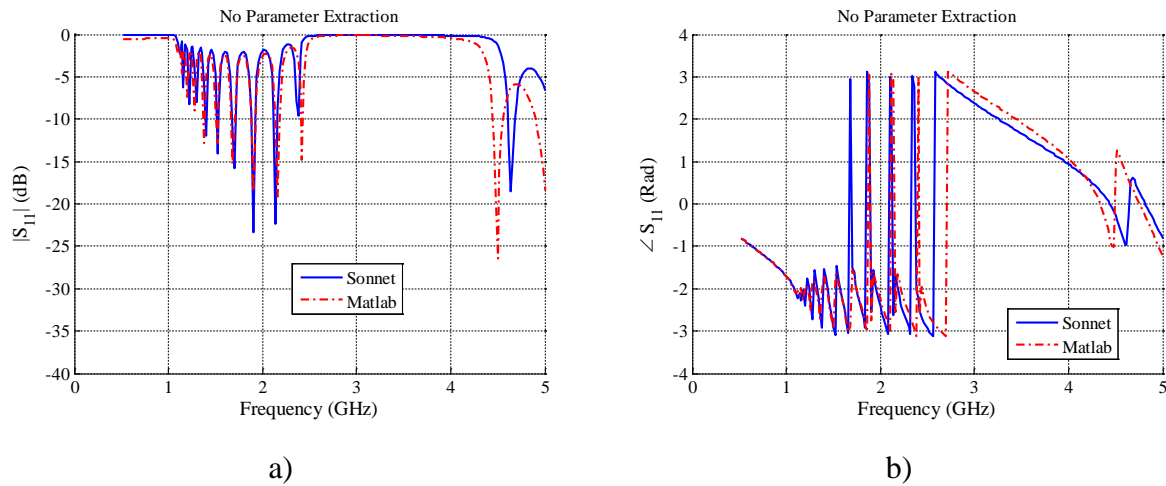


Fig. 7-34 S_{11} parameter response comparison between Matlab and Sonnet with no PE of the complete CRLH TL structure, illustrated in Fig. 7-1 (lossy case with bend and neglecting the slot): a) magnitude, b) phase.

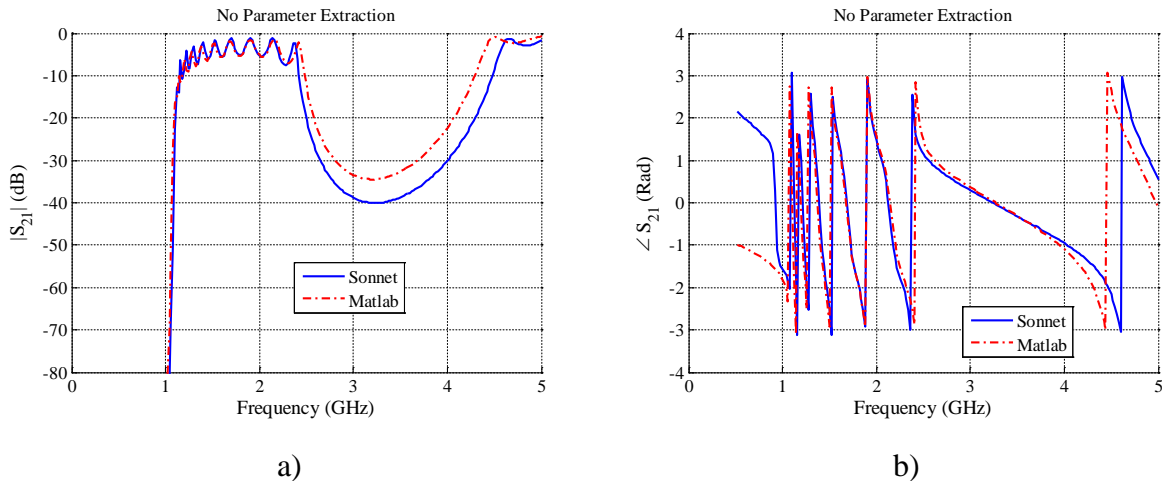


Fig. 7-35 S_{21} parameter response comparison between Matlab and Sonnet with no PE of the complete CRLH TL structure, illustrated in Fig. 7-1 (lossy case with bend and neglecting the slot): a) magnitude, b) phase.

below 1.1 GHz. Again, the differences between the EM and circuital responses are increased above 2.25 GHz.

By comparing Fig. 7-23-Fig. 7-24 with Fig. 7-34-Fig. 7-35, it is confirmed that the lossless approximation shows a slightly better match between the EM and circuital models, as expected. The increased mismatch in the lossy case, in the low frequency band, is due to our simplified circuital approximation of the metallic and dielectric losses. We use average per-unit

7. A Parameter Extraction Process for Equivalent Circuit Models of a CRLH TL

length parameter values, and due to the skin effect mainly, the resistive losses are increased with the frequency (see Chapter 5). Then, frequency dependent per-unit length loss parameters could be used to enhance the accuracy of the circuital model. For the sake of simplicity, our circuital models use only frequency independent per-unit length average values.

7.6. Conclusions

A methodology to extract the CRLH parameter values of an equivalent circuit, based on full-wave EM simulation of a metamaterial physical structure, was presented in this chapter. The unit-cell of the CRLH TL structure was decomposed into simpler conventional microstrip line structures, and its equivalent *RGLC* per-unit length values were extracted for each structure using Matlab. A comparison between Sonnet and Matlab S-parameter responses were presented and briefly discussed. An excellent match is obtained in the lossless case of each sub-structure by using per-unit length average values, although small differences arise using more complex structures. The lossy case shows a small mismatch in each sub-structure due to the simplicity of the circuital model e.g. the skin effect neglected, and as expected, the differences between EM and circuital responses are slightly increased when using more complex structures. In general, it was confirmed that a circuital model based on lumped components and simple transmission lines is able to capture the overall performance of this complex CRLH interconnect.

To increase the Matlab model accuracy, the slot could be modeled, and the circuital models of the lossy case could be built using frequency dependent per-unit length parameters.

General Conclusions

This thesis studied the basics of a transmission line (TL) theory, and circuitual model approximations, of purely right-handed (PRH), purely left-handed (PLH), and composite right/left-handed (CRLH) TL structures. The overall results indicate that the equivalent circuitual models, with parameter values extracted by optimization, yields a quite acceptable approximation of the CRLH TL responses obtained by full-wave electromagnetic simulations.

At first, the basic concepts of metamaterials and, the left-handed behavior were explained. The microstructure concept and its importance for artificial structures to create left-handed media, were explained. Two methodologies to create LH materials, as resonant and non-resonant structures, were introduced, including an example of each of these structures. The importance of having broad bandwidth in high-speed interconnections was briefly explained.

Then, the basic concepts of a conventional transmission line were presented to develop a simple model of the input impedance, and the voltage gain, using the ABCD-parameters in Matlab. These scripts can be used for lossless and lossy cases. It was demonstrated that simple PRH TL approximations can be achieved by using lumped element models in the frequency range where the *RGLC* transmission line model response is still valid.

Similarly, the basic concepts of a PLH TL were presented to develop a simple model of this component. The input impedance, the voltage gain, and S-parameter calculations were achieved using the ABCD-parameters of each interconnect element. It was possible to achieve acceptable results by using lossy PLH TL models. As in the PRH case, the LH conductance loss has a larger effect than the LH resistive loss in PLH transmission lines. It was demonstrated that simple LH TL approximations can be achieved by using TL element models in the frequency range where the *RGLC* TL model response is still valid.

The basic concepts of a CRLH TL were also presented to develop a simple model of this component. The S-parameter calculations were achieved using the ABCD-parameters of each interconnect element. It was observed that the right/left-handed conductance losses have larger effects than the right/left-handed resistive losses in CRLH TL. It was demonstrated that simple right/left-handed TL approximations can be achieved by using the TL and lumped element

models in the low frequency range, where the *RGLC* transmission line model is still valid.

A procedure to extract the equivalent circuit *RGLC* values of a PRH TL was described. It was demonstrated that simple direct parameter extraction (PE) process can be used to obtain the equivalent *RGLC* values of lumped element models from a target response, in the frequency range where the *RGLC* TL model is still valid. However, it was also demonstrated that these parameter extraction problems can be ill-conditioned at some frequency ranges, in which case a number of techniques can be applied to decrease the ill-condition effects, such as using penalty functions with suitable weighting factors, or reducing the number of optimization variables.

Then, a compilation of several physical implementations of CRLH TL structures were briefly described, and its S-parameter responses were also discussed. One structure using microstrip technology and ideal loading series capacitors was selected looking forward to extract its *RGLC* equivalent values.

Finally, a methodology to extract the CRLH parameter values of an equivalent circuit, based on full-wave EM simulation of a metamaterial physical structure, was presented. The unit-cell of the CRLH TL structure was decomposed into simpler conventional microstrip line structures, and its equivalent *RGLC* per-unit length average values were extracted for each sub-structure using Matlab. An excellent match is obtained in the lossless case of each sub-structure by using per-unit length average values, although small differences arise when using more complex structures. The lossy case shows a small mismatch in each sub-structure due to the simplicity of the circuit model, e.g. the skin effect neglected. Although the differences between EM and circuit responses are slightly increased when using more complex structures; in general, it was confirmed that a circuit model based on lumped components and simple TL is able to capture the overall performance of this complex CRLH interconnect.

As a possible continuation of this thesis work, I propose a number of ideas. APLAC or any other high-frequency circuit simulator, such as ADS, can be used as the circuit model approximation, and use the already existing circuit model approximations for each sub-component, such as the right-angle bend and the slot. Using the circuit simulator, the match between the 3D EM simulated responses and its circuit approximation responses, may be increased on the high-frequency range. Also, for real world applications, it is important to do some research on the dielectric material type that can provide low loss at the working frequency band. Similarly, if the SMT devices are used on the CRLH TL structure, their 3D models or their

equivalent non-ideal circuit models should also be included, such that the simulated results are closer to reality.

Appendix

A. List of Internal Research Reports

- [1] E. R. Villa-Loustaunau and J. E. Rayas-Sánchez, “A general introduction to metamaterials,” Internal Report *CAECAS-10-13-R*, ITESO, Tlaquepaque, Mexico, Dec. 2010.
- [2] E. R. Villa-Loustaunau and J. E. Rayas-Sánchez, “Modeling a right-handed transmission line in Matlab,” Internal Report *CAECAS-11-13-R*, ITESO, Tlaquepaque, Mexico, Aug. 2011.
- [3] E. R. Villa-Loustaunau and J. E. Rayas-Sánchez, “Modeling a left-handed transmission line in Matlab,” Internal Report *CAECAS-11-21-R*, ITESO, Tlaquepaque, Mexico, Nov. 2011.
- [4] E. R. Villa-Loustaunau and J. E. Rayas-Sánchez, “Modeling a composite right/left-handed transmission line in Matlab with equivalent circuits,” Internal Report *CAECAS-12-01-R*, ITESO, Tlaquepaque, Mexico, Jan. 2012.
- [5] E. R. Villa-Loustaunau and J. E. Rayas-Sánchez, “A parameter extraction process for equivalent circuit models of a purely right-handed transmission line in matlab”, Internal Report *CAECAS-12-10-R*, ITESO, Tlaquepaque, Mexico, June 2012.
- [6] E. R. Villa-Loustaunau and J. E. Rayas-Sánchez, “Physical implementations of composite right/left-handed transmission lines”, Internal Report *CAECAS-12-23-R*, ITESO, Tlaquepaque, Mexico, Dec. 2012.
- [7] E. R. Villa-Loustaunau and J. E. Rayas-Sánchez, “A parameter extraction process for equivalent circuit models of a composite right/left-handed transmission line”, Internal Report *CAECAS-13-10-R*, ITESO, Tlaquepaque, Mexico, Dec. 2013.

Bibliography

- [Averitt-06] R. D. Averitt, A. J. Taylor, and W. J. Padilla “Metamaterials for threat reduction applications: imaging, signal processing, and cloacking”, *Material Research Highlight*, Los Alamos National Laboratory, 2006.
- [Ballesta-09] F. Aznar Ballesta, *Caracterización de nuevos resonadores metamaterial, líneas de transmisión artificiales y aplicaciones en el diseño de circuitos de comunicaciones*, Doctoral Thesis, Universidad Autónoma de Barcelona, May. 2009.
- [Breed-07] G. Breed, “Metamaterials Allow Manipulation of EM waves from Low Frequencies to Light”, *High Frequency Electronics*, pp. 28-30, vol. 6, March 2007.
- [Caloz-02] C. Caloz and T. Itoh, “Application of a transmission line theory of left-handed (LH) materials to the realization of a microstrip “LH line”, in *IEEE Antennas and Propagation Society International Symposium*, vol. 2, pp. 412-415, Aug. 2002.
- [Caloz-06] C. Caloz and T. Itoh, *Electromagnetic Metamaterials*. Hoboken, New Jersey: Wiley-Interscience, 2006.
- [Cripps-06] S. T. Cripps, “Microwave bytes”, *IEEE Microwave Magazine*, pp 32-37, Dec. 2006.
- [Decoopman-04] T. Decoopman, O. Vanbésien, and D. Lippens, “Demonstration of a backward wave in a single split ring resonator and wire loaded fine”, *IEEE Microwave and Wireless Comp. Letters*, vol. 14, pp. 507-509, Nov. 2004.
- [Estrada-11] E. Estrada-Arámbula and J. E. Rayas-Sánchez, “Effects of discontinuities in the reference plane on the performance of microstrip lines,” Internal Report *CAECAS-11-07-R*, ITESO, Tlaquepaque, Mexico, Jun. 2011.
- [Gupta-96] K.C. Gupta, R. Garg, I. Bahl, and P. Bhartia, *Microstrip Lines and Slotlines*. Norwood, MA: Artech House, Inc., 1996.
- [Kogure-10] H. Kogure, Y. Kogure, and J.C. Rautio, *Introduction to RF Design Using EM Simulators*, Tokyo, Japan: UNI Agency, Inc., 2010.
- [Koziel-08] S. Koziel, Q. S. Cheng, and J. W. Bandler, “Space mapping,” *IEEE Microwave Magazine*, vol. 9, pp. 105-122, Dec. 2008.
- [Kshetrimayum-04] R. S. Kshetrimayum, “Introduction to metamaterials”, *IEEE Potentials*, pp. 44-46, Dec. 2004.
- [Lai-04] A. Lai, C. Caloz, and T. Itoh “Composite right/left-handed transmission line metamaterials”, *IEEE Microwave Magazine*, pp. 34-50, Sep. 2004.
- [Lai -07] A. Lai and T. Itoh, “Left-handed metamaterials for microwave applications”, in *Application Workshops for High-Performance Electronic Design*, Department of Electrical Engineering of UCLA, pp. 7-12, 2007.

- [Li-08] B. Li, J. Ping, and W. Wu, "A planar microstrip implementation of dual-composite right/left-handed transmission line", in *Int. Conf. on Microwave and Millimeter Wave Technology (ICMMT2008)*, Nanjing, China, April, 2008, vol. 4, pp. 1617 – 1619.
- [Ludwig-00] R. Ludwig and P. Bretchko, *RF Circuit Design*. Upper Saddle River, NJ: Prentice-Hall, 2000.
- [Madrid-05] L. J. R. Madrid, *Diseño de Dispositivos Pasivos Compactos en Tecnología Guiada y Materiales EBG*, Internal report, Universidad Politécnica de Valencia, Valencia, Oct. 2005.
- [Pendry-96] J. B. Pendry, A. J. Holden, W. J. Stewart, and I. Youngs "Extremely low frequency plasmons in metallic mesostructures", *Physical Review Letters*, vol. 76, pp. 4773-4776, June 1996.
- [Pendry-99] J. B. Pendry, A. J. Holden, D. J. Robbins, and W. J. Stewart, "Magnetism from conductors and enhanced nonlinear phenomena", *IEEE Trans. on Microwave Theory and Tech.*, vol. 47, pp 2075-2084, Nov. 1999.
- [Pendry -04] J. B. Pendry and D. R. Smith, "Reversing light: negative refraction", *Physics Today*, vol. 57, pp. 37-43, June 2004.
- [Pozar-05] D. M. Pozar, *Microwave Engineering*. Hoboken, NJ: John Wiley & Sons, Inc., 2005.
- [Qiang-10] L. Qiang, H. Lu, W. Zhao, J.-K. Wang, and B. Liu, "Simplified extended composite right/left-handed transmission line structure for dual-band applications", *Progress in Electromagnetics Research Letters*, 2010, vol. 15, pp. 137 – 144.
- [Rincón-07] J. G. Rincón, Diseño e Implementación de un Divisor de Potencia en banda dual con estructuras metamateriales basadas en CSRRs, Bachelor Memory, Universidad Autónoma de Barcelona, Bellaterra, Sep. 2007.
- [Sanchez-09] J. J. Sánchez-Martínez, E. Márquez-Segura, P. Otero, and C. Camacho-Peñaloza, "Artificial transmission line with left/right-handed behavior based on wire bonded interdigital capacitors", *Progress in Electromagnetics Research B*, 2009, vol. 11, pp. 245 – 264.
- [Siddiqui-03] O. F. Siddiqui, M. Mojahedi, and G. V. Eleftheriades, "Periodically loaded transmission line with effective negative refractive index and negative group velocity", *IEEE Transactions on Antennas and Propagation*, Oct., 2003, vol. 51, no. 10, pp. 2619 – 2625.
- [Suntives-07] A. Suntives, A. Khajooeizadeh, R. Abhari, "Characterization of metamaterial interconnects," in *Int. Conf. on Electrical Performance of Electronic Packaging*, Atlanta, GA, Oct., 2007, pp. 211 – 214.
- [Thierauf-04] S. C. Thierauf, *High-Speed Circuit Board Signal Integrity*. Norwood, MA: Artech House, 2004.
- [Wei-08] W. Wei, and H. Li, "Inhomogeneous composite right/left-handed transmission line", in *Int. Conf. on Microwave and Millimeter Wave Technology (ICMMT2008)*, Nanjing, China, April, 2008, vol. 3, pp. 1583 – 1586.
- [Veselago-68] V. G. Veselago, "The electrodynamics of substances with simultaneously negative values of ϵ and μ ", *Soviet Physics USPEKHI*, vol. 10, pp. 509-514, Jan. 1968.

Index

B

balanced case, 55, 56, 61, 62, 67, 68

Ch

characteristic impedance, 23, 33, 37, 40, 44, 54, 56, 73, 75, 109

C

complex propagation constant, 22, 53
composite right/left-handed, 1, 2, 17, 49, 51, 52, 62, 89, 90-92, 94, 95, 97-103, 131, 135, 138
conductance, 22, 36, 46, 48, 49, 64-70, 82, 85, 131
conductivity, 22, 79
conventional transmission line, 102
CRLH TL lossless model, 52, 54
CRLH TL lossy model, 56
cutoff frequencies, 42, 55, 56

D

dielectric constant, 73, 104
dispersion diagram, 18, 54

E

EC-SRR, 13-15
Edge-Coupled Split Ring Resonator, 13
effective homogeneity, 11
effectively homogenous, 10
electrical permittivity, 6, 7

G

group velocity, 9, 10, 16, 37, 54, 55, 138

I

ill-conditioned problem, 77, 81
input impedance, 1, 2, 21, 23-26, 31-35, 39, 41, 43-46, 48, 131
interdigital capacitors, 89, 90, 92-96, 138

L

left-handed materials, 35
Left-Handed Media, 10
left-handed parameters, 37, 43, 52, 60, 87
local minimizers, 72
loss tangent, 73, 79, 104
lossy parameters, 44, 48, 49, 64, 70, 124
lumped circuital models, 116, 118, 121

M

magnetic permeability, 6, 7, 13, 14
Matlab, v, 1, 2, 21, 25, 26, 27, 32-35, 38, 41-48, 51, 56, 58-69, 71, 72, 74-83, 84-87, 103, 104, 109-129, 131, 132, 135
metamaterials, 1, 5, 6, 8, 20, 131, 135, 137
microstrip technology, v, 1, 89, 96, 102, 132
Microstructure, 10

N

Nelder-Mead, v, 2, 72, 109
non-resonant approach, 5, 20

O

objective function, 77, 78
optimization algorithm, 109
optimization problem, 84
optimization variables, 84, 86, 87, 132

P

parameter extraction, v, 1, 2, 70, 71, 73-87, 102, 103, 115, 117, 132, 135
penalty term, 77, 78, 82
per unit-length parameters, 109
periodic structures, 16
periodicity, 12
permittivity, 6, 7, 8, 11, 14, 73
per-unit length, 17, 20, 25, 32, 36, 52, 56, 58, 63, 71, 109, 111-114, 116, 118, 121, 123-127, 129, 132
phase velocity, 23, 37, 54, 55, 73
PLH TL, v, 1, 35, 37-40, 44, 51, 131

propagation constant, 7, 22, 37, 52, 53
propagation direction, 9, 10, 105-107
propagation region, 94
purely left-handed, 36
purely left-handed TL, 17, 35
purely right-handed, v, 17, 53, 71, 87, 109, 131, 135

Q

quality factor, 15

R

reflection response, 74, 78, 109, 112-119, 121, 123-125, 127
resistance, 22, 30, 31, 37, 82, 84
resistive, 44, 46, 48, 49, 65-70, 124, 129, 131
right/left-handed losses, 56
right-angle bend, 107, 114-117

S

Sonnet, v, 2, 71-83, 85, 86, 96, 103-129
S-parameters, 35, 40, 41, 44, 51, 57, 58, 63, 74, 84
starting point, 71-75, 79, 81, 84
surface-mount technology, 89

T

T-junctions, 114
transition frequency, 18, 56, 61, 63, 68
transmission line, v, 1, 5, 16-18, 20-44, 46-49, 51, 52, 57-63, 65, 66, 70-72, 74, 79, 87, 89-91, 93, 95, 99-103, 109, 110, 112, 122, 124, 125, 131, 132, 135, 137, 138
transmission parameter, 15, 64-68

U

unbalanced case, 56, 62, 63, 68, 69
unit-cell, 1, 2, 14, 51, 57-64, 90, 92, 97, 98, 100, 101, 105, 107, 108, 109, 116-118, 120, 126, 127, 129, 132

V

voltage gain, 1, 2, 21, 27, 31-35, 38-41, 43-46, 48, 131

W

weighting factor, 76, 77, 81, 82, 84, 85